UNIVERSITY OF GENOVA

PHD PROGRAM IN BIOENGINEERING AND ROBOTICS

Developmental impact of blindness and sleep on neural multisensory processing

by

Helene Vitali

Thesis submitted for the degree of *Doctor of Philosophy* (36° cycle)

June 2024

Monica Gori	Supervisor
Claudio Campus	Co-supervisor
Paolo Massobrio	Head of the PhD program

Thesis Jury:

Claudia Lunghi, *Ecole Normale Supérieure, Paris*	External examiner
Andrew J. Bremner, *University of Birmingham*	External examiner
Matteo Bianchi, *University of Pisa*	External examiner

Dibris

Department of Informatics, Bioengineering, Robotics and Systems Engineering

Declaration

I hereby declare that except where specific reference is made to the work of others, the contents of this dissertation are original and have not been submitted in whole or in part for consideration for any other degree or qualification in this, or any other university. This dissertation is my own work and contains nothing which is the outcome of work done in collaboration with others, except as specified in the text and Acknowledgements. This dissertation contains fewer than 65,000 words including appendices, bibliography, footnotes, tables and equations and has fewer than 150 figures.

Helene Vitali
June 2024

Abstract

Objective. The objective of my Ph.D. project is to explore how visual impairment influences brain development during both awake and sleep states. Moreover, it examines the role of blindness and sleep in the neural processing of multisensory and spatial information in infants.

Approach. The primary technique employed in this research is electroencephalography (EEG), a non-invasive method that records the brain's electrical activity. EEG allows us to observe spontaneous electrical fluctuations generated by neural networks, providing valuable insights into brain functions. It remains one of the best techniques for studying brain activity in children due to its high temporal resolution and ability to capture neural activities and oscillations associated with various processes in near-ecological conditions. Four experiments were conducted using EEG recordings to address the research questions. Additionally, due to the lack of devices available for multisensory stimulation in children during EEG recordings and to overcome the limitations of existing devices, a new device was developed.

Main results. The findings indicate that the development of background brain activity during wakefulness differs between severely visually impaired (SVI) and sighted children. These differences, primarily involving the alpha rhythm (8-12Hz), increase the likelihood of motor disorders in the SVI group. While deviations from the typical development of the alpha rhythm become evident from age three, differences in the development of sleep spindles appear earlier. Sleep spindles, particularly fast spindles (13-16Hz), evolve alongside brain maturation and serve as markers of sensory information processing and consolidation during sleep. My research identified a decrease in fast spindle power in the sleep patterns of SVI children, devoid of the typical maturational decline. Reduced spindle power increases the risk of perceptual impairments within the first three years of life and heightens the likelihood of motor disorders from the fourth year onwards. These findings suggest that differences in multimodal responses observed in visually impaired infants compared to sighted peers may be partially attributed to mechanisms occurring during sleep, which favors the consolidation of more salient daily experiences. Early blindness leads to a prioritization of tactile cues over acoustic ones, also affecting sensory processing in non-canonical postures.

Indeed, blind children rely on bodily coordinates during their early years, prioritizing tactile spatial information, whereas sighted children transition towards an external reference frame, emphasizing environmental cues such as auditory information. Preliminary investigations into the effect of sleep on audio and tactile modulation of the alpha rhythm indicate that sleep enhances this difference in sensory preference, underscoring its crucial role in early sensory processing.

Significance. Neurophysiological differences between blind and sighted children can be interpreted within a broader context of divergent brain development, particularly concerning thalamocortical activity, which may represent the early impacted mechanisms. Highlighting these early impacted neural mechanisms is crucial for timely intervention during rehabilitation. Furthermore, enhancing the availability of devices for investigating these neural mechanisms could provide future insights, facilitating more precisely targeted individual rehabilitation.

Key-words: Brain Development; Blindness; EEG; Multisensory; Sleep; Sensorimotor.

Table of Contents

List of Figures

List of tables

Chapter 1

Introduction

Our senses constantly provide signals that contribute to the creation of a coherent representation of the external world. However, sensory systems are not mature at birth and undergo specific fine-tunings during the earliest stages of life. For instance, sensory perception is noisier with imprecise predicted sensory feedback mechanisms (Gori et al., 2012c; Meredith et al., 2018; Nardini et al., 2010), and different perceptual skills develop at different times within the same sensory modality (Gori et al., 2021, 2012a). This developmental timeline is asynchronous between modalities. As such, at a given time in childhood, the computation needed to discriminate a specific feature might be mature in a particular sensory modality but not the other, creating a discrepancy between percepts in each modality. Therefore, the least error-prone sense seems to become a priority to resolve this conflict and reduce ambiguity. Then, the continuous interaction among the senses enables their mutual refinement, fostering the acquisition of all the abilities essential for perceiving a unified multisensory environment. The development of these multisensory abilities implies a complex brain maturation process, which requires the involvement of different cerebral areas, the formation of new neural networks, and the evolution of brain rhythms. Furthermore, during sleep, the sensory information acquired while awake is reprocessed and consolidated trough the formation and destruction of new neural synapses (Cirelli, 2013). This reprocessing favors the child's maturation and the acquisition of multisensory and sensorimotor skills (Fernandez and Lüthi, 2020; Jaramillo et al., 2023; Tamaki et al., 2008). Indeed, an extended neural network is activated during sleep, favoring brain plasticity (Brzosko et al., 2019; Jones, 2020). Sleep-dependent neuromodulation promotes local effects on specific sensory systems and global effects on overall nervous system function. These effects foster the development of sensory systems, possibly incorporating memories from everyday sensory experiences.

What happens to multisensory skills when one sense is missing, as in the case of blindness? To what extent does the absence of vision impact the mechanisms of brain development? What is sleep's role in constructing a multisensory representation of the world, and how does this role change in the absence of vision?

The main aim of the thesis is to deepen how blindness affects the brain's multisensory processes during wakefulness and sleep. Chapter 2 of the thesis investigates how blindness affects the maturation of brain rhythms during wakefulness and sleep. Specifically, some brain processes crucial during childhood are considered to identify when blind children show a deviation from the typical developmental trajectory. Chapter 3 of the thesis investigates how blindness impacts the sensory neural processing of acoustic and tactile information in the first years of life and the role of sleep in sensory reprocessing. Chapter 4 of the thesis shows a new technological solution to investigate multisensory neural processing in children and the reliability value in children's EEG studies.

To reach its goal, this project involves studying and comparing different developmental mechanisms in blind and sighted children, specifically awake brain rhythm, sleep brain rhythm, and multisensory skills maturation. Subsequently, I preliminary investigate all these factors in order to understand their mutual relationship. The final considerations are linked to the technological and research evolution involving our future research.

Literature concerning the development of awake and sleep brain mechanisms, as well as the evolution of multisensory processing, shows which are the typical maturational processes that occur in childhood. Subsequently, in my experiments, I introduce the effect of the absence of vision within this complex intersection. The project aims to understand from a more comprehensive point of view how blindness impacts the child's development. From a clinical perspective, this understanding can help set up effective rehabilitation strategies to improve impaired multisensory skills in blind children.

1.1 Brain development

The brain undergoes a remarkable journey of development from birth through adolescence. This complex process involves intricate molecular, cellular, and structural changes that lay the foundation for sensorimotor and cognitive functions (Shonkoff and Phillips, 2000). Comprehending the typical brain developmental trajectory is essential for understanding when a deviation from that occurs. This chapter explores the multifaceted landscape of brain development, with a particular focus on the brain rhythms in the first decade of life. After a brief introduction to brain activity, the first part shows the maturation of neural activity rhythms during wakefulness. The second part delves into the brain patterns that characterize sleep.

1.2.1 The electrophysiological activity of the developmental brain

From the early stages of neurogenesis to the sculpting of neural circuits through synaptogenesis and pruning, the brain undergoes a dynamic transformation that shapes an individual's sensorimotor and cognitive abilities (Shonkoff and Phillips, 2000). To gain

deeper insights into this process, I focus on the realm of neurophysiology, specifically using the electroencephalography (EEG) technique, which provides a unique way to understand the evolution of neural activity during early development. EEG is a non-invasive technique that records the brain's electrical activity with higher temporal resolution. It allows us to observe the spontaneous electrical fluctuations generated by neural networks, as well as the brain response to stimuli, providing valuable information about brain function. To date, EEG remains one of the best techniques for studying brain activity in children (Bell and Cuevas, 2012).

One of the key features revealed by EEG is the presence of rhythmic patterns in the electrical activity of the brain. Typical oscillations are associated with different cognitive processes and states of consciousness. Theta, alpha, beta, gamma, and delta oscillations, for instance, are indicative of various mental states, including relaxation, arousal, and deep sleep (Buzsáki and Watson, 2012). Indeed, different oscillations play a causal role in different processes when the working brain is considered as a network. Therefore, cross-frequency interactions can inform how signal gating and inhibitions are allowed (Jensen and Mazaheri, 2010). Moreover, when sensory stimulation is applied, the generators of these rhythmic activities are coupled and act together in a coherent way, giving rise to event-related potentials (ERPs). ERPs can be regarded as originating from the reorganization of the spontaneous EEG in response to specific stimuli, offering a glimpse into the functional integrity of sensory pathways (Sur and Sinha, 2009). Understanding the maturation of these brain activities can shed light on the development of sensorimotor, attention, and overall cognitive abilities (Kandel et al., 2021). The first ten years of life witness significant milestones in their maturation, from the early emergence of basic sensory responses to the refinement of complex cognitive processing. In the following paragraphs, I illustrate how the wakefulness brain activity matures.

2.2.1 The maturation of neural rhythms during wakefulness

During everyday activities, our brain is continuously stimulated by signals coming from the external world. These random inputs keep thalamic and specific cortical cells in a depolarized state, generating the typical rapid rhythmic activity that characterizes the wakefulness state (Lopes da Silva et al., 1973). The primary cerebral rhythm is represented by alpha activity. It exhibits a typical locoregional distribution in the temporal-parietal-occipital area and demonstrates strong reactivity: it manifests as a synchronized rhythm during relaxed vigilance with closed eyes, which attenuates upon eye-opening, as well as during mental activity, sensory stimuli, etc. (Niedermeyer, 1997). In adults, alpha frequency fluctuates between 8 and 12 Hz, albeit this frequency changes during development.

In the early stages of life, slow oscillations characterize the neonatal brain, suggesting an initial phase of neural network organization. With the progression into childhood, alpha and beta rhythms become more prominent, reflecting the maturation of sensorimotor, attentional,

and high-cognitive processes (Angelini et al., 2023; Başar and Schürmann, 1994; Hofstee et al., 2022; Klimesch et al., 1997, 1993; Kwok et al., 2019; Vollebregt et al., 2015). Two different hypotheses have been presented about the effect of age on brain rhythms. The first one claims that the brain oscillations maintain the same frequency band playing, to some extent, the same functional role from the earliest stages of life (i.e., fixed bands hypothesis), (Başar-Eroglu et al., 1994; Başar, 2012; Basar and Bullock, 1992; Kolev et al., 1994; Yordanova and Kolev, 1996). Following this hypothesis, children under three years old show little spontaneous brain activity in the typical alpha frequency range. As they grow, alpha activity increases, manifesting earlier in the posterior regions and only later spreading to the frontal ones, becoming accentuated in elderly subjects (Basar and Bullock, 1992). This topographical shift matches brain area development: the rapid phase of synaptic growth is short and occurs early in the sensory areas (e.g., the visual cortex), while the association areas (e.g., the prefrontal cortex) take longer to mature. Sensory areas continue developing until age two or three, while association areas keep growing until age ten.

The second hypothesis, and the most accredited one, claims that a specific functional role is mediated by EEG bands shifting towards high frequencies with increasing ages (i.e., shifting bands hypothesis), (Mcsweeney et al., 2023; Niedermeyer, 1997; Stroganova et al., 1999). Thus, in early life, the alpha rhythm is slower than the conventional alpha band and tends to speed up with age. Initially, around 4 months old, a precursor of the alpha rhythm emerges with oscillations around 4Hz. Over time, its frequency gradually increases, reaching 6-8 Hz by the end of the third year. Between 3 to 5 years old, this rhythm stabilizes at 8 Hz but can occasionally be interrupted by slower wave sequences. Finally, the alpha rhythm continues to mature, resembling that of adults more closely, reaching a nearly complete maturation around age 16 (Marcuse et al., 2008). This shift to faster frequencies reflects the maturation of neural networks, which undergo significant changes in the myelination and modeling processes during development. Brain maturation is also manifested in the variation of alpha power: as we grow, the relative alpha power increases, mirroring structural changes in thalamocortical connectivity, while the overall alpha oscillatory power decreases due to synaptic pruning processes (Cragg et al., 2011; Mcsweeney et al., 2023; Tröndle et al., 2022; Whitford et al., 2007). Changes in the development of neural networks are also manifested in ERPs. For example, how alpha activity reorganizes itself after receiving sensory input shows how our information-processing abilities change as we get older (Yordanova and Kolev, 1997, 1996). Different brain rhythms occur in specific frequencies across various brain regions, speeding up internal communication and facilitating the transmission and processing of information (Basar and Bullock, 1992). This ability to reorganize the ongoing brain oscillations during stimulus processing reflects the development of brain maturation. For instance, three-year-old children did not consistently show alpha frequency components in the evoked auditory and visual potentials, and even those who do struggle to synchronize it with the stimulus (Başar-Eroglu et al., 1994; Başar et al., 1997; Kolev et al., 1994). During the school-age period, the alpha responses in children become stronger (increasing with age) but remain lower phase-locking than adults, as well as it is maximal over the posterior site

rather than central/frontal area (Başar et al., 1997; Yordanova and Kolev, 1996). These differences gradually diminish with age, although the alpha response system is not complete at the age of 11. The developmental dynamics of the alpha-band power imply that the activity or number of neurons involved in the alpha system changes with age.

Although the neurophysiological system involved in the genesis of alpha rhythm is not fully clear, its origin has been typically associated with a cortical origin, emerging by the activity of cortico-cortical networks (Lopes da Silva et al., 1973; Salvador et al., 2013), thanks to the firing of the intrinsically rhythmic neurons (Silva et al., 1991). However, an involvement of cortico-thalamic reverberating circuits in the generation of alpha activity was also hypothesized (Andersen and Andersson, 1968; Andersson and Manson, 1971) and demonstrated (Ching et al., 2010; Hughes and Crunelli, 2007), suggesting a thalamus influence in the activity of the corresponding cortical areas. Further evidence indicates that alpha generators should be extended to other structures, including the brainstem and hippocampus (Babiloni et al., 2009; Başar, 2012). The maturation of this distributed alpha system, which regulates the brain states, leads to changes in alpha activity observed with age, both during spontaneous and reorganized brain activity. Indeed, this distributed alpha system works under the "excitability of brain tissue" principle. Thus, if a neural population is able to show spontaneous activity in a given frequency range, then this neuronal group can be brought to a state of excitement in the same frequency range by sensory stimuli (Basar and Bullock, 1992). As a result, a shift towards faster frequencies with development will characterize both spontaneous and reorganized activity. On the contrary, slow activity will become less present in waking activity (Petersén and Eeg-Olofsson, 1971), remaining a specific physiological feature of sleep state.

3.2.1 The development of the sleeping brain

As the brain drifts into slumber, a gradual shift occurs in its electrical activity. The fast, low-amplitude neural oscillations begin to wane, giving way to slower, more rhythmic waves. The bustling activity of alpha and beta waves gradually gives way to the smoother patterns of theta and delta waves, sometimes organized in specific sleep patterns (e.g., slow waves and spindles). The electrical activity is transitioning from a busy state to a more relaxed one, ultimately leading to sleep. Indeed, this transition state is first characterized by a reduction of alpha activity, which changes unevenly depending on the brain region (Kalauzi et al., 2012). Initially, there is a reduction in prefrontal cortex activity, specifically associated with alertness. Then, further alpha activity decreases in the frontoparietal associative cortices occur. This decline reflects the diminishing engagement of higher cognitive functions at the beginning of the sleep onset. The primary sensory areas are affected only by progressing toward deeper sleep stages (Braun et al., 1997; Maquet et al., 1997). With this progression from drowsiness to deep sleep, we face the second phenomenon that characterizes the transition phase: an increase in the slower frequencies. Similar to the decrease in alpha

activity, the increase in slow waves shows a different regional distribution with an anteroposterior gradient at the onset of sleep. They appear first in the frontocentral regions (Marzano et al., 2013) and later in the posterior brain areas. Supporting such a temporal segregation of brain areas in the transition process, a study demonstrated the existence of two types of slow waves with different characteristics and spatial distribution processes that sequentially come into play during the transition to sleep (Siclari et al., 2014). However, the temporal dissociation of the two slow-wave synchronization processes in the falling asleep period is not yet present in young children (Spiess et al., 2018). This less structuring of sleep patterns, already evident in the transition phase, also occurs at the micro and macrostructural level and is related to an incomplete maturation of the sleep neural networks. Indeed, as during wakefulness, many changes occur in the sleeping brain in the first decade of life. Below, I delve into how sleep is characterized and how its specific structure is achieved during development.

At the macrostructural level, sleep is organized in cycles that repeat throughout the night. These cycles consist of different stages, including non-rapid eye movement (NREM) and rapid eye movement (REM) sleep. Each cycle typically has three NREM stages (N1, N2, N3) and one REM stage (Berry et al., 2020). Five cycles per night typically occur, but the relationship between NREM and REM stages is variable during the night. Deep sleep predominates in the first sleep cycles and then decreases, while the REM stage prevails in the last cycles (Le Bon, 2020). The total sleep time and the definition of the different sleep stages change with age, reflecting the crucial role of sleep in optimal brain development (Roffwarg et al., 1966). At birth, infants spend more hours sleeping than awake. Then, the total sleep time decreases, and the sleep period gradually consolidates during the night.

Meanwhile, also the distribution of sleep stages undergoes a maturational process, with a decrease in the intensity of slow wave activity (SWA), which characterized the N3 deep sleep, and a decline in the time spent in REM sleep (Eisermann et al., 2013; Galland et al., 2012; Scholle et al., 2011). Specifically, at 3 months of age, NREM and REM sleep stages are evenly distributed during the night (Yoshida et al., 2015), and most sleep onset is REM sleep. The shift from REM to NREM sleep onset occurs during infancy. At 6 months of age, NREM sleep is prevalent at the beginning of the night, while REM sleep occurs later. By around 1 year old, REM sleep decreases to about 30% of total sleep time; by age 5, it is around 20-25% (Grigg-Damberger, 2017). While REM sleep decreases, the percentage of NREM sleep increases with the N3 that occupies a greater proportion in infancy and early childhood (Scholle et al., 2011). From ages 5 to adolescence, the amount of REM sleep stays fairly steady, but there is an increase in N2 sleep and a decrease in N3 sleep (Peirano and Algarín, 2007; Scholle et al., 2011). The sleep EEG power spectrum also has a similar evolution during sleep; it evolves in keeping with maturation and neurodevelopmental milestones reflecting the activity of sleep microstructure. Indeed, during these dynamic changes in sleep cycle development, specific sleep patterns gradually shape, characterizing the sleep microstructure.

At the microstructural level, each sleep stage is characterized by specific sleep EEG patterns (Berry et al., 2020). The N1 manifests the V waves. They are sharply contoured waves distinguishable from the background activity, already characterized by a reduction/absence of dominant alpha rhythm. The N2 is defined by the appearance of K complexes and sleep spindles. The first one is a negative sharp wave followed by a positive component. In turn, the sleep spindle is a train of distinct sinusoidal waves that oscillate in the sigma band (10-16Hz). The N3 is characterized by the presence of SWA, consisting of slow-frequency waves oscillating in the delta band (0.5-4.75Hz) with high amplitude. Finally, the REM stage shows the sawtooth waves, an EEG hallmark composed of trains of sharply contoured or triangular waves. They are distinguishable from a low-amplitude, mixed-frequency background activity.

The first sleep EEG pattern that matures after birth is sleep spindles. Sleep spindles mirror the activity of the thalamocortical circuit (Fernandez and Lüthi, 2020; Halassa and Kastner, 2017; Steriade, 1999) and undergo important changes in the early life (D'Atri et al., 2018; Kwon et al., 2023). Spindles are typically evident by 3 months of age (Eisermann et al., 2013; Jenni et al., 2004; Sankupellay et al., 2011), and their synchronization increases during the first year of life, becoming bilateral symmetric by 2 years of age. Like adults, sleep spindles in children can occur independently at two different frequencies and topographies. Slow spindles oscillate in the low-sigma band (10–13 Hz) and prevail in the frontal area (Chatburn et al., 2013; Clemens et al., 2005; Doucette et al., 2015; Gruber et al., 2013; Hoedlmoser et al., 2014; Kurdziel et al., 2013; Tarokh et al., 2014). In turn, fast-spindles oscillate in the high-sigma band (13–16 Hz) and prevail in the central area (Barakat et al., 2011; Chatburn et al., 2013; Jaramillo et al., 2023; Schabus et al., 2007; Tamaki et al., 2008). Slow and fast spindles' different evolution reflects the maturation of their respective neural generators (D'Atri et al., 2018; McClain et al., 2016; Ricci et al., 2021; Shinomiya et al., 1999). In detail, the fast frequencies increase through a child's first 6 months, while the slow frequencies become less common (Louis et al., 1992). From 1 to 4 years of age, the slow spindles reverse this tendency and increase in density (D'Atri et al., 2018) while the fast spindles density decreases (D'Atri et al., 2018; Page et al., 2018). Afterward, fast spindles linearly increase until adolescence, while slow spindles decline with a sudden increase during puberty (Campbell and Feinberg, 2016; Shinomiya et al., 1999). The two types of spindles are also associated with different functional skills: slow spindles characteristics better reflect the high-level cognitive functions (e.g., intelligence and declarative learning), (Chatburn et al., 2013; Clemens et al., 2005; Doucette et al., 2015; Gruber et al., 2013; Hoedlmoser et al., 2014; Kurdziel et al., 2013; Tarokh et al., 2014). In turn, fast spindles are associated with sensorimotor processing (e.g., visuomotor performance, motor functioning, and motor learning), (Barakat et al., 2011; Chatburn et al., 2013; Jaramillo et al., 2023; Schabus et al., 2007; Tamaki et al., 2008). These changes mark the correct maturation of the underlying neural structures.

Precise temporal coordination of sleep spindles and slow oscillation is also a fundamental sleep marker during development (Jaramillo et al., 2023). SWA is another crucial sleep

feature that changes during development and is associated with sleep homeostasis and synaptic strength (Tononi and Cirelli, 2014). It is typically evident by 5-6 months of life (Campbell and Feinberg, 2009) and follows a U-shape trajectory during development: it increases progressively in early childhood before it declines during adolescence (Campbell and Feinberg, 2009; Feinberg and Campbell, 2010; Gaudreau et al., 2001; Jenni et al., 2004; Kurth et al., 2010). Meanwhile, the location of maximal SWA gradually shifts from posterior to anterior brain regions during this time (Castelnovo et al., 2023; Kurth et al., 2010). This evolution is associated with structural brain modifications (Buchmann et al., 2011; Shaw et al., 2008) and is related to acquiring regionally specific skills (Kurth et al., 2012, 2010). Recently, slow waves where classified into two types. The type I slow waves are generated by a likely subcortical-cortical, arousal-related synchronization process, giving rise to large, steep, widespread frontocentral slow waves that predominate early in the falling asleep period. In turn, the type II slow waves are probably generated by the cortico-cortical synchronization process that which gives rise to smaller, shallower and more circumscribed slow waves, which become the predominant feature towards stable sleep (Bernardi et al., 2018; Siclari et al., 2014). However, the high synchronization efficiency of type I slow waves shows a different origin and distribution in children, making them virtually indistinguishable from most other (type II) slow waves (Castelnovo et al., 2023). The numerous changes that occur in the sleeping brain during development report the important role that sleep has not only for correct brain maturation but also for signaling any deviations from the typical developmental trajectory.

4.2.1 The neurophysiological markers of brain maturation

As shown in the previous sections, numerous neurophysiological markers during wakefulness and sleep can be investigated. These biomarkers, which reflect fundamental processes such as myelination, brain growth, and synaptic pruning, can provide important insights into brain maturation during critical periods of development. Therefore, these markers can allow us to identify deviations from the normal developmental progression, allowing healthcare professionals to intervene early in the case of abnormalities in neurological development. Based on these assumptions, in Chapter 2, the thesis investigates the neural biomarker during wakefulness and sleep in blind and sighted children. By comparing neural evolution between blind and sighted children from birth, we can identify the sensitive period of interventions.

In addition, these biomarkers can provide insights into a specific condition's pathophysiology, helping us understand its altered physiological mechanisms and the potential structures involved. For example, both thalamocortical and cortico-cortical networks could be of our interest for different reasons. Firstly, both systems are involved in the genesis of alpha rhythm (P Andersen and Andersson, 1968; Andersson and Manson, 1971; Ching et al., 2010; Hughes and Crunelli, 2007). Secondly, thalamocortical and cortico-

cortical pathways generate specific sleep EEG patterns, such as different types of spindles and slow waves (Bernardi et al., 2018; Fernandez and Lüthi, 2020; Siclari et al., 2014). Thirdly, the thalamus is central in transmitting sensory information to the cortex, and the thalamocortical network is crucial for sensory neurodevelopment (Blumberg et al., 2022). Cortico-cortical connections are also essential for integrating multisensory stimuli (Murray et al., 2016). Both of these neural circuits appear to have a fundamental role in the child's brain and sensory development. However, only one of these mechanisms may be early impacted by blindness, helping to understand the role of vision in the maturation of neural networks. In Chapter 5, I delve deeper into this discussion in light of the findings of my Ph.D. project. However, before presenting the works carried out, I show the state of the art of multisensory development in the following subchapter.

1.2 The development of multisensory integration

In the early years of life, the communication between different senses is an intricate mechanism. At birth, sensory systems are not fully developed and undergo specific refinement as they mature. This maturation process varies between senses, with touch being the earliest to develop, followed by vestibular, chemical, and auditory senses, and then vision (Gottbield, 1972). However, until adolescence, the children's brain must continuously update the mapping between sensory and motor systems to accommodate differences in sensory development and changes in body size (Paus, 2005). Additionally, within each sensory system, different aspects develop at different rates. For instance, in visual perception, aspects like binocular vision and color perception within the first year (Atkinson, 2002), while complex form and motion perception continue to refine and improve until later childhood, typically between 5 to 14 years of age (Brown et al., 1987; Del Viva et al., 2006; Ellemberg et al., 2004; Gori et al., 2012a; Kovács et al., 1999; Sciutti et al., 2014). The auditory modality follows the same pattern, where the basic skills develop during infancy, such as temporal changes detection (Trehub et al., 1995) and auditory frequency discrimination (Olsho, 1984; Olsho et al., 1986), while more complex abilities take longer to fully develop and often require experience. Fall into this category, for example, understanding speech in noisy environments (Johnson, 2000) or accurately locating sounds in spatial bisection (Gori et al., 2012b). Similarly, the tactile system develops from infancy to childhood, contributing early to developing the body boundaries and peripersonal space - PPS (Làdavas and Farnè, 2004; Serino, 2019). Indeed, touch is the first of our senses to develop, providing us a tool to perceive our own bodies (Bremner and Spence, 2017). However, touch sense is strictly connected with action, favoring the maturation of the sensorimotor system during childhood.

This maturation involves several processes, including multisensory integration (MSI) and calibration between the senses, as well as the maturation of environmental reference metrics common to all senses. I present these concepts in detail in the following paragraphs.

1.2.1 The multisensory integration and the cross-sensory calibration theories

One challenging task for our brains is integrating signals from different senses that simultaneously vehicle the same environmental property, such as the size of an object or its spatial position. In adults, these redundant signals are typically combined in an optimal manner, enhancing the precision and accuracy of individual sensory estimates (Alais and Burr, 2004; Ernst and Banks, 2002; Trommershäuser et al., 2011). However, while some basic forms of integration, like reflexive orienting towards an audio-visual signal (Neil et al., 2006), develop early, others, such as integration of visual-haptic cues to understand orientation and size, take time to develop (Gori et al., 2008).

In detail, evidence on the cross-modal information transfer from touch to vision shows that newborns process and encode shape information derived from manual interaction with objects and discriminate between subsequently presented visual objects (Streri, 2003; Streri and Gentaz, 2004). Furthermore, newborns demonstrate the ability to recognize textures previously encountered through tactile experiences and, conversely, to tactually recognize textures previously observed visually (Sann and Streri, 2007). Studies have also observed that infants as young as one-month-old can leverage the tactile-oral properties of objects to aid in visual recognition processes (Gibson and Walker, 1984; Meltzoff and Borton, 1979). Moreover, the capacity to perceive audio-visual relations emerges early in human development (Lewkowicz and Turkewitz, 1980; Neil et al., 2006). Additionally, during the first months of life, infants benefit from multisensory synchronous information (Bahrick, 2001; Bahrick et al., 2004; Kuhl and Meltzoff, 1982; Scheier et al., 2003).

As children grow, their burgeoning motor, cognitive, and social competencies facilitate an augmented exploration of the multimodal surrounding environment. This experience allows them to refine their senses and complete the maturation of MSI processes initiated at birth. Indeed, some multisensory mechanisms appear in late childhood, following the maturation of individual senses (Gori et al., 2012b, 2012a, 2008; Nardini et al., 2013, 2010, 2008; Petrini et al., 2014). In the first period of life, individual senses often maintain dominance over integrated sensory experiences for specific tasks because the brain requires time to calibrate various sensory systems and acquire the skill to integrate redundant signals (Gori et al., 2008; Nardini et al., 2008). According to the cross-sensory calibration theory (Gori, 2015), the most accurate sense for a given task is used to fine-tune other senses when the body is undergoing rapid changes that affect sensory systems. Thus, the more accurate sense for a specific environmental property calibrates the less accurate one. For example, vision is the most accurate sense for spatial environmental property and continually recalibrates other sensory modalities during development to account for anatomical and physiological changes. In the following section, I delve into research on developing spatial metrics and the pivotal roles of vision for their optimal maturation.

1.2.2 The development of spatial metrics

From birth, infants begin to construct a spatial representation of their surroundings. However, it is essential to encode acquired spatial information using coordinate systems to fully establish this representation. Two primary reference frames exist: the body and external coordinate systems. In the body reference system, coordinates are relative to the perceiver's body, enabling the updating of spatial information in agreement with the relative movements in the environment. Conversely, in the external reference system, coordinates are based on salient environmental reference points and their relative positions (Palmiero, 2014; Ruggiero et al., 2016).

These reference frames emerge from the interplay between our senses and environmental interactions, undergoing a developmental journey. We harbor a partially formed body reference frame at birth due to the touch system's development during gestation (Bremner and Spence, 2017). The touch system, crucial for perceiving our bodies and interacting with the environment in the first months of life, strongly reinforces the development of the body reference frame and the relative PPS during infancy. With the development, vision becomes the predominant sense, offering a different perceptual experience of the environment and favoring the shift from body to external coordinates to represent the space (Bremner et al., 2013). However, this transition spans several years, beginning early in infancy, and requires the ability to integrate perceptual experiences of the environment to form a unified spatial representation (Röder et al., 2014; Ruggiero et al., 2016). In children, the default use of external coordinates, as in adults, emerges from the age of 5 years (Pagel et al., 2009) and is not complete before the age of 10 years (Röder et al., 2013). Indeed, to perceive a multisensory world, humans must merge spatial information from all sensory modalities into a cohesive spatial representation.

Vision appears to play a pivotal role in this process (Pasqualotto and Proulx, 2012), providing an immediate and comprehensive view of the surrounding environment with high spatial resolution (Tinti et al., 2006). Consequently, vision seems crucial for aligning neural representations of space across different sensory modalities (King, 2014; Welch and Warren, 1980). The dominance of vision in spatial inference becomes evident when interacting with other senses. For example, during sensorial conflicts, auditory and tactile perceptions are heavily influenced by concurrently presented visual-spatial information (Anderson and Zahorik, 2014; Bertelson and Aschersleben, 2003; Botvinick and Cohen, 1998; Flanagan and Beltzner, 2000). Furthermore, evidence suggests that during development, the auditory system's spatial representation is influenced by visual experience, indicating the visual system's role in calibrating the auditory system for spatial perception (Gori et al., 2012b; Loomis et al., 1998). Additionally, in infancy, only visual cues from one's own body allow the child to account for body position (Rigato et al., 2014), implying that visual signals also contribute to calibrating the proprioceptive system for spatial metrics. Animal studies

corroborate these findings, indicating that the development of multisensory interactions between vision and other senses relies on early perceptual experiences. For instance, visual adaptation with prismatic spectacles in juvenile barn owls alters their auditory spatial maps (Knudsen, 1998), while visual deprivation in young ferrets disrupts auditory spatial map development (King and Carlile, 1993). Similarly, in humans, short periods of adaptation to non-aligned auditory and visual stimuli can alter auditory spatial representation (Recanzone, 1998; Zwiers et al., 2003).

In summary, research across various fields confirms that vision provides the most precise and reliable information about the external world's spatial properties, thus exerting a dominant influence on spatial perception (Alais and Burr, 2004; Welch and Warren, 1980). However, the exact mechanisms through which vision shapes the development of spatial representation in early life are not fully understood. In the following section, I present current evidence on the neural mechanisms underlying the development of multisensory integration.

1.3 The neural basis of multisensoriality

In the context of studies investigating multisensory information processing, the conventional paradigm delineates a sequential progression (Stein et al., 2009). Sensory inputs are initially processed within subcortical structures, traversing cortical pathways. Within the cortical domain, these inputs undergo preliminary processing within specialized regions tailored to their respective modalities, such as the occipital area for vision, temporal for hearing, and central for touch. This segregated processing culminates in the convergence of sensory streams within the higher-order association cortices, where integration occurs.

Different subcortical structures, including the superior colliculus, the basal ganglia, and the putamen, were shown to contain multisensory neurons (Meredith and Stein, 1986, 1983; Stein and Meredith, 1993). In particular, the Superior Colliculus (SC) is the primary site where inputs from different senses converge. Then, its multisensory neurons project to motor-related areas involved in controlling orientation behavior (Stein & Meredith, 1993), initializing and managing the localization and orientation of motor responses. However, while the SC serves as the primary convergence site for multisensory inputs, cortico-SC projections are crucial in refining and adapting SC-mediated multisensory integration to a specific environmental context (Stein et al., 2009). Indeed, multisensory behavior has also been observed in many neurons in the cortex, particularly in associative brain regions, which contain neurons that respond to stimulation in more than one modality. These regions receive feedforward converging inputs from sensory-specific areas of the brain, allowing the merging of information from different senses. An activation of multisensory stimuli was shown in the temporal lobe, such as superior temporal sulcus (Beauchamp, 2005; Foxe et al., 2002), regions in the parietal lobe, such as the intraparietal sulcus and the superior parietal lobule (Bolognini et al., 2005; Bremmer et al., 2001; Bushara et al., 1999; Molholm

et al., 2006), as well as regions in the frontal lobe, such as the prefrontal cortex (Bushara et al., 1999; Laurienti et al., 2003).

Recent findings challenge the traditional views of a rigid distinction between early unisensory and late multisensory cortices, showing that multisensory processing also involves the earliest stages of stimulus processing in classical "unisensory" areas (Calvert et al., 1999, 1997; Cappe et al., 2010; Ghazanfar and Schroeder, 2006; Kayser et al., 2009; Murray et al., 2016, 2005). Therefore, multisensory integration could operate through feedback projections to the unisensory cortices from multisensory regions and direct connections between the unisensory areas themselves (Falchier et al., 2002; Rockland and Ojima, 2003). Many studies refer to the multisensory properties of the auditory cortex, showing both visual and somatosensory influences on auditory neurons (King and Walker, 2012; Musacchia and Schroeder, 2009). However, the same has been seen also for visual and somatosensory neurons (Chanauria et al., 2019; Kuehn and Pleger, 2018). A still open question concerns the functional implication that multisensory convergence at low-level cortical processing may have on the perceptual experience. Investigating the mechanisms underlying sensory processing and multisensory integration during early development may help our comprehension of the low-level integration functional.

1.3.1 The development of multisensory neural networks

In most multisensory areas, the capacity to integrate stimuli from different sensory modalities is not present at birth but progressively develops during life. This phenomenon has been primarily studied in the SC. The immature cells in the SC may exhibit some multisensory behavior but cannot integrate inputs of different modalities (i.e., they do not show multisensory enhancement and depression), (Stein et al. 2009). Moreover, the acquisition of integrative capacities strictly depends on the experience of cross-modal inputs (Wallace et al., 2001, 2004). The development of descending afferents from two distinct extra-primary cortical regions, namely the Anterior Ectosylvian Sulcus and the rostral segment of the Lateral Suprasylvian Sulcus, is thought to be pivotal in acquiring these integrative capacities (Stein et al. 2009). Indeed, blocking these descending inputs results in the loss of integrative capabilities within the SC (Jiang et al., 2006, 2001).

The integration of multisensory information at the cortical level is also a process that takes many years to complete. One approach to probing the evolution of cortical multisensory integration abilities is investigating the evoked neural response during multimodal stimulation. When two stimuli are integrated, the multimodal stimulation evokes a potential with greater amplitude (or smaller) than the sum of the unisensory responses (Murray et al., 2005). This superadditivity (or subadditivity) effect indicates a nonlinear interaction between the neural responses and multisensory stimuli. Using this approach, it was evident that multisensory integration in adults occurs in associative areas at later latencies, as well as unisensory areas at early latencies (<100ms) (Fort et al., 2002; Foxe et

al., 2000; Foxe and Schroeder, 2005; Gobbelé et al., 2003; Molholm et al., 2004, 2002; Murray et al., 2005, 2004; Taylor-Clarke et al., 2002). For instance, audio-tactile stimuli were integrated starting from ~50ms in the central area contralateral to the hand stimulated with touch cues (Foxe et al., 2000; Murray et al., 2005).

This method has been used to comprehend the mechanisms of multisensory integration (MSI) from the first moments of life. It has been observed that the ability to integrate audio-tactile information when they are present in the PPS emerges immediately after birth (Ronga et al., 2021). This integration appears in the frontocentral area around 300ms (P2). The primary sensory areas' involvement in facilitating audio-tactile interaction compared to auditory-only stimuli on N1 response during a social task appears before the first year of life (Tanaka et al., 2018). A consistent audio-tactile integration is evident in school-age children and involves early latencies (Brett-Green et al., 2008). Indeed, an early audio-tactile integration in central regions between 60–80 ms in the hemisphere contralateral to the side of somatosensory stimulation was found in school-age children (Brett-Green et al., 2008). Between 110–150 ms, the MSI occurs in the hemisphere ipsilateral to the side of somatosensory stimulation. Finally, around 200 ms effect of MSI was found also on the associative areas. Other findings also reported the involvement of temporal regions starting from 100ms in the audio-tactile MSI (Russo et al., 2010). Differently, a significant audiovisual integration on associative areas starting from 100ms (N1) seems to mature between 7 to 16 years of age (Brandwein et al., 2011; Molholm et al., 2020; Stefanou et al., 2020). In adolescents, both audiovisual and visuotactile MSI are evident already at early latencies (<100ms) as well as in the trimodal response (Dwyer et al., 2022). However, an effect of visual influence on auditory responses on N450 over frontotemporal sites was found in 3-month-old infants (Hyde et al., 2010).

Analyzing the neural response during multiple sensory stimulations also allows us to understand the development of spatial metrics. EEG studies in newborns suggest a primitive coding system for body boundaries during audio-tactile stimulation emerges shortly after birth (Maitre et al., 2020; Ronga et al., 2021). The ability to detect the colocation of auditory and tactile stimuli is important to relate body sensory experiences (tactile) with external stimuli (audiovisual). Nevertheless, a spatial recalibration by vision is necessary for learning a precise spatial perception. For instance, the ability to accurately identify tactile stimuli delivered to the hands while in a non-canonical body position (i.e., crossed-hand posture) is a skill that emerges between the ages of 6 and 10 months (Rigato et al., 2014). A neural correlate associated with this spatial remapping at EEG starts to manifest around the 8th month and becomes more established by the 10th month. However, it is noteworthy that the vision of the hand is crucial at this developmental stage. Indeed, as delineated in the preceding section, visual experience is essential for transferring spatial decoding pertaining to body coordinates onto a reference system predicated upon external coordinates.

Overall, the study of evoked potentials can be an important tool for investigating the development of spatial and multisensory abilities in the early periods of life. Nonetheless, confining the analysis solely to ERPs would be restrictive. Indeed, EEG analysis affords the

opportunity to explore brain rhythms, offering deeper insights into the maturation of the neurophysiological mechanisms involved in processing multimodal information.

1.3.2 The brain rhythms during sensory processing

In the first section of this Chapter, I discussed how the brain rhythms mature in the first decades of life. But what happens when sensory stimulations are provided? How do the neural circuits in the brain organize their rhythmic activity to convey the message?

For unisensory stimulation, findings report that both auditory and tactile senses mainly modulate alpha-range oscillations already in infancy. Specifically, a vibrotactile stimulation applied to an infant's hand triggers an alpha rhythm desynchronization (i.e., decrease in power) in the contralateral central area, also called mu rhythm (Drew et al., 2018; Meltzoff et al., 2019; Saby et al., 2015; Shen et al., 2021). These results are consistent with findings in adults (Anderson and Ding, 2011). Indeed, early in life, the somatotopic organization of the basic body map in infants mirrors that of older children and adults with a similar mu rhythm response (Dall'Orso et al., 2018; Meltzoff et al., 2019; Saby et al., 2015; Shen et al., 2020). However, during infancy, the peak frequency of mu activity increases with age, as with alpha activity. Consequently, the frequency range of brain activity during tactile stimulation depends on the maturation of the mu rhythm, typically ranging from 4-6Hz in younger infants to 6-9Hz in older infants (Berchicci et al., 2011; Marshall et al., 2002; Shen et al., 2021; Thorpe et al., 2016), until reaching adult-like frequency range (see section 1.1.2). Essentially, as infants grow, there is an increase in mu frequencies modulated by tactile stimulation, accompanied by greater contralateral desynchronization (Shen et al., 2021). This aligns with findings on action production in older infants and the observation that infants' behavioral responses to tactile stimuli become more efficient with age (Cuevas et al., 2014; Leed et al., 2019; Somogyi et al., 2018). Similarly, auditory stimulation induced suppression of background alpha activity in the bilateral temporal electrodes (called tau rhythm) in infants and children (Fujioka et al., 2011; Fujioka and Ross, 2008), as well as in adults (Kim et al., 2023; Lehtelä et al., 1997; Niedermeyer, 1997; Tiihonen et al., 1991). Again, the modulated spectral frequencies, as do mu and alpha oscillations, increase with age.

Instead, in adults, cross-modal interaction and multisensory integration show involvement of faster and slower frequencies (for a review, see Keil and Senkowski, 2018). Briefly, the dynamic feed-forward-feedback processing between unisensory and multisensory areas is primarily reflected in gamma and beta-band power. In addition, information processed within one cortical area can modulate ongoing activity in another region, for example, through delta- and theta-band phase resetting. In tasks requiring top-down control, intersensory attention is reflected in local alpha- and beta-band power, as well as alpha- and beta-band functional connectivity networks. The exact mechanisms seem to be also involved in spatial attention and in shifting from body-centered to external coordinates

(Anderson and Ding, 2011; Heed et al., 2015; Ossandón et al., 2020; Schubert et al., 2019, 2015).

To the best of our knowledge, few studies investigated the role of neural oscillations in multisensory processing in infants (Drew et al., 2018; Tanaka et al., 2018). These studies evidenced that high-frequencies in the beta band already modulate cross-modal influences and multisensory integrations. However, future studies should further investigate brain rhythm development in multisensory processing. Another less explored area is the role of sleep and its neural oscillations in sensory and multisensory processing.

1.3.3 The sleep and multisensoriality

It is a common situation that everyday sensory experiences are reflected in dreams. They represent a multisensory experience in an altered state of consciousness, which varies in sensory-deprived humans (Vitali et al., 2022). Although the nature of dreams remains elusive, their occurrence underscores the role of sleep in sensory information processing, evident not only during REM sleep but also during NREM stages. Notably, sleep has been shown to facilitate visual plasticity (Aton et al., 2009; Frank et al., 2001). Studies in cats and humans demonstrate that visual plasticity is enhanced during subsequent sleep following monocular deprivation (MD), primarily through slow wave and spindle oscillations (Aton et al., 2013; Menicucci et al., 2022). Particularly in humans, a strong correlation between visual plasticity and changes in slow wave rate and sharp, as well as in sigma power, in the visual area has been observed (Menicucci et al., 2022). This evidence further supports the notion of thalamocortical interaction modulation as a homeostatic response to MD. The idea that these rhythms are involved in sleep sensory processing is reinforced by studies investigating multisensory integration and multisensory memory reactivation during sleep (Faivre et al., 2017; Rothschild, 2019) as well as the formation of sensorimotor memories during sleep (Miyamoto, 2023).

Recently, a review has highlighted the role of sleep in processing multisensory and sensorimotor information in children, underscoring its significance in typical and atypical neurodevelopment (Blumberg et al., 2022). Further discussion on the interplay between multisensorial experiences and sleep are presented in Chapters 3 and 5, where, respectively, I show preliminary data on the impact of sleep on the reinforcement of auditory and tactile stimuli in sighted and visually impaired infants, and I provide a comprehensive analysis of the thesis results.

1.4 Objectives of the thesis

Considering the recent advancements outlined in the introduction, the first step of the thesis involves the study of the development of neural mechanisms during wakefulness and sleep

in children with and without visual impairment. Subsequently, it delves into understanding how vision influences the ability to localize multisensory stimuli and the corresponding neural processes involved. Finally, the thesis provides insights into the role of sleep in shaping sensory perception and neural development, as well as the advancements in technology used to study these phenomena. Each paragraph begins with a comprehensive review of the literature about blind individuals, setting the stage for the subsequent discussion.

Specifically, Chapter 2 delves into the intricate brain oscillations that exhibit distinct maturation patterns between blind and sighted children during waking and sleeping states. This exploration underscores the pivotal role of vision in shaping brain maturation processes. In Chapter 3, the thesis elucidates the underlying brain mechanisms contributing to behavioral disparities in audio and tactile stimulus localization across different body positions in blind infants compared to their sighted counterparts. Chapter 4 highlights the significance of advancing multisensory technological tools for assessing brain activity in children. By leveraging cutting-edge technology, researchers can gain deeper insights into the complex interplay of sensory processing and neural dynamics.

Nearly a century ago, Charles Scott Sherrington described the plastic nature of the brain as: "*Swiftly the head mass becomes an enchanted loom where millions of flashing shuttles weave a dissolving pattern, always a meaningful pattern though never an abiding one; a shifting harmony of subpatterns"* (Sherrington, 1956). Today, our understanding extends beyond the confines of the cortex, recognizing the dynamic interactions encompassing deeper subcortical regions. In the concluding Chapter 5, I synthesize the critical discoveries of this thesis, contextualizing them within the framework of existing literature. It mainly focuses on the pivotal role of thalamocortical connections in shaping the intricate landscape of multisensory brain development.

I address the objectives of this thesis using Electroencephalography (EEG) as an investigative tool. With its remarkable temporal resolution and non-invasive nature, EEG remains the gold standard for studying brain development in children. It also allows the investigation of brain oscillations and their dynamics in multisensory stimulations. Additionally, the use of high-density electroencephalography, as in Chapters 3 and 4, offers a good topographical representation of the brain between temporal and spatial resolution for investigating neural mechanisms. Figure 1.1. shows the general framework of the thesis and the included studies.

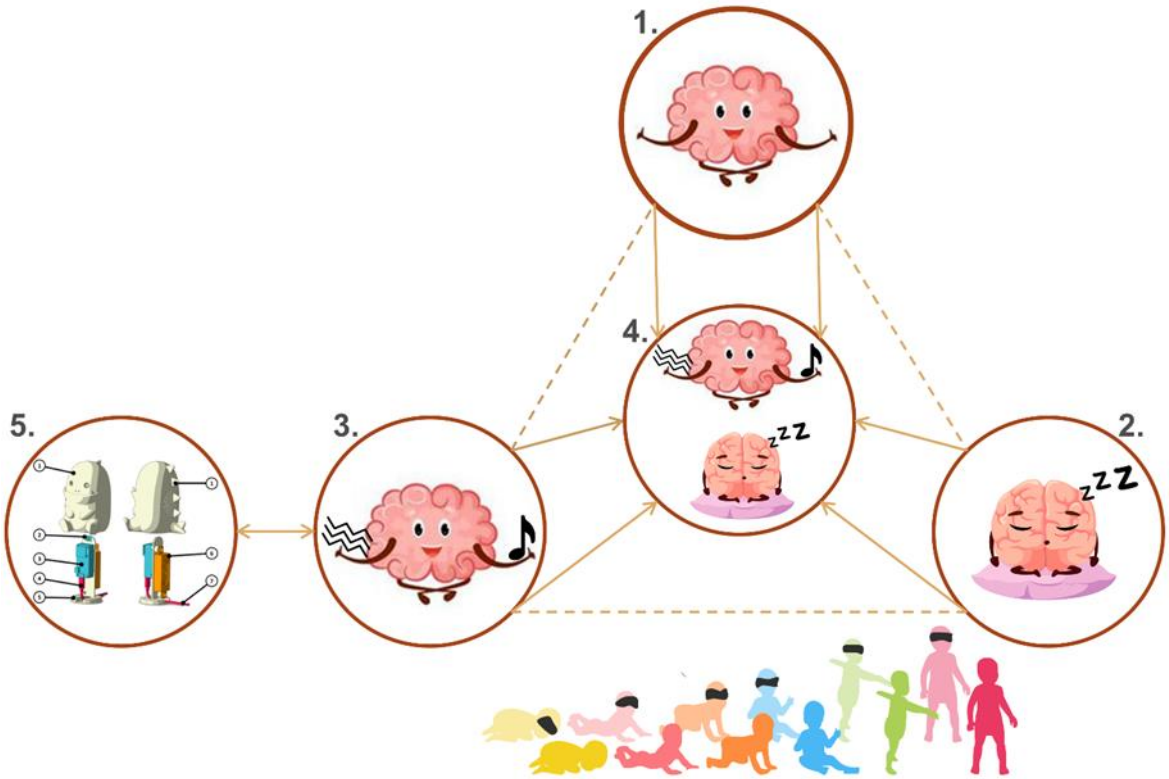

Figure 1.1 General Framework. *Each circle shows one of the five studies included in the thesis. Studies 1 and 2 are included in Chapter 2. Studies 3 and 4 are included in Chapter 3. Study 5 is included in Chapter 4.*

Chapter 2

Brain development in blindness

In Chapter 1, I introduced how neurophysiological biomarkers can be measurable indicators that provide valuable insights into the underlying mechanisms of brain development, allowing researchers and clinicians to identify deviations from typical developmental trajectories. This chapter explores how this approach can be applied to children with peripheral blindness. Indeed, the absence of visual input from birth or early infancy can lead to profound alterations in brain structure and function, affecting sensory, motor, and social abilities (Bollini et al., 2023; Cappagli et al., 2019, 2017; Gori et al., 2021; Houwen et al., 2009, 2007). Neuroimaging studies in blind children revealed significant changes in different brain areas, such as the occipital cortex (Inuggi et al., 2020), ToM (Theory of Mind) brain regions (Richardson et al., 2023), and thalamocortical connections (Lin et al., 2022), as well as a neural reorganization of the sensory networks and the development of some compensatory mechanisms (Lin et al., 2022; Ortiz-terán et al., 2017). Numerous cross-modal plasticity changes in the human brain were also confirmed by studies in congenitally blind adults (Amedi et al., 2007, 2002; Gori et al., 2018; Kujala et al., 1995; Röder et al., 2000; Striem-Amit et al., 2012; Uhl et al., 1991). While compensatory neural mechanisms are essential for daily activities, they may leave gaps in acquiring specific concepts, such as spatial representation (Gori et al., 2014).

By employing neural biomarkers, researchers can further understand the role of sensory experience in shaping brain development and identify the specific sensitive period of interventions. Therefore, in the first experiment, I focus on the development of brain rhythm during wakefulness comparing sighted with blind children in the first decade of life. In turn, I am focusing on the sleep period in the second experiment.

2.1 Exp.1: Developmental trajectory of alpha activity in blind and sighted children

Alpha activity (8–12 Hz) represents the main brain rhythm that develops during childhood. It dominates the occipital EEG activity (Bazanova and Vernon, 2014; Lopes Da Silva, 1995; Steriade et al., 1990), and its maturation is a visual-dependent mechanism. Indeed, alpha oscillations are reduced or missing in blind adults (Akiyama et al., 1964; Birbaumer, 1971; Cohen et al., 1961; Enge et al., 1973; Jan and Wong, 1988; Kriegseis et al., 2006; Noebels et al., 1978; Novikova, 1974; Ossandón et al., 2023). Evidence shows that the alpha1 (8-10Hz) and alpha2 (10-12Hz) sub-bands are linked to different perceptual-cognitive functions (Petsche et al., 1997), with alpha1 associated with attention, expectation, and encoding, and alpha2 linked to memory and semantics (Doppelmayr et al., 2002; Klimesch, 1997; Klimesch et al., 1994). However, whether there is a specific association between different alpha sub-bands and blindness has not yet been studied. Some studies also explored the EEG spectral activity in blind children, confirming a reduction of alpha rhythm and an overrepresentation of delta activity in late childhood (Akiyama et al., 1964; Cohen et al., 1961; Jan and Wong, 1988; Jeavons, 1964; Red'ka and Mayorov, 2014). Most of the studies are qualitative, include wide age ranges and variability in visual impairment, and fail to include a control group, keeping it unclear whether and how alpha activity develops in blind children. A better understanding of alpha activity's developmental trajectory could help clarify the brain processes linked to reduced alpha activity in blindness.

This reduced occipital alpha power observed in blind individuals may stem from two primary mechanisms: weakened inhibitory circuits (Sherman and Spear, 1982) or structural alterations in regions crucial for alpha rhythm generation (Inuggi et al., 2020). Studies suggest that alpha waves may primarily originate from the thalamocortical network (Per Andersen and Andersson, 1968; Andersson and Manson, 1971) and/or the cortico-cortical connections (Pfurtscheller and Lopes da Silva, 1999). Both networks may be affected by visual deprivation. First, the lateral geniculate nuclei (LGN) of the thalamus are atrophied following blindness in animals (Berman, 1991; Rakic et al., 1991) and humans (Breitenseher et al., 1998). Second, alpha rhythms within the visual cortex may also arise from cortical layers IV and V, with pyramidal cells in layer V possessing intrinsic rhythm-generating properties. These neural connections are altered in cases of early visual deprivation (Sherman and Spear, 1982).

Based on previous information, two questions remain unanswered. When does the differentiation of alpha activity between sighted and visually impaired individuals emerge during development? What mechanisms are associated with the impairment of this activity? So, in this study, I explore the EEG spectral composition's developmental trajectory, specifically the occipital alpha activity in congenital blind/severely visually impaired (BSI) children and sighted (S) controls. I investigate four hypotheses. The first two hypotheses

argue, respectively, that the differences in occipital area activity between blind and sighted children increase with age and that these differences arise mainly from activity in the visual areas of the brain. Then, I hypothesize that congenital visual deprivation also influences the entire EEG spectrum in favor of lower frequencies. Finally, I hypothesize a possible association between perceptual disorders resulting from blindness and some motor dysfunctions.

2.1.1 Methods

Participants

EEG recordings at rest for 60 blind/severely impaired (BSI) individuals and 66 sighted (S) individuals aged 20 days to 10 years and 11 months were included in this study and subdivided into three age bins: from 0 to 3 years with 19 BSI (9F) and 17 S (9F) children; from 3 to 6 years with 19 BSI (10F) and 22 S (8F); and, from 6 to 11 years with 22 BSI (11F) and 27 S (13F). Table 2.1. presents details about the BSI group. None of the children had a history of prenatal infections, distress during delivery, genetic syndromes, or metabolic disorders. All the participants in this study presented with good general health status; some of them had slight developmental delay, especially in the motor domain, motor coordination impairment, and/or hypotonia, as is often described in visually impaired children (Dale et al., 2017; Dale and Sonksen, 2002; Fazzi et al., 2005). None were epileptic or cognitively impaired. Developmental and cognitive assessment was evaluated using standardized tests according to the age of the child - i.e., Griffiths Mental Development Scales (Luiz et al., 2001), Leiter-R (Leiter, 1980), Wechsler scales (Wechsler, 2003) or Raven matrices test (Raven et al., 1996). BSI children were assessed with the Reynell-Zinkin Scale (Reynell, 1978) and the verbal subscales of the Wechsler scales. In 38 children, a normal or altered psychomotor development level was defined based on clinical evaluation and information on the child's adaptive behavior and school functioning provided by parents and teachers. Furthermore, all BSI participants were exclusively affected by congenital disorders of the peripheral visual system (i.e., involving pre-chiasmatic structures). Cerebral visual impairment was excluded based on anamnesis, clinical and instrumental visual function assessment, and neurological examination.

Code	Biological sex	Age (Y)	Degree of visual impairment	Diagnosis
1	M	0.06	severely impaired	Inherited congenital retinal dystrophy
2	M	0.44	severely impaired	Optic nerve hypoplasia
3	M	0.86	severely impaired	Ocular albinism
4	M	1.04	totally blind	Inherited congenital retinal dystrophy
5	F	1.2	severely impaired	Nystagmus
6	F	1.23	severely impaired	Inherited congenital retinal dystrophy
7	F	1.34	totally blind	Inherited congenital retinal dystrophy

8	F	1.34	totally blind	Inherited congenital retinal dystrophy
9	M	1.45	totally blind	Inherited congenital retinal dystrophy
10	F	1.48	totally blind	Nystagmus
11	M	1.65	totally blind	Ocular malformation
12	F	1.66	totally blind	Inherited congenital retinal dystrophy
13	M	1.83	totally blind	Inherited congenital retinal dystrophy
14	M	2.17	totally blind	Inherited congenital retinal dystrophy
15	F	2.32	severely impaired	Ocular malformation
16	M	2.61	totally blind	Inherited congenital retinal dystrophy
17	F	2.65	severely impaired	Ocular albinism
18	M	2.76	severely impaired	Inherited congenital retinal dystrophy
19	F	3.55	totally blind	Inherited congenital retinal dystrophy
20	F	3.66	totally blind	Inherited congenital retinal dystrophy
21	F	3.7	severely impaired	Nystagmus
22	F	3.8	severely impaired	Inherited congenital retinal dystrophy
23	F	3.84	totally blind	Inherited congenital retinal dystrophy
24	M	3.87	severely impaired	Optic nerve hypoplasia
25	M	4.24	totally blind	Inherited congenital retinal dystrophy
26	M	4.29	severely impaired	Inherited congenital retinal dystrophy
27	F	4.62	totally blind	Inherited congenital retinal dystrophy
28	M	4.78	severely impaired	Inherited congenital retinal dystrophy
29	F	4.95	severely impaired	Optic nerve atrophy
30	F	4.99	severely impaired	Optic nerve hypoplasia
31	F	5.08	totally blind	Inherited congenital retinal dystrophy
32	M	5.14	severely impaired	Nystagmus
33	F	5.35	severely impaired	Inherited congenital retinal dystrophy
34	M	5.44	totally blind	Inherited congenital retinal dystrophy
35	M	5.65	severely impaired	Inherited congenital retinal dystrophy
36	F	5.66	totally blind	Inherited congenital retinal dystrophy
37	M	5.83	totally blind	Inherited congenital retinal dystrophy
38	M	6.1	totally blind	Inherited congenital retinal dystrophy
39	F	6.1	totally blind	Inherited congenital retinal dystrophy
40	F	6.26	totally blind	Optic nerve hypoplasia
41	M	6.31	severely impaired	Inherited congenital retinal dystrophy
42	F	6.33	totally blind	Inherited congenital retinal dystrophy
43	F	6.51	severely impaired	Congenital cataract
44	M	6.53	severely impaired	Nystagmus
45	F	6.72	totally blind	Retinopathy
46	M	6.76	totally blind	Inherited congenital retinal dystrophy
47	F	6.91	totally blind	Inherited congenital retinal dystrophy
48	M	7.29	totally blind	Inherited congenital retinal dystrophy
49	F	7.35	totally blind	Inherited congenital retinal dystrophy
50	M	8.64	severely impaired	Inherited congenital retinal dystrophy
51	F	8.79	totally blind	Inherited congenital retinal dystrophy
52	M	8.97	severely impaired	Optic nerve hypoplasia
53	F	9.07	totally blind	Congenital cataract
54	M	9.47	totally blind	Inherited congenital retinal dystrophy
55	M	9.47	totally blind	Inherited congenital retinal dystrophy

56	F	9.55	totally blind	Inherited congenital retinal dystrophy
57	M	9.56	totally blind	Inherited congenital retinal dystrophy
58	M	9.6	severely impaired	Inherited congenital retinal dystrophy
59	M	10.31	totally blind	Inherited congenital retinal dystrophy
60	F	10.47	totally blind	Inherited congenital retinal dystrophy

Table 2.1. Clinical details of the blind group. *The table shows identification code, the biological sex, age expressed in decimal years (i.e., age in days/365), the degree of visual impairment, and the diagnosis. Different colors represent different age bins.*

Data acquisition and preprocessing

EEG data were collected with a 512 Hz sampling frequency using a Nicolet vEEG 5.94 system; missing or artifacted electrodes were interpolated to obtain a complete montage of 72 derivations. For each participant, a resting-state period in sensory deprivation conditions with opened eyes in a dark, silent, and comfortable room was recorded. These conditions are reportedly the best for recording resting state in infants/children (Stroganova et al., 1999). An operator continuously monitored the state of participants using EEG and infrared camera recordings. In a later scoring phase, based on the EEG and video recording, periods in which subjects were moving or falling asleep from the analysis were excluded. Then, the EEG recordings were filtered between 0.1 and 100 Hz. Transient high-amplitude artifacts were removed using artifact subspace reconstruction (ASR), an automated artifact rejection method available as a plug-in for EEGLAB software (Delorme and Makeig, 2004; Mullen et al., 2015). ASR uses a sliding window technique whereby each window of EEG data is decomposed via principal component analysis and compared with data from a clean baseline EEG recording. Within each sliding window, the ASR algorithm identifies principal subspaces that deviate from the baseline; it then reconstructs these subspaces using a mixing matrix computed from the baseline EEG recording. Here, a sliding window of 500 ms and a threshold of 3 std to identify corrupted subspaces was used. Moreover, channels were removed if their correlation with other channels was below 0.85 or if the line noise-to-signal ratio exceeded 4 std from the channel population average. Time windows were removed after applying the previously described criteria – i.e. when the fraction of contaminated channels exceeded the threshold of 0.25. With the cleaned data of each participant (mean segment duration = 333s, 95% CI = [195, 638]s), the power spectral density (PSD) expressed in uV^2/Hz was computed), applying the *spectopo* function of EEGLAB, which returns a PSD estimate via Welch's method. Finally, spectral activity for delta1 (0.5-2)Hz, delta2 (2-4)Hz, theta (4-8)Hz, alpha1 (8-10)Hz and alpha2 (10-13)Hz spectral bands was considered. The spectral activity was normalized to make it comparable among children by computing the relative spectral power, which measures the ratio of the absolute spectral power to the total power in the signal.

Statistical analysis

Statistical analyses were performed based on the a priori hypotheses. Based on the first hypothesis, whether differences exist in the activity of visual areas between blind and sighted children was investigated, as well as whether these differences become more significant with age. Therefore, in the first analysis, the effect of age and visual impairment on spectral activity in the occipital area was tested, measured as the average spectral activities in O1, Oz and O2 electrodes. For each spectral band, an independent ANOVA with relative band power as the dependent variable and group (i.e., BSI or S) and age bin (i.e., [0-3)Y, [3-6)Y or [6-11)Y) as between-subject factors was performed. Post-hoc comparisons were also computed using unpaired two-tailed t-tests, retaining significant comparisons with $p < 0.05$ after a Bonferroni correction.

As per the second hypothesis, whether differences in spectral activity between blind and sighted children are primarily associated with visual areas was tested. The spectral activity across the entire scalp for each spectral band and age bin between the BSI and S groups was compared. Unpaired two-tailed t-tests were conducted for each electrode, considering significance at $p<0.05$ after FDR correction for all electrodes.

According to the third hypothesis, whether blindness affects the overall EEG spectrum was examined, including the shift of the alpha peak and activity at lower frequencies. The peak frequency of background EEG activity (Freeman, 2004) for each participant was measured using a three-stage approach to investigate the shift of the alpha peak. First, the peak was identified in the raw spectrum. Then, the peak was identified in the spectrum after detrending using an exponential decay function. Both in the raw and detrended spectrum, the *findpeaks* function of the *pracma* package (Borchers, 2019) for R (R Core Team, 2021) was used to automatically identify peaks in the background. Finally, the automatic peak estimates from the first two stages were compared to select the most reliable peak position through visual inspection. Changes in peak frequency were assessed using ANOVA, with group and age bins as between-subject factors. Post-hoc comparisons were conducted using unpaired two-tailed t-tests, considering significance at $p<0.05$ after Bonferroni correction.

To test the fourth hypothesis, it was examined whether lack of vision leads to motor difficulties. Therefore, the existence of a specific association of these dysfunctions with the activity of visual area was investigated. To do that, the association between the spectral activity and specific clinical scores that reflect motor dysfunction – namely motor coordination impairment (MCI) and hypotonia – was measured in the BSI group using logistic regression models. This model can predict the likelihood of MCI and hypotonia based on EEG band power for each age bin.

2.1.2 Results

This study measured alpha activity at rest in 60 BSI and 66 sighted S children ranging in age from 20 days to 11 years, subdivided into three age bins. It shows that BSI children manifest posterior alpha activity during the first three years of life, although weaker and slower developing than sighted participants. The first great differentiation between blind and sighted subjects occurs between 3 and 6 years of age. Starting from this period, lower alpha activity increases the probability of motor impairment in blind children. In the following paragraphs, I present the specific results for each hypothesis.

Neural activity differences between blind and sighted increase with age

The first finding of this study evidences that there is a difference between blind and sighted children in the alpha activity of the occipital area, which is crucially related to visual processes. This difference is weak at birth and increases with age. Moreover, within the alpha rhythm, the first sub-band showing differences between groups is alpha1, starting from the first years of life, while alpha2 diverges later at 6 to 11 years of age (see Figure 2.1.). Figure 2.1.A. shows the occipital alpha1 relative power compared at different ages. A significant interaction occurs between the group and age bin ($F(2,120)=3.94$, $P=0.02$, $\eta p2=0.13$). Specifically, S children have stronger alpha1 activity at all ages relative to BSI children, and the gap between groups increases with age ([0-3)Y: $t(34)=3.22$, $P=0.008$, (Cohen's) $d=1.08$; [3-6)Y: $t(39)=2.9$, $P=0.02$, $d=0.91$; [6-11)Y: $t(47)=4.76$, $P=0.00006$, $d=1.37$). Moreover, in BSI children, alpha1 activity increases from the youngest to the middle age bin, ($t(36)=3.15$, $P=0.01$, $d=1.02$) but not from the middle to the oldest age bin ($t(39)=0.52$, $P=0.5$, $d=0.16$). Conversely, alpha1 of S children increases both from the youngest to the middle ($t(37)=3.45$, $P=0.004$, $d=1.12$ and from the middle to the oldest age bin ($t(47)=2.50$, $P=0.04$, $d=0.72$). Figure 2.1.B. shows occipital alpha2 relative power for each age bin. Also, occipital alpha2 exhibits a significant interaction between group and age bin ($F(2,120)=3.65$, $P=0.03$, $\eta p2=0.47$). BSI and S groups have similar alpha2 activity in the youngest ($t(34)=2.23$, $P=0.1$, $d=0.74$) and middle ($t(39)=0.5$, $P=1$, $d=0.16$) age bins. In the oldest age bin, S children have higher alpha2 than the BSI group ($t(47)=2.82$, $P=0.02$, $d=0.81$). Within the BSI group, alpha2 behaves similarly to alpha1, increasing from the youngest to the middle ($t(36)=2.91$, $P=0.02$, $d=0.94$), but not from the middle to the oldest age bins ($t(39)=0.72$, $P=0.5$, $d=0.23$). In S children alpha2 increases both from the youngest to the middle ($t(37)=2.82$, $P=0.02$, $d=0.91$) and from the middle to the oldest age bins ($t(47)=2.92$, $P=0.02$, $d=0.84$).

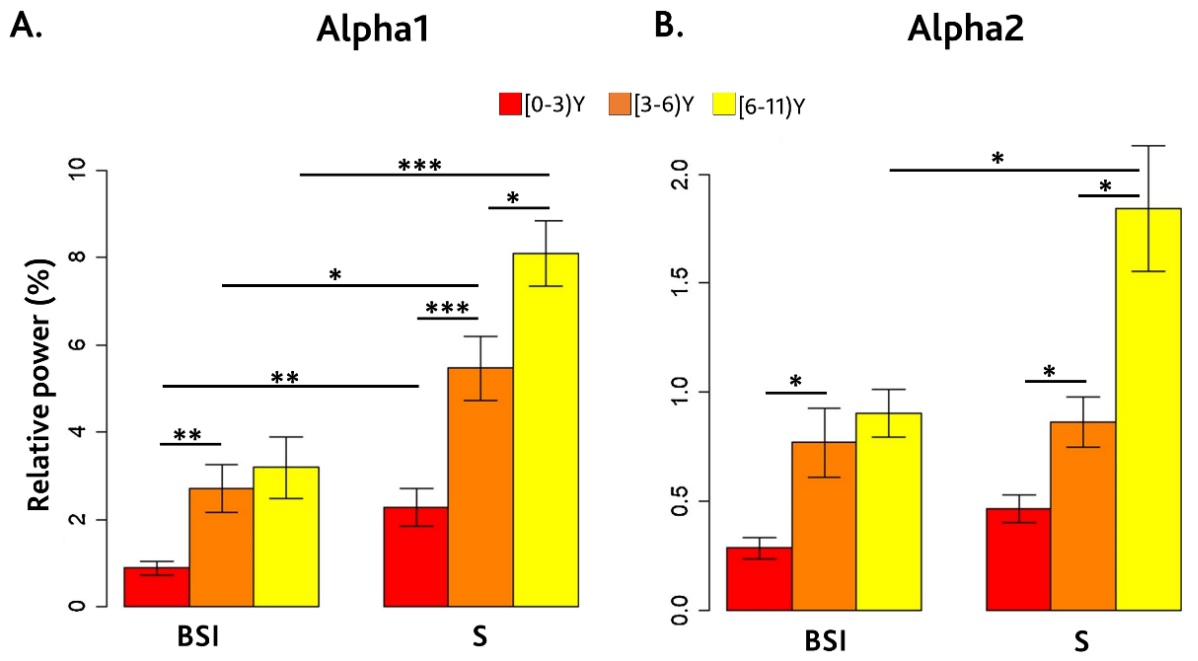

Figure 2.1. Relative alpha power in the Occipital area. *A. Relative power of alpha1 activity (8-10) Hz in Occipital area (O1, O2 electrodes) of blind/severely impaired (BSI) compared with sighted (S) children. Bars represent means, and error bars represent standard errors in means (sem). B. Relative power of alpha2 activity (10-13) Hz in the Occipital area of BSI compared with S children. In both figures, different colors represent different age bins.*

Considering other typical EEG frequency bands, a significant interaction between group and age-bin for the occipital delta2 relative power was found ($F(2,120)=3.60$, $P=0.03$, $\eta p2=0.1$), with an opposite trend with age respect to the alpha band (Figure 2.2.). Specifically, the two groups show similar delta2 activity in the youngest age-bin ($t(34) = 0.50$, $P = 1$, $d = 0.17$), while at older age-bins S children have lower delta2 activity with an increased difference with age ([3-6)Y: $t(39)=2.64$, $P=0.03$, $d=0.83$); [6-11)Y: $t(47)=5.46$, $P=0.000005$, $d=1.57$). Indeed, delta2 does not change with age in the BSI group, both from the youngest to the middle age-bins ($t(36)=1.88$, $P=0.2$, $d=0.61$), and from the middle to the oldest age-bins ($t(39)=0.18$, $P=0.5$, $d=0.06$). Instead, it decreases in S children both from the youngest to the middle ($t(37)=2.90$, $P=0.02$, $d=0.94$) and from the middle to the oldest age-bins ($t(47)=3.03$, $P=0.01$, $d= .87$).

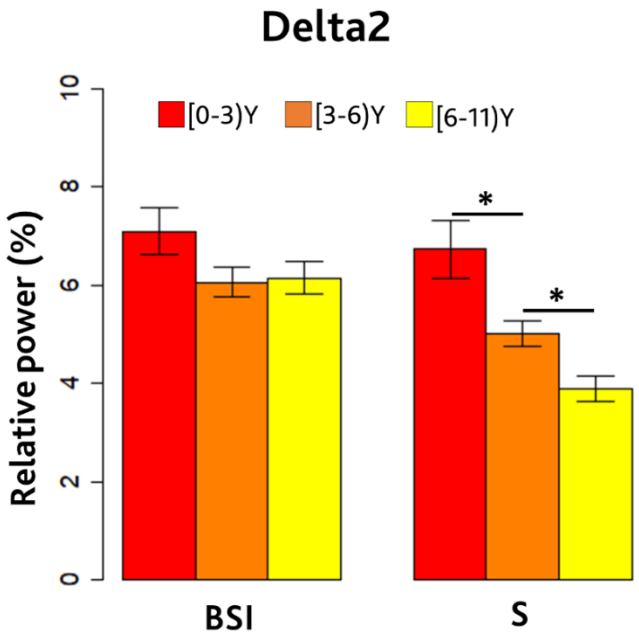

Figure 2.2. Relative delta2 power in the Occipital area. *The relative power of delta2 activity (2-4) Hz in Occipital area (O1, O2 electrodes) of blind/severely impaired (BSI) compared with sighted (S) children. Bars represent means, and error bars represent standard errors in means (sem). Different colors represent different age-bins*

Neural activity differences between blind and sighted increase with age

In the second analysis, the entire scalp was examined, showing that the spectral differences in brain activity between blind and sighted children are specifically ascribable to the activity of visual areas, while activity in other areas is not significantly affected during the earliest stages of life. Figure 2.3. presents the significant ($p<0.05$ after FDR correction) comparisons (non-significant differences in green) using a topographic map for each age bin (columns), frequency bands (alpha1, alpha2, and delta2, see rows), and group. Differences are primarily located in the occipital areas. They specifically involve the alpha1 band for the middle age bin, while in the oldest age bin, differences are greater and tend to involve a larger scalp area and different bands.

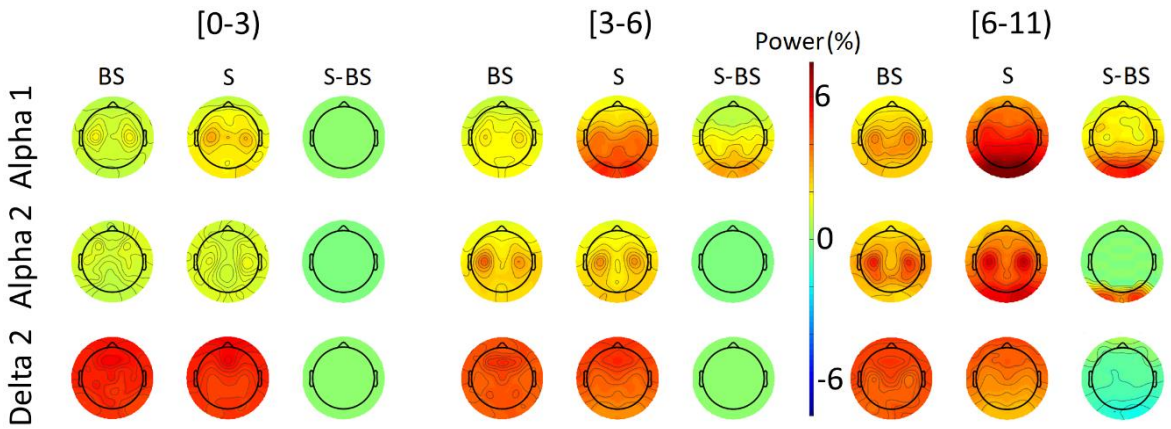

Figure 2.3. Spectral power on the entire scalp. *Topographic maps of alpha1, alpha2, and delta2 relative power compared between groups. For each age bin, the first column represents the BSI group, the second represents the S group, and the third represents the significant difference ($p<0.05$ after FDR correction) between groups. Green areas correspond to non-significant differences, reddish areas to S > BSI, and bluish regions to S < BSI.*

Whole spectrum differences

In agreement with the third hypothesis, results evidence that the lack of vision also affects the EEG spectrum at a global level. Indeed, the spectral composition of the EEG varies with age and marks typical brain development (Anderson and Perone, 2018; Eisermann et al., 2013; Gasser et al., 1988; Miskovic et al., 2015). Specifically, blindness causes both a slower shift of the alpha peak and slower decay of activity at a lower frequency. Figure 2.4. provides an overview of how the entire spectrum evolves with age in both groups. In sighted individuals, as they grow older, the background brain activity tends to shift towards higher frequencies, becoming more noticeable with sharper and more pronounced peaks. In the youngest age group, the background activity exhibits two components: one around 4.5 Hz and another around 8.5 Hz. The power at lower frequencies progressively decreases with age. However, in BSI children, the shift in background activity towards higher frequencies is slower, and the power is reduced. Additionally, BSI individuals show a strong over-representation of low frequencies compared to sighted participants while maintaining similar power across all age groups. In both groups, the two alpha components observed in the youngest age group merge as age increases, resulting in a single prominent peak within the conventional alpha band observed in adults.

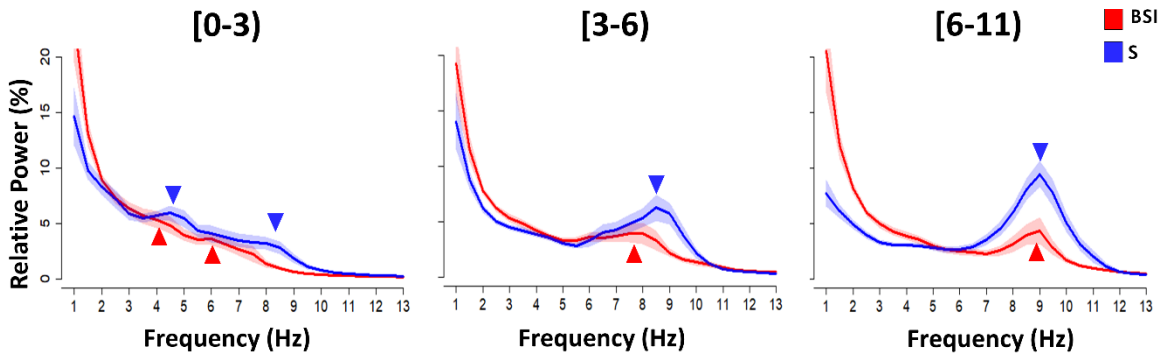

Figure 2.4. The whole power spectrum evolution. *Whole spectrum for each group and age bin. Lines represent mean and shadowed areas sem. Triangles indicate background activity peaks.*

The ANOVA on peak frequencies of background activity revealed a significant interaction between group and age bin ($F(2,113)=7.37$, $P=0.001$, $\eta_p^2=0.12$). In S children, peak frequencies increased from the youngest to the middle ($t(38)=5.63$, $P<0.001$, $d=1.71$) and from the middle to the oldest age bins ($t(47)=2.55$, $P=0.04$, $d=0.93$). In turn, BSI individuals maintain the same peak frequencies with age (youngest to middle: $t(32)=0.10$, $P=0.5$, $d=0.05$; to the oldest age bin: $t(33) = 1.11$, $P = 0.05$, $d = 0.36$). Accordingly, compared with BSI individuals, the peak frequencies of S group were lower in the youngest age bin ($t(33)=-2.23$, $P=0.048$, $d=0.69$), although differences are just barely hinted, and higher in the middle ($t(37)=2.77$, $P=0.01$, $d=0.97$) and for the oldest age bins ($t(43) = 2.30$, $P=0.04$, $d=0.79$).

Association with motor dysfunctions

In the final analysis, motor dysfunctions in blind children seem to be associated with the alpha activity in the visual areas. Specifically, Logistic Regression Models revealed significant associations between alpha activities and clinical examination scores. Figure 2.5. displays that, for the [3-6) years age-bin, a lower relative alpha1 activity is associated with an increased probability of both motor coordination impairment (MCI, $\chi2(1)=12.99$, P=0.0003, Accuracy=0.91), and hypotonia ($\chi2(1)=8.96$, P=0.003, Accuracy=0.88). Similarly, in the [6-11) years age bin, lower alpha1 and alpha2 activity is associated with increased probabilities of MCI and hypotonia (alpha1: MCI: $\chi2(1)=8.38$, P=0.004, Accuracy=0.83; hypotonia: $\chi2(1)=10.89$, P=0.001, Accuracy=0.88; alpha2: MCI: $\chi2(1)=12.79$, P=0.0004, Accuracy=0.90; hypotonia: $\chi2(1)=17.62$, P=0.00003, Accuracy=0.95). Alpha2 activity emerges as the strongest predictor for clinical scores. Models using age as a predictor variable did not yield significant results.

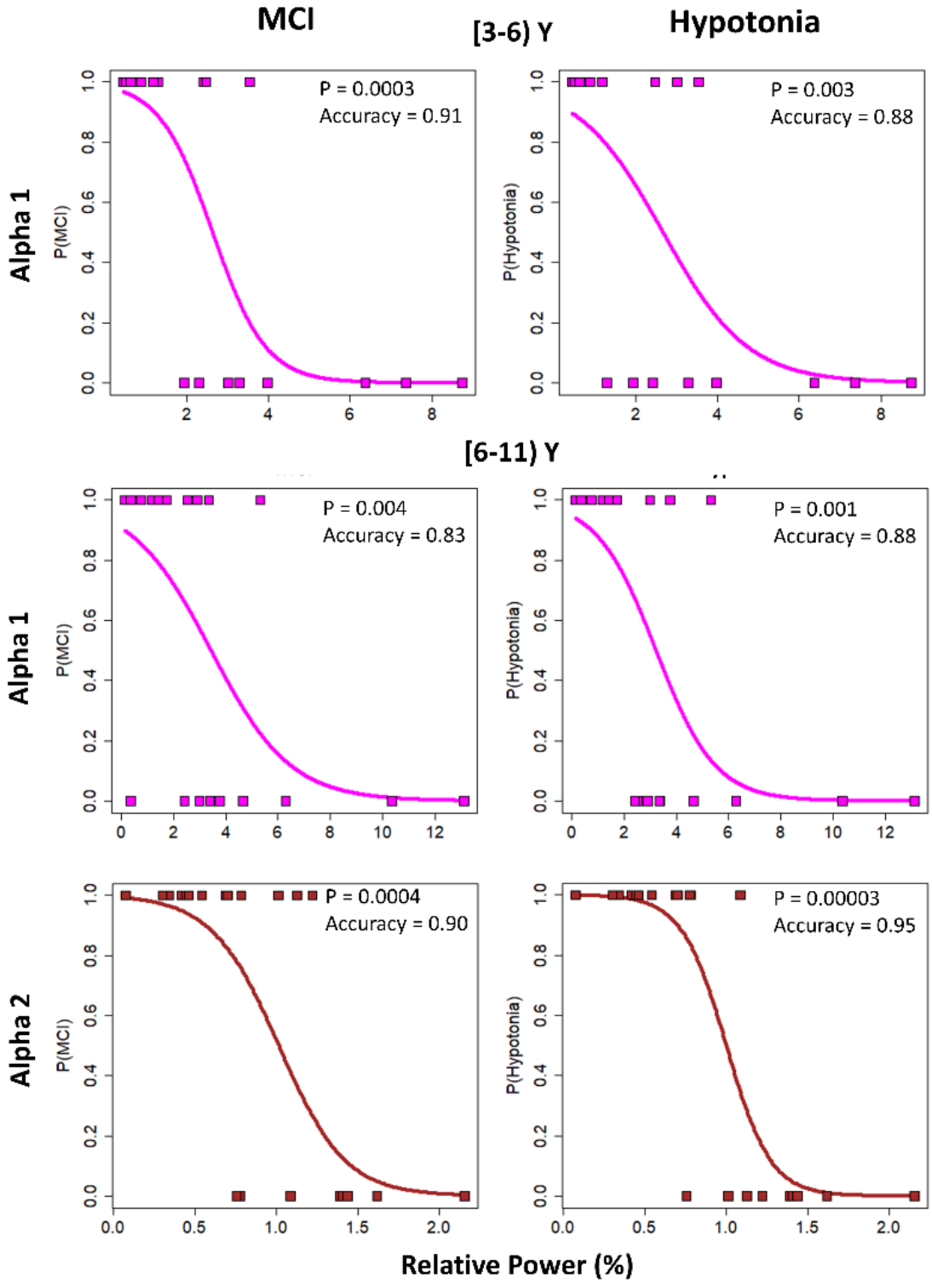

Figure 2.5. Association with clinical scores. *Results of the Logistic Regression models for the [3-6) and [6-11) years age bin. The curve represents the probability of altered clinical findings (motor coordination impairment and hypotonia) as a function of relative power. Each square represents the values of a single subject.*

2.1.3 Discussion of results

The current study investigates spectral activity development in sighted and blind children to shed light on the effect of visual deprivation on the evolution of brain rhythms during childhood. To understand how reduced visual experience influences the EEG spectra during development, I adopted two complementary approaches, integrating the fixed and shifting bands hypotheses, described extensively in Chapter 1. The first analysis focused on the evolution of occipital activity in the conventional frequency bands. Meanwhile, my third analysis assessed how vision, relative to age, influences the entire EEG spectrum in the occipital area, especially the peak of background activity. These two approaches show similar parallel results, and rather than being in opposition, they seem to coexist. Both the first and the third analyses identify differences, progressively increasing with age, between blind and sighted children both in terms of increasing alpha activity and decreasing low frequencies. Moreover, the spectrum analysis reveals that two distinct peaks in the EEG spectra can be observed in the youngest age bin. One peak aligns with the standard alpha band across all age groups, supporting the fixed band hypothesis. The other peak, stronger and shifting towards higher frequencies with age, merges more with the first peak as individuals grow older, aligning with the classical shifting band hypothesis. This suggests a compatibility between the two approaches.

These two analyses also agree with the mechanisms generating alpha rhythm develop similarly in the early years of life for blind and sighted children, suggesting that visual deprivation may partially suppress or alter alpha activity later in childhood. Specifically, the major difference appears in the age range between 3 and 6 years. This period is extremely important, as it is fundamental for children's development. During this stage of life, children begin kindergarten, enhance their language abilities, and initiate social interactions with peers. This phase is characterized by increased social and perceptual stimuli, which play a pivotal role in the refinement of visual functions such as visual acuity and visual evoked potentials (Lenassi et al., 2008), as well as multisensory integration in complex tasks (Mix et al., 1996), visuospatial and visuomotor processes (Freier et al., 2017; James and Kersey, 2018; Maffongelli et al., 2019; Moll et al., 2013; Schipke et al., 2012). Notably, the findings of this study reveal that differences in alpha activity between blind and sighted children first emerge in the alpha1 sub-band, followed by alpha2, indicating that visual deprivation primarily impacts attention-related neural processes and only later alters processes related to semantics and memory. From the shifting band hypothesis perspective, I can speculate that the slower shift results in an initial difference in the alpha1 frequency, followed by a subsequent one in the alpha2 sub-band.

The analysis of the topographical distribution of spectral power over the whole scalp shows that these differences between blind and sighted children are attributable to the activity of the visual area since the occipital region is mainly involved. This is of interest when I consider the associations with motor dysfunctions. Indeed, lower alpha activity in

blind children heightens the likelihood of both motor coordination impairment and hypotonia. This supports the speculation that a perceptual deficit resulting from a lack of vision can reduce a person's capacity to interact with their external environment, with potentially negative consequences for motor development over time. This speculation is supported by the idea that alpha activity plays a fundamental role in the functional inhibition of task-irrelevant areas, allowing for the correct allocation of resources (Jensen and Mazaheri, 2010). Inadequate development of this inhibitory network could lead to a broader range of disorders with growth. However, it is still also possible that a common factor underlying both visual processing differences and sensorimotor abilities could be at play. Thus, both occipital visual processing and motor difficulties could be due to a broader common experiential factor of visual deprivation (i.e., visual deprivation could lead to different visual processing, and it could also lead to impoverished motor experience). In agreement with previous results, the regression findings indicate that this association primarily emerges in the [3-6)Y age group, involving only the alpha1 band, before extending to include the alpha2 band in the [6-11)Y age group.

In conclusion, the results of this study provide important points of discussion about the brain mechanisms associated with alpha activity generation and that are affected by visual deprivation, which will be better addressed in the general discussion in Chapter 5. In the next section, I investigate the sleep counterparts of brain rhythms development related to sensory processing.

The reported data have been partially extracted and adapted from *Campus C, Signorini S, Vitali H, De Giorgis V, Papalia G, Morelli F, and Gori M. Sensitive period for the plasticity of alpha activity in humans (2021). Dev Cogn Neurosci.* Figures were reproduced with permission.

2.2 Exp.2: Sleep differences in children with and without visual impairment

Sleep research in blind children is lacking (Vitali et al., 2022), although recent studies provide new evidence (Adhikari et al., 2023; Ingram et al., 2022). The first findings about sleep in blind children focused on sleep-wake cycle disorders because results in adults with visual impairments show that they often present a disrupted sleep pattern. This disruption can lead to non-24-hour sleep-wake disorder (N24SWD), where the sleep-wake cycle does not align with the 24-hour day. It is rare in standard clinical practice but affects approximately 72.2% of blind patients (Aubin et al., 2016; Dirks et al., 2019). This condition influences daily activities, mood, and overall well-being. However, unlike adults, circadian disturbances appear to be rare in children and adolescents born completely blind (Hartley et

al., 2018). It is hypothesized that structured routines imposed by parents and educators, such as regular meals, work patterns, and physical activity, may act as alternative synchronizers for blind children, promoting a more regular sleep-wake cycle (Tahara et al., 2017). The loss of these patterns in independently living adults could contribute to the development of circadian disorders.

Despite the absence of circadian disorders, blind children often experience lower sleep quality compared to sighted children, as well as higher sleep complaints (Adhikari et al., 2023; Fazzi et al., 2008; Hayton et al., 2021; Ingram et al., 2022; Leger et al., 2002, 2001, 1999). For example, a questionnaire-based study involving 156 children (77 blind) aged between 3 and 18 years showed that 17.4% of blind children (against 2.6% of controls) have reported sleeping less than 7 hours a night, and 13.4% of blind children (vs. 1.3% of controls) have daily episodes of involuntary sleepiness (Leger et al., 1999). Additionally, increased difficulty falling asleep in childhood is common among blind children (Fazzi et al., 2008; Leger et al., 2001, 1999). Another study shows that a large majority (89%) of visually impaired children have clinically significant sleep problems, as indicated by elevated scores on the Children's Sleep Habits Questionnaire, compared to normative data (Ingram et al., 2022). In addition, differences in the sleep macrostructure are also reported. Specifically, blind children have lower total sleep time (TST) and sleep efficiency (Adhikari et al., 2023; Leger et al., 2002, 2001). Moreover, sleep latency is increased, and REM sleep is disturbed (with longer latency, the percentage decreases).

Conversely, none of the studies investigates their sleep microstructure, leaving unrevealed which neurophysiological mechanisms could be impacted by visual deprivation. Indeed, the investigation of specific sleep patterns could provide further insights. For instance, sleep spindles are a marker of the role of sleep in brain development and in sensory information processing, mirroring the activity of the thalamocortical loop (Fernandez and Lüthi, 2020; Halassa and Kastner, 2017; Steriade, 1999; Steriade et al., 1985). Indeed, while people sleep, the sensory information acquired during daily activities is reprocessed and consolidated (Fernandez and Lüthi, 2020; Fogel and Smith, 2011; Gruber and Wise, 2016). Sleep-dependent neuromodulation promotes local effects on specific sensory systems and global effects on overall nervous system function, fostering brain plasticity and sensory neurodevelopment (Blumberg et al., 2022; Brzosko et al., 2019; Jones, 2020). Studies on monocular deprivation show that visual plasticity modulates spindles spectral activity (Aton et al., 2013; Menicucci et al., 2022), suggesting that congenital visual deprivation from birth may influence their generation due to a plastic reorganization of the sleep brain networks.

Spindles can be subdivided into slow (10–13Hz) and fast (13–16Hz), as described in Chapter 1, each associated with different functions. Specifically, fast spindles oscillate in the high-sigma band, prevail in the central region, and are associated with sensorimotor processing (e.g., visuomotor performance, motor functioning, and motor learning), which is affected by visual deprivation (Barakat et al., 2011; Chatburn et al., 2013; Jaramillo et al., 2023; Schabus et al., 2007; Tamaki et al., 2008). Therefore, given the strong association with

sensorimotor processing, I hypothesize that fast spindle development may be specifically impacted in blind children.

Therefore, this study investigates whether blindness may influence sleep microstructure, specifically sleep spindles. My analyses focus on three potential spindle biomarkers and their associations with clinical indices: the spatial spindle-frequency distribution on the scalp, spindle characteristics, and spindles' event-related spectral perturbation (ERSP).

2.2.1 Methods

Participants

Sleep EEG recordings for 114 children were included in the study; 50 participants were blind or severely visually impaired (BSI), and 64 were sighted (S). Both groups were subdivided into two age bins: the first bin included children from 5 months to 3 years and had 27 BSI (13 F, mean age = 1.65, sd=0.71) and 28 S (13 F, mean age = 1.58, sd=0.80); the second bin had children from 3 to 6 years and included 23 BSI (16 F, mean age = 4.46, sd=0.85) and 36 S (12 F, mean age = 4.40, sd=0.87). A t-test was performed between the BSI and S groups' ages for each age bin. They were non-significant for both the 0-3 ($t(53)=0.36$, $P= 0.72$, 95% CI=[-0.34, 0.48]y) and the 3-6 ($t(57)=0.30$, $P= 0.80$, 95% CI=[-0.40, 0.52]y) age-bins. However, considering the maturational changes known to happen in the first decade of life, like cortical rewiring, further analyses were performed considering age as a continuous predictor. The analyses provided results that supported the adopted age bin subdivision. Table 2.2 presents details about the BSI group. The inclusion and exclusion criteria were similar to the previous experiment.

Code	Biological Sex	Age (Y)	Degree of visual impairment	Diagnosis
001	M	0.37	totally blind	Inherited congenital retinal dystrophy
002	M	0.43	totally blind	Optic nerve hypoplasia
003	M	0.85	severely impaired	Ocular albinism
004	F	0.88	totally blind	Eye maldevelopment
005	M	1.02	totally blind	Inherited congenital retinal dystrophy
006	M	1.11	severely impaired	Nystagmus
007	F	1.19	severely impaired	Nystagmus
008	F	1.21	totally blind	Inherited congenital retinal dystrophy
009	M	1.23	totally blind	Inherited congenital retinal dystrophy
010	F	1.32	totally blind	Inherited congenital retinal dystrophy
011	F	1.32	totally blind	Inherited congenital retinal dystrophy
012	M	1.43	totally blind	Inherited congenital retinal dystrophy
013	F	1.45	totally blind	Nystagmus
014	F	1.46	totally blind	Retinopathy
015	F	1.59	severely impaired	Inherited congenital retinal dystrophy
016	F	1.64	totally blind	Inherited congenital retinal dystrophy

017	M	1.76	totally blind	Inherited congenital retinal dystrophy
018	M	1.81	totally blind	Inherited congenital retinal dystrophy
019	F	1.99	totally blind	Inherited congenital retinal dystrophy
020	M	2.14	severely impaired	Inherited congenital retinal dystrophy
021	F	2.28	severely impaired	Eye maldevelopment
022	M	2.41	totally blind	Inherited congenital retinal dystrophy
023	F	2.61	totally blind	Ocular albinism
024	M	2.66	severely impaired	Eye maldevelopment
025	F	2.71	severely impaired	Inherited congenital retinal dystrophy
026	M	2.72	severely impaired	Inherited congenital retinal dystrophy
027	M	2.92	totally blind	Eye maldevelopment
028	F	3.34	severely impaired	Nystagmus
029	F	3.50	totally blind	Inherited congenital retinal dystrophy
030	F	3.61	totally blind	Inherited congenital retinal dystrophy
031	M	3.62	severely impaired	Eye maldevelopment
032	F	3.65	severely impaired	Nystagmus
033	F	3.70	totally blind	Eye maldevelopment
034	F	3.75	severely impaired	Inherited congenital retinal dystrophy
035	F	3.76	totally blind	Inherited congenital retinal dystrophy
036	F	3.79	totally blind	Inherited congenital retinal dystrophy
037	M	3.82	severely impaired	Optic nerve hypoplasia
038	M	4.18	severely impaired	Inherited congenital retinal dystrophy
039	M	4.23	totally blind	Inherited congenital retinal dystrophy
040	F	4.55	totally blind	Inherited congenital retinal dystrophy
041	M	4.71	severely impaired	Inherited congenital retinal dystrophy
042	F	4.88	totally blind	Optic nerve hypoplasia
043	F	4.92	severely impaired	Optic nerve hypoplasia
044	F	5,00	severely impaired	Optic nerve hypoplasia
045	F	5,01	totally blind	Inherited congenital retinal dystrophy
046	F	5,28	totally blind	Inherited congenital retinal dystrophy
047	M	5,58	severely impaired	Inherited congenital retinal dystrophy
048	F	5,58	totally blind	Inherited congenital retinal dystrophy
049	F	5,99	totally blind	Inherited congenital retinal dystrophy
050	M	6,01	totally blind	Inherited congenital retinal dystrophy

Table 2.2. Clinical details of the blind group. *The table shows identification code, the biological sex, age expressed in decimal years (i.e., age in days/365), the degree of visual impairment, and the diagnosis. Different colors represent different age bins.*

Data acquisition and preprocessing

Daytime naps were recorded with a 512Hz sampling frequency using a Nicolet Video-EEG 5.94 system. The recordings included EEGs from 19 derivations following the International 10-20 System (Mecarelli, 2019), and further polygraphic channels included ECG, pneumogram (PNG), EMG, and electrooculogram (EOG), depending on the children's compliance. Along with their parents (or legal guardians), the participants arrived at the laboratory at their scheduled time and were prepared for the EEG recording. Then, the

children were placed in a dark, silent, and comfortable room while an expert EEG technician continuously monitored their state. Starting from the first drowsiness period that appears on the EEG trace, the participant had 50 minutes of sleep possibility.

Sleep scoring and the pre-processing analysis were performed offline. Specifically, The sleep recordings were processed using EEGLAB (Grandchamp and Delorme, 2011) and Hume (https://github.com/jsaletin/hume) software. Any missing or artifacted electrodes were interpolated. The EEG was filtered using a notch (50+-5 Hz) and a band-pass filter between 0.16 and 100 Hz; in turn, it was subsampled to 256 Hz and re-referenced to the average of all the electrodes. Data were scored for sleep stages using 30-s epochs in accordance with the AASM manual criteria (Berry et al., 2020).

Data were subsequently pre-processed to examine both macro- and micro-structural sleep aspects. The macrostructural analysis involved the examination of sleep statistics and spectrograms. Spectrograms were computed by dividing each scoring page into 6 non-overlapping 5-second segments. The power spectral density (PSD) was then calculated for each segment using the *Pwelch* function, averaging across segments within each 30-second epoch. The power of sigma and delta frequency bands was measured for each 30-second epoch and normalized to the mean power of total sleep time (TST). The microstructural analysis focused on sleep spindles. The detect spindles EEGLAB plug-in (Ray et al., 2015) was employed to automatically detect the sleep spindles (10-16Hz) using a minimum duration threshold of 0.5 seconds. The spindle events on the Frontal (F3, F4, Fz) and Central (C3, C4, Cz) electrodes during the N2 and N3 sleep stages were considered. An event-related spectral perturbation (ERSP) in dB of spindle events was also computed. Data were segmented from 1s before to 4s after spindle onset, with the period from -1s to 0s serving as a baseline. ERSP was calculated using the *newtimef* function of EEGLAB. For each participant, the whole time-frequency distribution was extracted from 3 to 32 Hz using a Morlet Wavelet (cycles starting from 3 at the lowest frequency and increasing with a 0.1 factor with frequency). The low-sigma, high-sigma, and the observed clear modulation within the high-beta (25-30Hz) bands were considered. For each band, the mean ERSP was computed within the Frontal and Central ROIs (Region of Interests), while considering the temporal evolution over the whole epoch time course (Figure 2.6.A). Subsequently, I evaluated the ERSP within 1s time-windows from sleep onset to 4s after, considering the ERSP mean for each time-window (Figure 2.6.B).

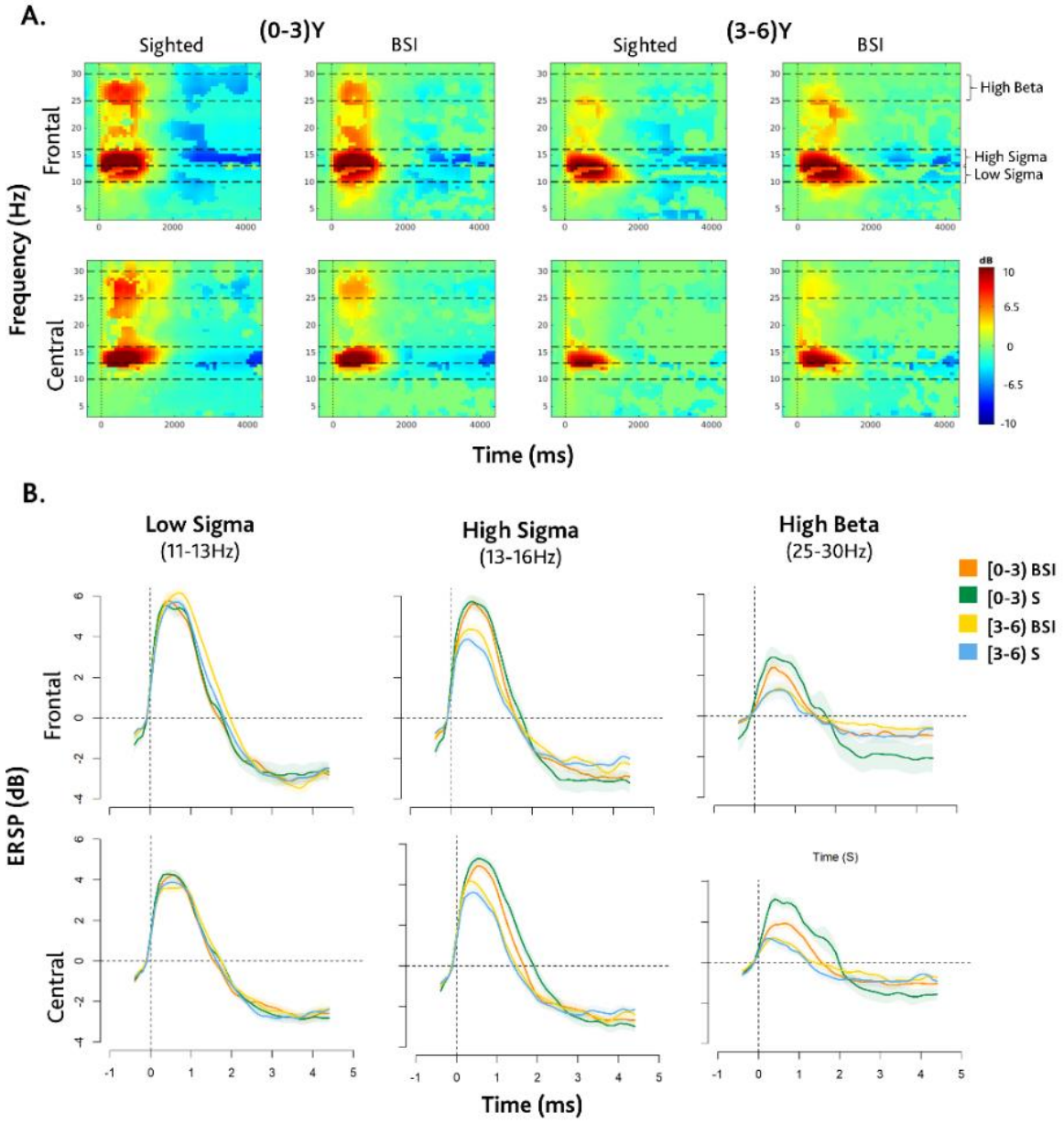

Figure 2.6. ERSP power of sleep spindles. *A) Plot of time-frequency distribution for each group, age-bin, and ROIs. (B) ERSP curve representation of the low-sigma, high-sigma, and high-beta on the Frontal and Central ROIs for each group and age bin.*

Statistical analysis

Statistical analyses were conducted in the R environment (R Core Team, 2021). Linear mixed models (LMMs) were fitted using the *lmer* function of the *lme4* package (Bates et al., 2015). The predictors were evaluated using Type III Wald $\chi 2$ tests, as implemented in the

Anova function of the car package. Where not otherwise specified, the contrasts were further investigated with the *emmeans* function of the *emmeans* package (Lenth, 2022) by obtaining their estimated marginal means (EMMs). Instead, linear models (LMs) were fitted using the *lm* function. The predictors were evaluated using an F test implemented in the *Anova* function of the *car* package (Fox and Weisberg, 2018). The analyses were repeated while considering continuous age to evaluate the maturational effects in more detail. Indeed, it is always suboptimal to dichotomize continuous variables. Thus, the planned contrasts were investigated with the *emtrends* function while considering age as a continuous covariate. All the effects were considered significant when $P<0.05$ after the Bonferroni correction. Following, I show the specific statistical analysis performed for sleep macro- and microstructures.

For the sleep macrostructure, the effects of the groups (S and BSI) and age bin ((0–3)Y, Young and (3–6)Y, Old) were evaluated on the sleep statistics and spectrogram activities in the sigma and delta bands. For the sleep statistics, the TST in minutes and the percentage of stages N1, N2, N3, NREM, and REM on TST were considered. LM was fitted considering each sleep statistic independently as the dependent variable, while group and age bin served as the predictors. Because only a small percentage of participants reached the REM stage, this data was excluded from the subsequent analysis. The delta (0.5-4.75 Hz) and sigma (10-16 Hz) activities were extracted from the spectrogram, normalized, and then averaged separately for N1, N2, and N3. LMM was fitted for each independent band with mean power as the dependent variable and group, age bin, and sleep stage as predictors. According to Wilkinson's notation (Wilkinson and Rogers, 1973), the models fitted were:

Sleep statistics: *Sleep stage ~ group (S/BSI)*age_bin(Young/Old)*

Spectrogram: *Mean_power ~ group(S/BSI)*age_bin(Young/Old)*sleep_stage + (1|participant)*

For sleep microstructures, separate analyses were performed for sleep characteristics and spindle ERSP. Firstly, the mean spindle frequency (SF) was evaluated by fitting an LMM, considering SF as the dependent variable, group and age-bin as the between-subject factors, and ROI as the within-subject factor. Secondly, the characteristics (spindle density in #/min and duration in s) of slow and fast spindles on the separate ROIs were investigated by fitting LMMs considering spindle characteristics as the dependent variables, while the group, age bin, and frequency band as the predictors. The analyses were repeated while considering continuous age to evaluate the maturational effects in more detail. Thirdly, The ERSP modulations were assessed by fitting a LMM model considering the ERSP mean as the dependent variable, while the group, age bin, and time-window ([0-1]s, [1-2]s, [2-3]s, [3-4]s) were evaluated in the LMM. Afterward, we also investigated the peak power within the spindle time-window ([0-2]s) for each frequency band and ROI using the *aov* function to consider the interindividual variability. According to Wilkinson's notation (Wilkinson and Rogers, 1973), the models fitted were:

Mean spindle frequency: *spindle frequency ~ group (S/BSI)*age bin(Young/Old)* ROI(Central/Frontal) + (1| participant)*

Spindles characteristics: *spindle feature ~ group (S/BSI)*age bin(Young/Old)* frequency band(Fast/Slow) + (1| participant)*

Spindles ERSP mean: *ERSP mean ~ time window ([0-1]s, [1-2]s, [2-3]s, [3-4]s)*group (S/BSI)*age bin(Young/Old) + (1| participant)*

Spindles ERSP peak: *ERSP peak ~ group (S/BSI)*age bin(Young/Old)*

The analyses were repeated while considering continuous age to evaluate the maturational effects in more detail.

Finally, a possible association between the neurophysiological biomarkers and the selected clinical indices was examined. First, if the severity of visual impairment (i.e., Sighted (S) =0, Severely Visually Impaired (SVI) =1, and Blind (B) =2) could be predicted from the investigated spindle measures was evaluated, applying ordinal regression models using the *orm* function of the *rms* package. According to Wilkinson's notation (Wilkinson and Rogers, 1973), the models fitted were:

Association with mean spindle frequency: *Visual impairment index ~ group (S/BSI)*age bin(Young/Old)* ROI(Central/Frontal)*spindle frequency*

Association with spindles characteristics: *Visual impairment index ~ age bin(Young/Old)*frequency band(Fast/Slow)*spindle feature(duration/density)*

Spindles ERSP mean: *Visual impairment index ~ time window ([0-1]s, [1-2]s, [2-3]s, [3-4]s)*age bin(Young/Old)* ERSP mean*

Spindles ERSP peak: *Visual impairment index ~ age bin(Young/Old)* ERSP peak*

The analyses were also repeated with continuous age instead of age bins.

Subsequently, in the BSI children only, the spindle biomarkers were related to the specific clinical scores that reflect sensory, environmental interaction, and motor dysfunction: MCI and hypotonia evaluated through neurologic examinations; and social adaptation, spatial exploration, verbal comprehension, and expressive language, measured with subscales of the RZS (Reynell, 1978). Then, to identify more reliable factors, a factorial analysis was performed in which all these indices were included (Drasgow, 2004; Revelle, 2009). This factorial analysis was based on a polychoric correlation matrix. Parallel analysis suggested that 2 clinical factors were most appropriate. The first clinical factor was *environmental interaction*, which accounted for spatial exploration, social adaptation, and language indices. The second clinical factor was *motor disorders*, which accounted for motor coordination impairment and the hypotonia indices. For each clinical factor, the related scores were computed. Then, two extracted factors, instead of the original 6 indices, were used to test their possible associations with electrophysiological biomarkers, fitting linear regression models. According to Wilkinson's notation (Wilkinson and Rogers, 1973), the models fitted were:

Association with mean spindle frequency: *clinical factor ~ group (S/BSI)*age bin(Young/Old)* ROI(Central/Frontal)*spindle frequency*

Association with spindles characteristics: *clinical factor ~ age bin(Young/Old)* frequency band(Fast/Slow)*spindle feature(duration/density)*

Spindles ERSP mean: *clinical factor ~ time window ([0-1]s, [1-2]s, [2-3]s, [3-4]s)*age bin(Young/Old)* ERSP mean*

Spindles ERSP peak: *clinical factor ~ age bin(Young/Old)* ERSP peak*

The analyses were also repeated with continuous age instead of age bins.

2.2.2 Results

This study investigates the hypothesis that the development of fast sleep spindles may be specifically affected in blind children by being strictly associated with sensory information processing. I show here both macro- and micro-structural aspects. Macrostructural analyses did not show significant differences between BSI and S children. Microstructural analyses were focused on three potential spindle biomarkers and their association with clinical indices: spatial spindle-frequency distribution on the scalp, spindle characteristics (density and duration), and spindle ERSP in different ROIs. The findings revealed that BSI children lacked the evolution of developmental spindles within the central area. Specifically, young BSI children presented low central high-sigma and high-beta ERSP and showed no signs of maturational decrease. High-sigma and high-beta activity in the BSI group correlated with clinical indices predicting perceptual and motor disorders. In the following paragraphs, I present the specific results.

Sleep Macrostructure

No relevant differences emerge between the BSI and S children in sleep statistics (see Table 2.3). There is only a small difference in the percentage of N3 ($F(1,107) = 3.94$, $P = 0.049$). Regarding developmental differences, the sleep statistics show an increase in NREM ($F(1,107) = 4.3$, $P = 0.04$) and a decrease in REM sleep ($F(1,107) = 4.3$, $P = 0.04$) in the old age bin compared with the young age-bin, as expected by the typical sleep macrostructural development. In addition, an increase of sigma activity is found during N3 with age, $\chi2(1)=6.69$, $P=0.01$. Considering age bin analysis, no significant differences emerge between the BSI and S children in the spectrogram activity.

Sleep Statistics								
	S		BSI		Group effect		Age bin effect	
	(0-3)Y	(3-6)Y	(0-3)Y	(3-6)Y	F(Dfn,Dfd)	p	F(Dfn,Dfd)	p
TST (min ± se)	43.0 ± 1.4	43.1 ± 1.2	40.4 ± 2.4	40.4 ± 2.2	2.18(1,107)	0.14	0.00(1,107)	0.99
% Stage 1 ± se	17 ± 2.2	20 ± 1.9	20 ± 2.7	19 ± 2.0	0.28(1,107)	0.60	0.19(1,107)	0.66
% Stage 2 ± se	39 ± 2.7	44 ± 2.2	45 ± 13.2	49 ± 3.1	3.18(1,107)	0.08	2.52(1,107)	0.12
% Stage 3 ± se	39 ± 3.5	33 ± 3.4	27 ± 3.7	31 ± 4.2	3.93(1,107)	**0.049*** **(S>BSI)**	0.26(1,107)	0.61
% NREM ± se	95 ± 1.5	97 ± 1.4	92 ± 2.3	98 ± 1.2	0.51(1,107)	0.48	4.3(1,107)	**0.04*** **(O>Y)**
% REM ± se	5 ± 1.5	3 ± 1.4	8 ± 2.3	2 ± 1.2	0.51(1,107)	0.48	4.3(1,107)	**0.04*** **(Y>O)**

Table 2.3. Sleep Macrostructural Statistics. *Results from the macrostructure parameters of the sleep statistics analysis. Significant results are in bold. The meaning of the interaction is stated within brackets; these show the relationships between the sighted (S) and the blind/severely impaired (BSI) groups as well as the 0-3 years and the 3-6 years age-bins.*

The specificity of the central area

Figure 2.6. provides an overview of spindle topography distribution, showing the effects of group, age bin, and ROIs on mean spindle frequency (SF), $\chi 2(1)=99.89$, $P<0.0001$. Fast spindles are mainly localized in the central area, while slow spindles in the frontal area. Indeed, SF is higher in the central than the frontal ROI in all groups and age bins: young S, $Z=11.21$, $P<0.0001$, young BSI, $Z=13.94$, $P<0.0001$, old S, $Z=27.24$, $P<0.0001$, and old BSI group, $Z=22.74$, $P<0.0001$. Additionally, S children show reduction with age in both frontal, $Z=-5.03$, $P<0.0001$, and central, $Z=-3.07$, $P=0.03$, ROIs; this reduction is not evident in BSI children. Continuous age analyses provide evidence of a selective absence of SF maturation in only the central ROI in BSI children. Indeed, the statistic shows a significant reduction with age in both frontal and central ROIs in S children, $Z=-4.6$, $P<0.0001$ and $Z=-3.09$, $P=0.002$, respectively; and only in the frontal region, $Z=-3.50$, $P=0.0005$, in the BSI group. Between-group contrasts provide evidence of significant interaction in the central area, $Z = 2.08$, $P=0.04$.

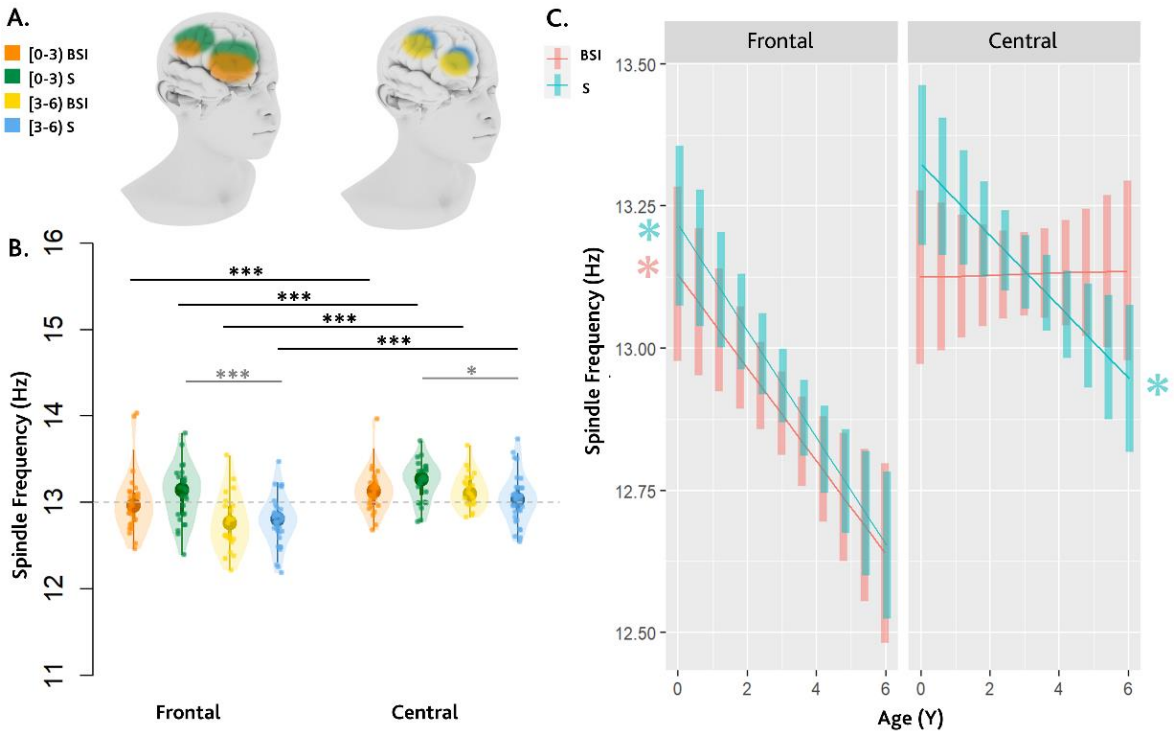

Figure 2.7. Topographical distribution of mean spindle frequency. *(A) The 3D models represent the group differences between the two age bins and the different ROIs. (B) Plot of mean spindle frequency (violin plot), the median (box plot) and related 95% CI (vertical line), and the single subjects spindle frequency (scattered plot) for each age-bin, group, and ROIs. The stars represent the significant p values: The grey stars represent the interactions within the ROIs; the black stars represent the interactions between the ROIs. (C) Plot of the frontal and central spindle frequency evolution considering age as a continue variable.*

Slow and fast spindle evolution

Figure 2.7. shows the changes in the characteristics of slow and fast spindles. BSI children exhibit distinct patterns in spindle duration, $\chi2(1)=125$, $P<0.0001$, and density, $\chi2(1)=11.60$, $P=0.0003$, compared to their S counterparts in the central area. In S children, fast spindles are longer than slow spindles in the young age bin, $Z=19.34$, $P<0.0001$, while slow spindles are longer in the old age bin, $Z=-8.10$, $P<0.0001$. There is a reduction in fast spindle duration between age bins, $Z=-3.3$, $P=0.01$, confirmed by continuous age analysis, $Z=-4.62$, $P<0.0001$. In contrast, BSI children show longer fast spindles in the young age bin, $Z=6.04$, $P<0.0001$, with minimal changes with age. Continuous-age analysis reveals a slight reduction in fast spindle duration with age, $Z=-2.20$, $P=0.03$. Regarding spindle density, fast spindles are denser than slow spindles in young S children, $t(106)=5.4$, $P<0.0001$, while no difference is observed in young BSI children. Maturation with age of both slow and fast spindles is evident only in S children. Fast spindles are denser in the young age bin, $t(212)=-3.1$, $P=0.02$, while slow spindles are denser in the old age bin, $t(212)=3.8$, $P=0.003$. Continuous age analysis confirms that fast spindle density decreases with age in S children,

t(220)=-3.47, P=0.0006, while slow spindle density increases with age, t(220)=4.12, P=0.0001. Contrasts between BSI and S children show significant differences in the development of both slow, t(220)=-3.34, P=0.001, and fast spindles, t(220)=2.20, P=0.03.

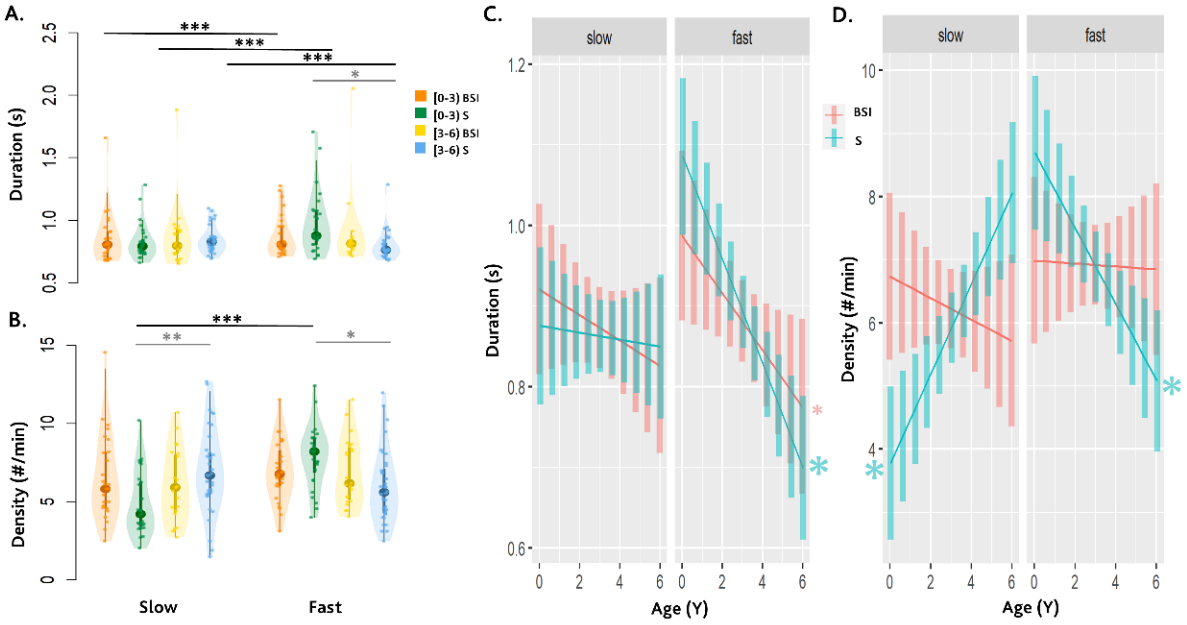

Figure 2.8. Characteristics of slow and fast sleep spindles. *(A)and (B) plot, respectively, the mean spindle duration and density (violin plot), the median (box plot) and related 95% CI (vertical line), and the single subjects spindle duration (scattered plot) for each age-bin, group, and frequency band. The stars represent the significant P values: the grey stars represent the interactions within the spindle frequency band; the black stars represent the interactions between the spindle frequency band. (C) and (D) plot, respectively, the slow and fast-spindles evolution of duration and density considering age as a continue variable. The bigger stars represent a significant P value < 0.001; the small star represents a significant P value < 0.05.*

Slow and fast spindle evolution

ERSP allows us to delve beyond global spindle descriptors, exploring frequency distribution and timing of activation during spindle events. Indeed, a preliminary visual inspection of spindle ERSP sometimes indicates increased high-beta power (Figure 2.6). Previous studies reported concurrent high-frequency activity with spindles in animals (Averkin et al., 2016) and humans (Clemens et al., 2011). Only one presented evidence of a concurrent component time-locked to the spindle, spanning from ~ 24 to 30 Hz, in the centro-parietal areas (Laventure et al., 2018). Thus, the analysis was extended to explore this frequency band. Using LMMs, the effects of age and group on mean ERSP were evaluated separately for each ROI in 1-second time windows from 0 to 4 seconds after spindle onset. Differences between age groups and between BSI and S children are evident in the high-sigma and high-

beta bands in the central area, as Table 2.4 shows. Specifically, young S children exhibit higher activity than their BSI peers in the high-sigma band in the second time window, and this difference persists in continuous age analysis, including both spindle time windows. Moreover, power is significantly higher in young compared to older S children, while a developmental difference is almost absent in BSI children. Similarly, the high-beta band power is higher in young than in old S children, while no developmental differences were found in the BSI children. These effects also persist with continuous age.

		Low Sigma				High Sigma				High Beta			
Mean ERSP Age-bin *Mean frequency ~ time window*group*age bin + (1|subject)*													
		χ^2(Df)		**p**		**χ^2(Df)**		**p**		**χ^2(Df)**		**p**	
time_window*group*age_bin		1.46(3)		0.69		9.36(3)		0.02		11.66(3)		0.009	
Post Hoc for each time window													
		[0-1]s		**[1-2]s**		**[0-1]s**		**[1-2]s**		**[0-1]s**		**[1-2]s**	
		t(Df)	**p**	**t(Df)**	**p**	**t(Df)**	**p**	**t(Df)**	**p**	**t(Df)**	**p**	**t(Df)**	**p**
BSI-S contrast	(0-3)Y	-	-	-	-	-	-	-2.87 (377)	0.004	-1.98 (392)	0.048	-2.92	0.004
BSI-S contrast	(3-6)Y	-	-	-	-	-	-	-	-	-	-	-	-
(0-3)Y – (3-6)Y contrast	BSI	-	-	-	-	-	-	2(377)	0.046	-	-	-	-
(0-3)Y – (3-6)Y contrast	S	-	-	-	-	3.62 (377)	0.0003	5.13 (377)	<0.000 1	3.59 (392)	0.0004	3.75 (392)	0.0002
Mean ERSP Age *Mean frequency ~ time window*group*age bin + (1|subject)*													
		χ^2(df)		**p**		**χ^2(df)**		**p**		**χ^2(df)**		**p**	
time_window*group*age		2.17(3)		0.5		9.09(3)		0.03		14.31(3)		0.002	
Post Hoc for each time window													
		[0-1]s		**[1-2]s**		**[0-1]s**		**[1-2]s**		**[0-1]s**		**[1-2]s**	
		t(Df)	**p**	**t(Df)**	**p**	**t(Df)**	**p**	**t(Df)**	**p**	**t(Sf)**	**p**	**t(Df)**	**p**
BSI-S contrast		-	-	-	-	2.04 (384)	0.04	2.59 (384)	0.01	1.91 (393)	0.056	2.21 (393)	0.03
BSI		-	-	-	-	-	-	-2.17 (384)	0.03	-2.07 (393)	0.04	-	-
S		-	-	-	-	-4.64 (384)	<0.0001	-6.46 (384)	<0.0001	-5.31 (393)	<0.0001	-4.66 (393)	< .0001

Table 2.4. Statistics of mean spindle ERSP. *LMM results on Central ROI were reported. Models are expressed with the Wilkinson notation.*

To consider interindividual variability, the effects of group and age on peak power in the spindle time window ([0–2]s) were also investigated, showing similar results in the age-bin and continuous age analysis, as reported in Table 2.5.

		Low Sigma		High Sigma		High Beta	
Peak ERSP Age-bin *Peak frequency ~ group*age bin*							
		F(Dfn, Dfd)	**p**	**F(Dfn, Dfd)**	**p**	**F(Dfn, Dfd)**	**p**
Group*age bin		0.03(1,110)	0.87	4.02 (1,110)	0.047	7.1(1,110)	0.0087
Post Hoc							
		t(Df)	**p**	**t(Df)**	**p**	**t(Df)**	**p**
BSI-S contrasts	(0-3)Y	-	-	-	-	3.65(110)	0.0016
BSI-S contrasts	(3-6)Y	-	-	-	-	-	-
(0-3)Y – (3-6)Y contrasts	BSI	-	-	-	-	-	-
(0-3)Y – (3-6)Y contrasts	S	-	-	-5.06(110)	<0.0001	-5.45(110)	<0.0001
Peak ERSP Age *Peak frequency ~ group*age*							
		F(Dfn, Dfd)	**p**	**F(Dfn, Dfd)**	**p**	**F(Dfn, Dfd)**	**p**
Group*age		2.17(1,110)	0.87	6.66(1,110)	0.011	7.57(1,110)	0.0069
Post Hoc							
		t(Df)	**p**	**t(Df)**	**p**	**t(Df)**	**p**
BSI-S contrast		-	-	2.58(110)	0.011	2.75(110)	0.0069
BSI		-	-	-	-	-	-
S		-	-	-5-32(110)	<0.0001	-5.95(110)	<0.0001

Table 2.5. Statistics of peak spindle ERSP. *LMM results on Central ROI were reported. Models are expressed with the Wilkinson notation.*

Association with clinical scores

Finally, the association between spindle biomarkers and specific clinical indices predicting perceptual and motor disorders was examined, as shown in Figure 2.8. First, the findings reveal that sleep density and spindle ERSP are robust predictors of the visual impairment index (VII). Notably, a significant interaction between spindle frequency band, density, and age bin, $\chi^2(1) = 12.39$, $p=0.0004$, as well as continuous age, $\chi^2(1) = 12.02$, $p=0.0005$, is found. A lower density of fast spindles in the young age bin corresponded to a higher probability of being classified as a blind child, whereas a higher density in the old age bin is associated with a higher likelihood of being classified as a blind child. Conversely, slow spindle patterns exhibit an opposite trend. The SVI group demonstrates a mixed pattern between S and B groups.

Furthermore, significant interactions are observed between age-bin and mean ERSP in both the high-sigma, $\chi^2(2) = 10.51$, $p=0.005$, and high-beta, $\chi^2(2) = 10.31$, $p=0.006$, bands.

These interactions persist when age is considered a continuous variable, showing results of $\chi^2(2)=11.59$, $p=0.003$ and $\chi^2(2)=8.44$, $p=0.01$, respectively. Similarly, significant interactions between age bin and peak ERSP in both high-sigma, $\chi^2(1)=6.99$, $p=0.008$, and high-beta, $\chi^2(1)=4.8$, $p=0.03$, frequency bans. Once again, these interactions are confirmed when considering age as a continuous variable, showing results of $\chi^2(1)=9.91$, $p=0.002$ and $\chi^2(1)=5.17$, $p=0.02$, respectively. From an interpretative point of view, both frequency bands showed a similar behavior as for fast spindle density.

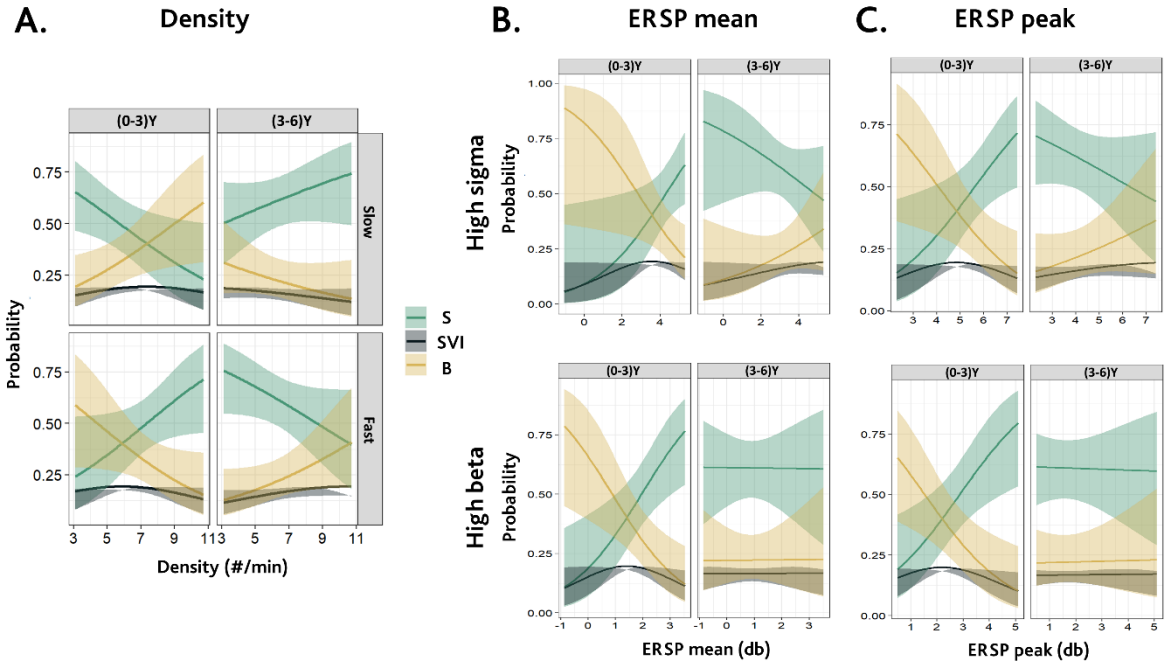

Figure 2.9. Association with clinical indices: Visual impairment index (VII). *Figure (A) shows the association between VII and density. Figure (B) shows the association between VII and ERSP mean. Figure (C) shows the association between VII and ERSP peak. Different colors represent different visual impairments, specifically S=sighted, SVI=Severely visually impaired, and B=blind.*

Regarding the *environmental interaction* and *motor disorders* factors, a trend is observed for the interactions between age-bin, time window, and ERSP mean in the high-sigma band for the *motor disorders*, $F(1,78)=3.7$, $p=0.057$. This trend becomes fully significant when age is considered continuously, $F(1,78)=5.7$, $p=0.02$. Specifically, higher high-sigma activity within the [0-1]s time window in the old age bin is associated with increased motor disorder scores. Finally, a main effect of a high-beta ERSP peak for the *motor disorders* factor is found, $F(1,39)=4.89$, $p=0.03$, which shows a negative association. These results are illustrated in Figure 2.9.

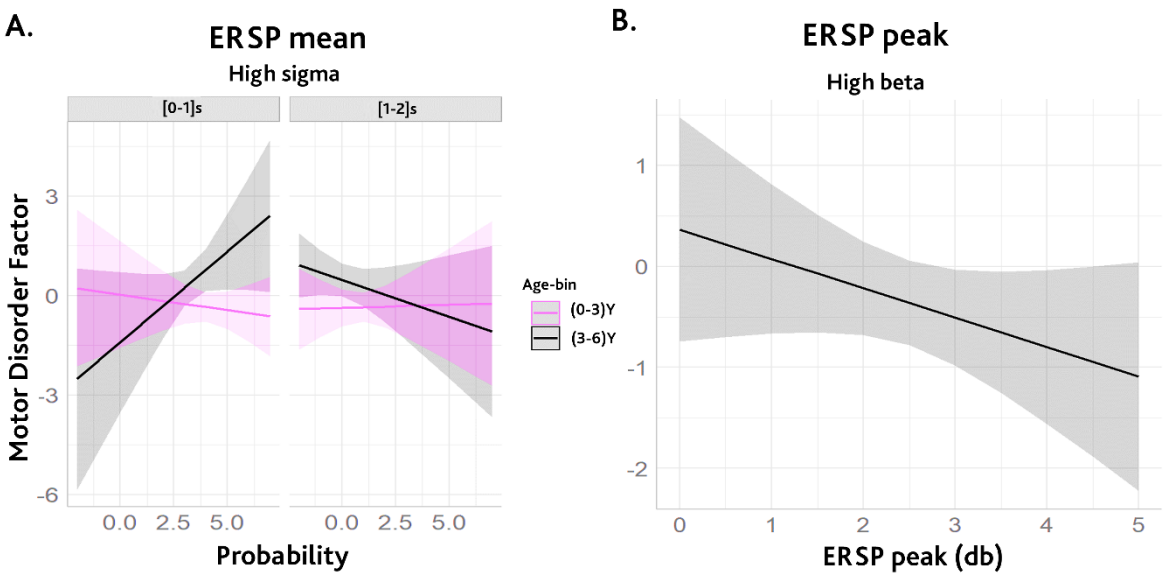

Figure 2.10. Association with clinical indices: Motor disorder factor. *Figure (A) shows the association between the motor disorder factor and ERSP mean results. Different colors represent different age-bin. Figure (B) shows the results of the association between the motor disorder factor and ERSP peak.*

2.2.3 Discussion of results

Spindles are a hallmark of sensory information processing during sleep (Fernandez and Lüthi, 2020; Fogel and Smith, 2011; Gruber and Wise, 2016), and can be a marker of normal or abnormal neurodevelopment. Here, I propose that blindness might trigger brain reorganization, affecting spindle development, and especially fast spindles due to their association with sensorimotor processing (Barakat et al., 2011; Chatburn et al., 2013; Jaramillo et al., 2023; Schabus et al., 2007; Tamaki et al., 2008). The results indicate that blind children show a unique absence of mean spindle frequency reduction in the central region, indicating impaired involvement of the sensorimotor area. Typically, a decrease in mean frequency is present in children between ages 2 to 5 years cause of neural development processes, such as synaptic pruning, that occurs from infancy to adolescence (D'Atri et al., 2018; Kwon et al., 2023; McClain et al., 2016). The absence of frequency reduction in blind children suggests delayed cortical maturation in the central area, possibly due to altered synaptic changes in early life.

These results align with findings on fast spindles and spectral power. Indeed, fast spindle density and duration development are either absent or slight in blind children in the central area. Fast spindles are crucial for sensorimotor (Schabus et al., 2007) and neural processing (Geiger et al., 2011; Lustenberger et al., 2012; Maquet, 2010) and undergo significant changes during early development following the trajectory of cortical growth (Kwon et al., 2023). The lack of spindle evolution in blind children suggests compromised neural

processes essential for optimal brain maturation. Analysis of spindle ERSP similarly showed a specific impact of blindness on high-sigma and high-beta power evolution with age in the central region.

Overall, this study indicates that the typical developmental trajectory of the fast spindles does not occur in blind children, suggesting that vision is extremely important in the proper development of the neural structures underlying brain rhythms. The high frequencies and central regions' selective involvement provide evidence of a strong link with sensory and motor information processing. A recent study demonstrated that fast spindles could be a crucial developmental biomarker in infancy, predicting sensorimotor scores (Jaramillo et al., 2023). Here, I also show that different spindle biomarkers can be good predictors of visual impairment in early life and motor disorders starting from the three years of life. This suggests that the age of three seems critical in delineating developmental differences between blind and sighted children.

Fast spindles and their concurrent beta modulation could serve as important early biomarker in blind children, reflecting early neurophysiological mechanisms and predicting future impairment. This study highlights the importance of investigating the sleeping brain to identify the early biomarkers of developmental divergence in blind children. It provides new insights into how sensory deprivation produces neural divergence from the typical developmental trajectory. In conclusion, Chapter 2 demonstrates the presence of significant neurophysiological mechanisms impacted by visual deprivation with age, both in wakefulness and sleep. These mechanisms may be linked to the same neural networks related to thalamocortical activity, contributing to increasing the knowledge about the influence of blindness on the development of brain structures. Further discussion about the neural mechanisms will be provided in Chapter 5.

The reported data have been partially extracted and adapted from *Vitali H, Campus C, Signorini S, De Giorgis V, Morelli F, Varesio C, Pasca L, Sammartano A, Gori M. Blindness affects the developmental trajectory of the sleeping brain (2024). Neuroimage*. Figures were reproduced with permission.

Chapter 3

Sensory and spatial representation in blind infants

In Chapter 1, I emphasized that vision is the most reliable sense to represent spatial information. Given the role of visual experience, it is conceivable that the absence of vision from birth may interfere with the development of spatial representation. However, research findings regarding spatial performance after visual loss have produced conflicting outcomes.

Historically, investigations into the functioning of the blind brain have predominantly focused on the compensatory capacity of visual areas to process non-visual information (Frasnelli et al., 2011; Kupers and Ptito, 2011; Renier et al., 2014; Sadato et al., 1996). The "sensory compensatory hypothesis" posits that blind individuals exhibit exceptional perceptual abilities in their remaining sensory modalities to compensate for visual deprivation (Miller, 1992). Experimental evidence supporting this hypothesis in the realm of spatial representation includes studies demonstrating enhanced skills among early blind individuals in tasks such as peripheral sound localization in the horizontal plane (Lessard et al., 1998; Röder et al., 1999; Zwiers et al., 2001), cognitive mapping for auditory localization (Fortin et al., 2008; Tinti et al., 2006), tactile spatial acuity (Goldreich and Kanics, 2003; Legge et al., 2008; Van Boven et al., 2000; Wong et al., 2011), relative distance discrimination (Kolarik et al., 2013; Voss et al., 2004), and hand-pointing localization tasks (Rossetti et al., 1996).

Compensatory mechanisms at the neural level may elucidate the augmented spatial perceptual abilities observed in blind individuals across their remaining senses (Collignon et al., 2009; Gougoux et al., 2005; Voss and Zatorre, 2012). The remarkable plasticity of the brain enables the adoption of compensatory mechanisms to sustain spatial skills. Indeed, significant structural and functional reorganization occurs at both subcortical and cortical levels following visual deprivation. For instance, the visual occipital cortex of blind individuals exhibits discernible responses to somatosensory and auditory stimuli (Collignon et al., 2011, 2009; Gougoux et al., 2005; Poirier et al., 2005; Renier and De Volder, 2005;

Striem-Amit and Amedi, 2014; Voss and Zatorre, 2012; Weeks et al., 2000). Contemporary research posits that while the deprived visual cortices retain specific task specializations, they are engaged by non-visual input (Dormal and Collignon, 2011), a phenomenon referred to as sensory-independent supramodal cortical organization (Ricciardi et al., 2014), or task-specific sensory-independent organization of the brain (Heimler et al., 2015). The absence of visual input also fosters increased functional connectivity between the primary auditory cortex and occipital regions (Collignon et al., 2013), as well as changes in non-visual auditory (Elbert et al., 2002) and somatosensory (Park et al., 2009) cortices. Intriguingly, the brain reorganization extends to subcortical structures such as the volume of the lateral geniculate nuclei (Cecchetti et al., 2016).

While, on the one hand, the absence of vision can adopt compensatory mechanisms, on the other hand, it has also been demonstrated that the lack of visual input can detrimentally impact the development of some additional processes. The "perceptual deficiency hypothesis" posits that improvements in auditory and tactile skills following visual deprivation are not uniform and appear contingent upon various factors (e.g., age of onset, severity of blindness, nature of task, etc.). For example, visually impaired individuals exhibit deficits in estimating the absolute distance of auditory cues (Kolarik et al., 2017, 2013), performing tasks involving spatial imagery (Cattaneo et al., 2008), metric representation of auditory space (Gori et al., 2014), auditory distance discrimination, or proprioceptive reproduction (Cappagli et al., 2017). Researchers have also reported deficits in blind individuals regarding the representation and updating of haptic spatial information (Pasqualotto and Proulx, 2012), tactile perception during non-canonical body position (Röder et al., 2004), and changes in multisensory bodily perception (Radziun et al., 2024).

These results raise questions regarding the extent of cross-modal plasticity in cases of vision loss. Neurophysiological evidence indicates that lateralized visual activation in response to sounds, serving as an amodal indication of spatially oriented auditory attention, is discernible in congenitally blind individuals (Amadeo et al., 2019). Consequently, the auditory activation of the visual area does not require visual experience, which, conversely, seems to facilitate the cross-modal reorganization. However, in scenarios requiring the construction of intricate spatial representations, such as spatial bisection tasks, the specific occipital response to sounds in blind individuals seems to be linked not to the physical position of the stimulus (as in sighted individuals) but to the “virtual” position of the stimulus inferred from the time delay (Campus et al., 2019). Thus, the sensory-independent supramodal organization of visual areas is contingent, at least in certain instances, upon visual experience. However, most of these spatial difficulties do not manifest in late blind individuals (Cappagli et al., 2017; Collignon et al., 2011; Finocchietti et al., 2015; Gori et al., 2010; Lehtinen-Railo and Juurmaa, 1994; Voss et al., 2008), suggesting that the first years of life can constitute a sensitive period for the development of spatial metrics.

Only one study investigates the multisensory spatial perception in blind infants, revealing that they encounter challenges in localizing tactile stimuli but not auditory stimuli during

non-canonical body positions (Gori et al., 2021). Specifically, in auditory tasks, blind infants demonstrate comparable levels of accuracy and reaction times (RTs) to their sighted peers across both uncrossed and crossed-hands body postures. In contrast, sighted infants exhibit slower and less accurate responses during tactile tasks in the crossed-hands condition, whereas visually impaired infants do not. Thus, changes in body posture do not influence the responses of visually impaired infants. These findings validate the significant role of vision in influencing body representations on tactile perception during infancy.

In the next section, I illustrate possible cortical mechanisms underlying audio and tactile spatial perception in severely visually impaired infants (section 3.1). Results demonstrate that visual experience is a prerequisite for developing neural correlates associated with external spatial coordinates. Moreover, I present some preliminary data investigating the role of sleep in the modulation of alpha activity during audio and tactile stimulation (section 3.2). Indeed, an extended neural network is activated during sleep, favoring brain plasticity (Brzosko et al., 2019; Jones, 2020). Sleep-dependent neuromodulation promotes local effects on specific sensory systems and global effects on overall nervous system function. These effects foster the development of sensory systems, possibly incorporating memories from the most salient sensory information relevant to everyday experience. The findings of Chapter 3 offer important insights into the changes in neural mechanisms when the vision inputs are lacking in the early sensitive period.

3.1 Exp.1: The absence of vision in early life impairs the somatosensory body remapping

Upon perceiving touch, our brain takes into account the current position of our limbs to determine the touch's location in external space, regardless of limb resting position (Azañón et al., 2010b; Azañón and Soto-Faraco, 2008; Gori et al., 2021; Heed and Azañón, 2014; Rigato et al., 2014). In situations involving non-canonical limb positions, additional neural networks are engaged. Indeed, when adults attempt to locate a tactile stimulus on the hand during a crossed-hands posture, the touch is not attributed to the stimulated hand but rather to the corresponding side of external space (Heed and Azañón, 2014; Maij et al., 2020). These phenomena, known as "crossed-hand effects," are evident both in behavior and neural responses: the tactile ERP deviates from its typical contralateral pattern and becomes ipsilateral to the stimulated hand. The process of localizing a touch on the body entails a double mechanism. First, the stimulus is localized on the body, and later, it is mapped onto external space by considering the arrangement of the limbs (Longo et al., 2010). ERPs mirror this two-step process, with an early period, around ~50ms, during which the tactile stimulus is mapped to the body's coordinates (Azañón et al., 2010a; Azañón and Soto-Faraco, 2008; Soto-Faraco and Azañón, 2013); and a subsequent later period, around ~100ms, that marks

the completion of the shift to the external reference space (Eimer et al., 2004; Heed and Röder, 2010; Rigato et al., 2013; Soto-Faraco and Azañón, 2013). The first step reflects the activity of the primary somatosensory cortex (SI) (Allison et al., 1992, 1989; Hämäläinen et al., 1990). Then, activity extends to the secondary somatosensory cortex (SII), posterior parietal regions (PPC), and frontal areas (Mauguière et al., 1997). The involvement of SII and its associated network indicates the phase of remapping of tactile information, probably influenced by back-projections from the PPC to somatosensory cortices (Buchholz et al., 2011; Macaluso et al., 2000; Schubert et al., 2008).

Regarding brain oscillations, tactile remapping appears to be associated with alpha activity. Specifically, different frequencies of brain activity have been observed when localizing touch with uncrossed- and crossed-hand postures. This suggests that specific frequency bands correspond to distinct spatial processes and reference frames (Heed et al., 2015). Alpha-like (mu) and beta activities in central areas seem to indicate skin-based, anatomical coding of stimuli. Conversely, a modulation of alpha-like activity in centro-parietal regions is linked to external tactile coordinates. Indeed, crossing the hands reduces the lateralization of alpha-band activity in the posterior parietal cortex, indicating that attention is influenced by external spatial coordinates (Buchholz et al., 2013, 2011; Fabio et al., 2024; Ossandón et al., 2020; Schubert et al., 2019, 2015).

The ability to remap tactile stimuli develops in the first stages of life, driven by the shift from a body-centered to an external primary reference frame. However, as previously reported, visual feedback plays a crucial role in developing these spatial skills (Rigato et al., 2014). Indeed, congenitally blind adults and infants lack the crossed-hand effects observed in sighted individuals (Eardley and van Velzen, 2011; Gori et al., 2021; Ley et al., 2013; Röder, 2012; Röder et al., 2004), as well as the related modulation of alpha activity during tactile remapping (Schubert et al., 2019, 2015). However, it remains unexplored to what extent brain activity is influenced by limb position when blind infants experience tactile stimuli and whether a clearly defined two-step process is evident in brain responses in sighted infants. I hypothesize that neural processes related to somatosensory perception and body mapping are modulated by vision in a specific functional temporal hierarchy, and the absence of visual experience may alter these neural patterns. Conversely, I predict that limb position may not noticeably impact brain responses to auditory stimulation, considering that auditory stimuli are directly mapped on external reference frame from the first stages of sensory processing.

3.1.1 Methods

Participants

Twelve severely visually impaired (SVI) infants (6F, median age=28.1 months, age range=10-54 months) and twelve sighted (S) infants (5F, median age=31 months, age range=12-52 months) with similar ages ($t(20)=0.51$, $p=0.61$) were included in this study. Informed consent was obtained from the infants' parents before commencing the study. Table 3.1 shows demographic and clinical details. It is challenging to gather large samples of SVI infants while meeting our exclusion criteria (see below). However, according to a statistical t-test, with $\alpha = 0.05$ and power = 0.80, 12 participants are needed to achieve a significant result if a large effect size ($d = 1.2$) is expected, as shown in a previous study (Gori et al., 2021). Grating acuity was measured with Teller acuity cards as appropriate for pre-verbal children and infants (Teller et al., 1986). None of the participants had a history of prenatal infections, fetal and perinatal distress, metabolic disorders, and cognitive impairment. All the participants in this study presented with good general health status. All participants demonstrated a normal psychomotor development level based on a clinical evaluation and the Reynell-Zinkin Scale (Reynell, 1978). Cerebral visual impairment was excluded based on anamnesis, clinical and instrumental visual function assessment, and neurological examination. The parents/legal guardians signed the informed consent form, according to the Declaration of Helsinki, before the beginning of the experiment.

Code	Biological Sex	Age (m)	Group	Diagnosis
001	M	10.13	Severely visually impaired	Ocular albinism
002	M	10.7	Severely visually impaired	Inherited congenital retinal dystrophy
003	F	11.53	Severely visually impaired	Eye maldevelopment
004	M	12.7	Severely visually impaired	Ocular albinism
005	M	13.07	Severely visually impaired	Inherited congenital retinal dystrophy
006	F	19.67	Severely visually impaired	Optic nerve hypoplasia
007	F	36.5	Severely visually impaired	Inherited congenital retinal dystrophy
008	M	37.23	Severely visually impaired	Inherited congenital retinal dystrophy
009	F	37.8	Severely visually impaired	Inherited congenital retinal dystrophy
010	M	38.1	Severely visually impaired	Inherited congenital retinal dystrophy
011	F	48.7	Severely visually impaired	Nystagmus
012	M	53.5	Severely visually impaired	Inherited congenital retinal dystrophy
013	M	12.17	Sighted	-
014	M	16.2	Sighted	-
015	M	21.83	Sighted	-
016	F	21.9	Sighted	-
017	F	27.5	Sighted	-
018	F	29.37	Sighted	-
019	F	32.63	Sighted	-
020	F	33	Sighted	-

021	M	35.6	Sighted	-
022	M	36.83	Sighted	-
023	M	46.43	Sighted	-
024	M	51.47	Sighted	-

Table 3.1. Demographic and clinical details. *The table shows identification code, the biological sex, age expressed in decimal months, the group, and the diagnosis (for SVI participants).*

Data acquisition

In this experiment, two different sensory stimuli (tactile and auditory) were presented to infants during two different hand postures (uncrossed and crossed), with each condition occurring a maximum of 12 times (6 times in each posture). The stimulation protocol was repeated when possible to increase the number of trials. During the testing phase, the infant, seated on a parent's lap, wore an EEG cap while a digital video camera recorded their movements. The auditory and vibrotactile stimuli were delivered to the infant's palms using custom-built stimulators (Gori et al., 2019). The vibrotactile stimulus was a continuous pure tone (112 Hz). The sound was a 926 Hz pure tone pulsed at a frequency of 5 Hz. Each stimulus lasted for 1000 ms, followed by an 8000 ms interval for the infant to react. Stimulus-linked signals were sent to a visual stimulator behind the infant to signal stimulus onset and offset to the behavioral coder via the video recording. This enabled the infants' behavior to be observed and coded in a stimulus-locked manner without indicating which hand the stimulus was presented to. In this way, the behavioral coders were unaware of the location of the stimulus. Brain electrical activity was recorded continuously using a Hydrocel Geodesic Sensor Net, consisting of 128 silver–silver chloride electrodes evenly distributed across the scalp. The vertex served as the reference.

Two experimenters, E1 and E2, conducted the test. E1 interacted with the infant and manipulated their arms into the correct postures, while E2 triggered the stimuli via a Matlab program. For each trial, E1 played a game with the infant "bouncing" their hands into the correct position and saying "1,2,3, bù". The hands were placed in the allocated posture just before "bù", and the "bù" also functioned as a cue for E2 to trigger a stimulus. If a trial was marked as bad, it was repeated, with an average of 3 trials per participant. Following stimulus delivery, E1 held the infant's arms in place until they moved or until 8000 ms had elapsed. In the 8000 ms period following each stimulus, E1 oriented their face to the floor so as not to distract the infant. The study continued until all trials were completed or until the infant and parent were unwilling to continue cooperating. Figure 3.1 represents the experimental design.

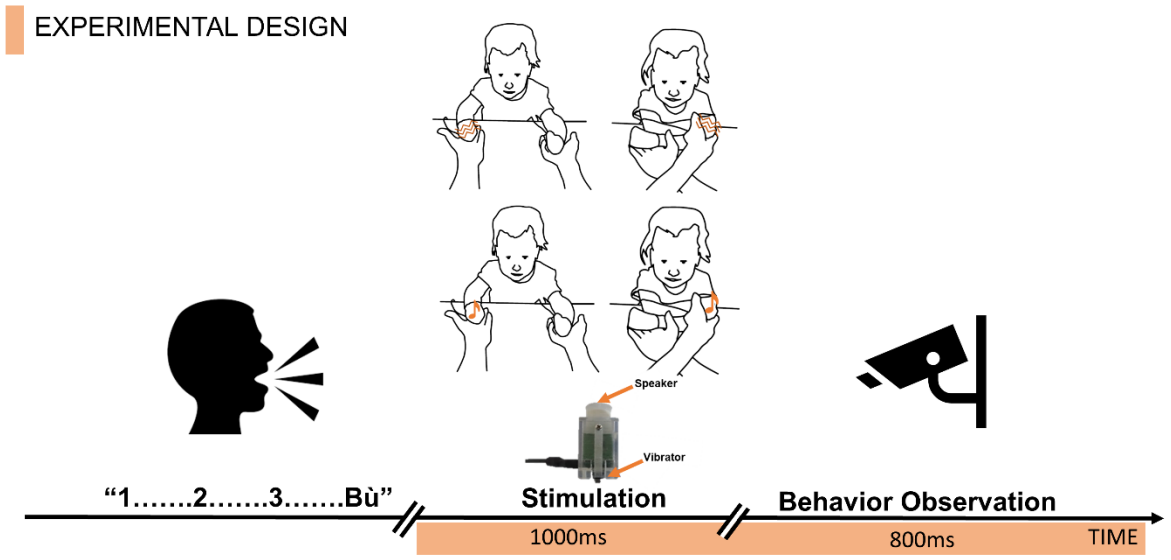

Figure 3.1. Experimental Design. *Representation of the temporal sequence of the experimental design.*

Preprocessing

Regarding behavioral data, the direction, latency, and type of the infants' first orienting responses to the stimuli on each trial were coded from the video records by two raters who were naive to the purpose of the study. During the 8000 ms period following the stimulus on each trial, lateral eye movements (saccades), lateral head movements, and unilateral hand/arm movements were all coded as orienting responses. Therefore, the orienting response was a binary variable in which ‘‘1’’ coded an orienting response to the stimulated limb. ‘‘0’’ coded an orienting response to the unstimulated limb. Where infants made bilateral, symmetrical arm movements, these were coded as null responses, and the trial was terminated. The hand/arm movements, coded as orienting responses, included fine movements (i.e., flexions and extensions of the elbow, wrist, and finger joints) and gross withdrawal movements (the arm and hand pulled back towards the infant’s trunk).

As per EEG data, the signal was filtered between 0.1 and 30 Hz. Then, a visually supervised automated approach in which bad channels were removed by artifact rejection tools was adopted. The bad channels were identified based on the classification of flat signals, abnormal periodograms, and outlier channels. Next, transient high-amplitude artifacts were removed using an ASR (Chang et al., 2018), available as a plug-in for EEGLAB software (Delorme and Makeig, 2004). In this study, a sliding window of 500 ms and a threshold of 10 std to identify corrupted subspaces was used. Furthermore, channels were removed if they were less correlated than 0.95 to an estimate based on the other channels or if their line noise relative to the signal was more than 4 std from the channel population mean. Time windows were removed when, after applying the previously

described criteria, the fraction of contaminated channels exceeded the threshold of 0.25. Other parameters were kept as their default. EEG data were further cleaned using ICA. Specifically, to select artefactual components based on quantitative criteria, a visually inspected classification based on the EEGLAB IC_Label toolbox (Pion-Tonachini et al., 2019) was applied, keeping all parameters as their default and following the criteria reported in the corresponding validation papers. Data were then referenced to the average. EEG data were averaged in synchrony with the stimulus presentations to obtain ERPs, considering a period of 200 ms before the first sound onset as a baseline. Mean ERP amplitude was computed by averaging the voltage in an early (45-65 ms) and in a late time window (105-120 ms). The association between ERP response and participant performance was investigated using linear regression of individual mean ERP amplitude in each time window against the percentage of trials in which the participant perceived the stimuli. A further analysis was implemented to investigate how experimental manipulation could precisely modulate brain activity at each frequency. To this aim, ERSP was calculated using the *newtimef* function of EEGLAB. For each participant, the whole time-frequency distribution was extracted from 4 to 32 Hz using a Morlet Wavelet (cycles starting from 1 at the lowest frequency and linearly increasing with a 0.5 factor with frequency).

To perform an analysis related to the physical characteristics of the stimuli (and increase statistical power), the electrode montage was swapped for conditions where stimuli were provided to the right hand separately for each group, posture, and sensory modality. Therefore, responses were considered as contralateral or ipsilateral relative to the stimulated hand. To evaluate tactile activations, the centro-parietal (CP) regions of interest were considered: contralateral CP (channels E98, E102, E103) and ipsilateral CP (channels E41, E46, E47). In turn, for auditory activation the temporal-posterior (TP) regions of interest were considered: contralateral TP (channels E82, E83, E88, E89, E90, E94, E95, E96, E97, E99, E100, E101, E107, E108) and ipsilateral TP (channels E45, E50, E56, E57, E58, E63, E64, E65, E68, E69, E70, E73, E74)

Statistical analysis

Statistical analyses were carried out in the R environment (R Core Team, 2021). Results were deemed significant when $p < 0.05$. Where multiple comparisons were used to follow up significant interactions, a Bonferroni correction was applied. For two-way interactions, the correction was applied against all meaningful contrasts. Generalized Linear mixed models (GLMMs) and Linear Mixed Models (LMMs) were fitted using the *lmer* function of the *lme4* package (Bates et al., 2015). The predictors were evaluated using Type III Wald $\chi 2$ tests, as implemented in the *Anova* function of the *car* package (Fox and Weisberg, 2018). For GLMM, all models included random intercepts, allowing for individual differences in baseline performance, but did not have enough power to estimate participant-specific slopes. Where not otherwise specified, the contrasts were further investigated with the *emmeans* function of the *emmeans* package (Lenth, 2022) by obtaining their estimated marginal means

(EMMs). Effect sizes were estimated using the *eff_size* function of the emmeans package, utilizing the sigma and the edf estimated by every single model. Below, I show the specific statistical analysis performed for the behavioral outcomes, EEG data, and associations between the two.

For behavioral analysis, the percentages of the infants' orienting responses directed to the stimuli were calculated in all groups and conditions. In all the analyses, the stimulated hand was considered the correct response. Effects and interactions of Posture, Stimulus condition, Group, and Age (in months) were evaluated by fitting GLMMs. According to Wilkinson's notation (Wilkinson and Rogers, 1973), the models fitted were:

Auditory localization (Auditory only condition): *Stimulus response ~ Group(SVI/S)*Posture(Uncrossed/Crossed)*Age in months + (1|participant);*

Tactile localization (Tactile only condition): *Stimulus response ~ Group(SVI/S)*Posture(Uncrossed/Crossed)*Age in months + (1|participant).*

Different analyses were performed for EEG data considering ERP, ERSP, and microstates. First, effects and interactions of Posture, Laterality, Group, and Age (in months) of ERP were evaluated with LMMs for each time window and sensory modality. The following models were fitted:

Auditory localization (Auditory only condition): *ERP mean ~ Group(SVI/S)*Posture(Uncrossed/Crossed)*Laterality(ipsi/contra) + (1|participant);*

Tactile localization (Tactile only condition): *ERP mean~ Group(SVI/S)*Posture(Uncrossed/Crossed)*Laterality(ipsi/contra) + (1|participant).*

Second, an analysis based on ERSP was performed to investigate the functional specificity of different frequencies within brain activity by computing t-tests with false discovery rate (FDR) correction for multiple comparisons.

Third, a microstate analysis was performed, which can naturally describe inter-subject and inter-trial variability. Moreover, it has been shown that microstates correlate with MRI patterns and thus may be interpreted as functional states of the brain (Britz et al., 2010; Habermann et al., 2018; Michel and Koenig, 2018; Van De Ville et al., 2010). Microstate analysis could validate the hypothesis-driven defined time windows and possibly reveal coherent functional states. Therefore, for each group, sensory modality, and posture, a microstate analysis was performed using the Microstate EEGlab toolbox (Poulsen et al., 2018). Specifically, a well-established K-means clustering method was applied. The number of random initializations of the algorithm (restarts) was kept to 10 (default value), and the best restart based on global explained variance (GEV) was selected. Temporal smoothing was applied to microstate label sequences to avoid short segments, imposing a minimum 10 ms microstate segment duration. Four measures of fit, namely GEV, cross-validation criterion, dispersion, and normalized Krzanowski-Lai criterion, were calculated in a range

between 3 and 8 microstates to decide the amount of microstate clusters. Finally, a qualitative decision was made based on these measures and the quality of the topographical maps.

The Association between EEG and behavioral data was evaluated with linear regressions, GLMMs, and MVPA analysis. For each group (SVI and S), sensory modality (tactile and auditory), posture (crossed and uncrossed), laterality (ipsi and contra), and time window (early and late), an independent linear regression was performed, considering ERP mean as independent and accuracy (% of the correct answer) as dependent variables. A series of GLMMs was also fitted for each time window and sensory modality to generalize the results of regression analyses. Then, the ERP data were preliminarily Z-transformed to make data more comparable among participants. The models fitted were:

Auditory localization (Auditory only condition): *Accuracy ~ Group(SVI/S)*Posture(Uncrossed/Crossed)*Laterality(ipsi/contra)*ERP mean + (1|participant);*

Tactile localization (Tactile only condition): *Accuracy ~ Group(SVI/S)*Posture(Uncrossed/Crossed)*Laterality(ipsi/contra)*ERP mean + (1|participant).*

Finally, a Multivariate Pattern Analysis (MVPA) was also performed. It involves using machine learning classification techniques to discriminate between patterns of neural activation associated with stimuli, experimental conditions, participant characteristics, or responses. By analyzing neural activation patterns, MVPA aims to understand how these patterns relate to specific stimuli or responses. In this study, MVPA was conducted using the MVPAlab Matlab toolbox (López-García et al., 2022). Each group was analyzed separately. All trials were combined from each group to enhance statistical power. Finally, for decoding related to infants' perception, trials based on the participants' behavioral responses within each group, posture, and sensory modality were classified. The classification model used for the decoding analysis was a Support Vector Machine (SVM). Linear classifiers were used for decoding analysis (linear kernel). A k-fold cross-validation technique was used, setting the number of folds to 5. To evaluate the performance of the decoding models, mean accuracy was used, a metric that is quick and easy to compute, defined as the number of correct predictions divided by the total number of evaluated trials. Feature weights obtained from training the SVM models were considered to measure their contribution to the model's decision boundary. The Haufe procedure was applied to transform these feature weights, allowing them to be interpreted as the origins of neural processes in space, leading to more accurate predictions (46). The contribution of each electrode to the classification performance was evaluated at each time point and then averaged within the time windows of interest. A t-test was applied to compare accuracy between different time windows, and Bonferroni correction was used for multiple comparisons to draw statistical inferences. To improve our statistical power, for each group separately, all the participants' trials were merged. Then, decoding related to participants'

perception for each group, posture, and sensory modality was performed, trying to classify trials based on the accuracy of the children, i.e., trials with correct vs. incorrect responses.

3.1.2 Results

This study compared neural responses during auditory and tactile localization in both uncrossed- and crossed-hand postures between sighted (S) and severely visually impaired (SVI) infants. Results show that vision uniquely shapes tactile, but not auditory, neural processes related to external space. S and SVI infants display a contralateral somatosensory response early on, which only in SVI infants closely tied to their behavioral responses. Conversely, sighted infants exhibit a later ipsilateral somatosensory response consistent with their behavioral reactions. These results suggest that in early development, SVI children maintain a reliance on body coordinates. In contrast, sighted children transition towards an external frame of reference, indicating a two-step somatosensory processing mechanism. In the following paragraphs, I present the specific results.

Behavioral orienting responses

The behavioral responses were investigated by examining the orienting responses of S and SVI infants to auditory and tactile stimuli presented on their hands in different hand positions (uncrossed and crossed). The results confirm previous findings (Gori et al., 2021), showing differences between S and SVI infants only when tactile stimuli are presented in a crossed-hand posture. In this condition, sighted infants show less accurate responses than SVI infants. However, significant differences are not found between the two groups in auditory localization accuracy for both uncrossed- and crossed-hand postures, nor in tactile localization accuracy for the uncrossed-hand posture (see Table 3.2 and Figure 3.1).

% Orienting response in tactile and auditory localization

Sensory Modality	**Tactile**				**Auditory**			
GLMMs	***accuracy ~ Group*Posture*Age in months + (1|participant)***				***accuracy ~ Group*Posture*Age in months + (1|participant)***			
	χ^2(df)		**P**		**χ^2(df)**		**P**	
Group	15.911(1)		<0.001*		0.160(1)		0.689	
Posture	21.331(1)		<0.001*		0.389(1)		0.533	
Age	0.556(1)		0.456		0.056(1)		0.813	
Group:Posture	18.899(1)		<0.001*		0.263(1)		0.608	
Group:Age	0.402(1)		0.526		0.062(1)		0.803	
Posture:Age	0.017		0.897		0.489(1)		0.484	
Group:Posture :Age	0.063		0.802		0.639(1)		0.424	
Post hoc								
Comparisons for posture	**Uncrossed**		**Crossed**		**Uncrossed**		**Crossed**	
	t(df)	**p**	**t(df)**	**p**	**t(df)**	**p**	**t(df)**	**p**
S-SVI contrast	0.115(36)	0.909	-5.865(36)	<0.001*	-	-	-	-
Comparisons for group	**S**		**SVI**		**S**		**SVI**	
	t(df)	**p**	**t(df)**	**p**	**t(df)**	**p**	**t(df)**	**p**
Uncrossed-crossed contrast	6.293(19)	<0.001*	0.167(19)	0.869	-	-	-	-

Table 3.2. Behavioral results. *Results of the percentages of sighted (S) and visually impaired (SVI) infants' head and manual orienting responses, which were made toward the stimulated hand across stimulus conditions (tactile/auditory) and posture (uncrossed/crossed) conditions.*

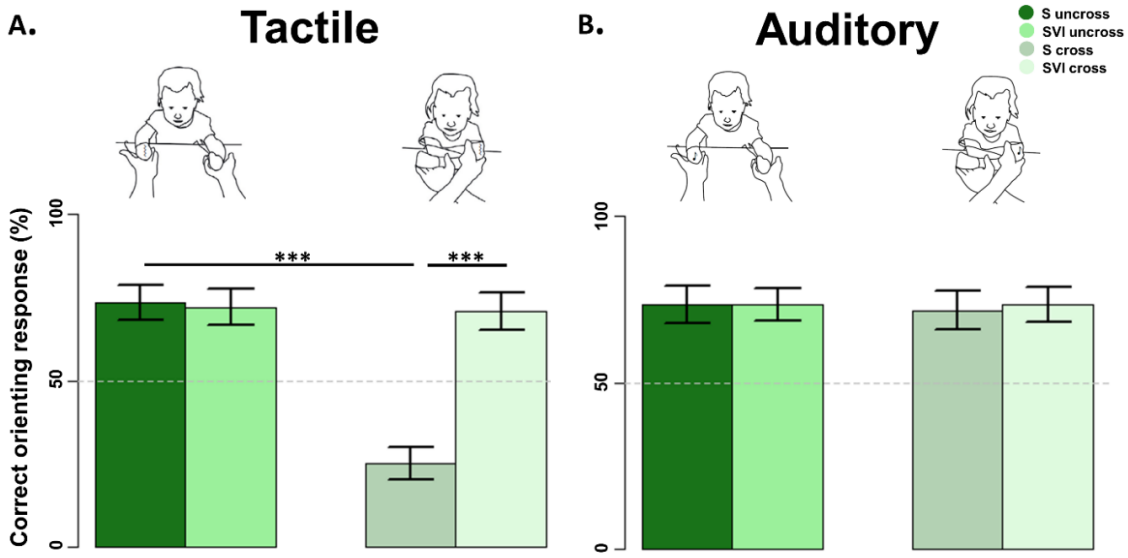

Figure 3.2. Percentages of orienting responses to tactile and auditory stimulation*. For each condition, posture, and group, the bars represent the percentages of head and manual orienting responses (mean and sem). The stars represent the significant P values P<0.001). (A) only Tactile condition. (B) only Auditory condition.*

Auditory localization

No difference is observed in the audio processing between the two groups. Both groups showed an evident response in the temporal-posterior region contralateral to the stimulated hand during uncrossed posture and ipsilateral to the stimulated hand during crossed posture in the early [45-65]ms time window (see Table 3.3 and Figure 3.2). ERSP analysis also shows no differences between blind and sighted children, with only a main effect on posture. Figure 3.3 illustrates the results of the microstates analysis.

Auditory localization ERP results in the [45-65]ms time widow

	Posture uncrossed				**Posture crossed**			
Linear models of the ERP mean	***Erp_mean ~ laterality* group + (1|subject)***				***Erp_mean ~ laterality * group + (1|subject)***			
	χ^2(df)		**P**		**χ^2(df)**		**P**	
laterality	214.3(1)		<0.001*		162.8(1)		<0.001*	
group	0.986(1)		0.321		0.024(1)		0.878	
laterality:group	0.782(1)		0.782		0.07(1)		0.791	
Post hoc								
Comparisons for laterality	Ipsi		Contra		Ipsi		Contra	
	t(df)	p	t(df)	p	t(df)	p	t(df)	p
S-SVI contrast	-	-	-	-	-	-	-	-
Comparisons for group	S		SVI		S		SVI	
	t(df)	p	t(df)	p	t(df)	p	t(df)	p
Ipsi-contra contrast	-9.519(274)	<0.001*	-11.12(274)	<0.001*	8.618(226)	<0.001*	9.411(226)	<0.001*

Table 3.3. ERP results of Auditory only condition. *Statistics of the LMM for each time window and posture which evaluate the effects of laterality and group on ERP amplitude.*

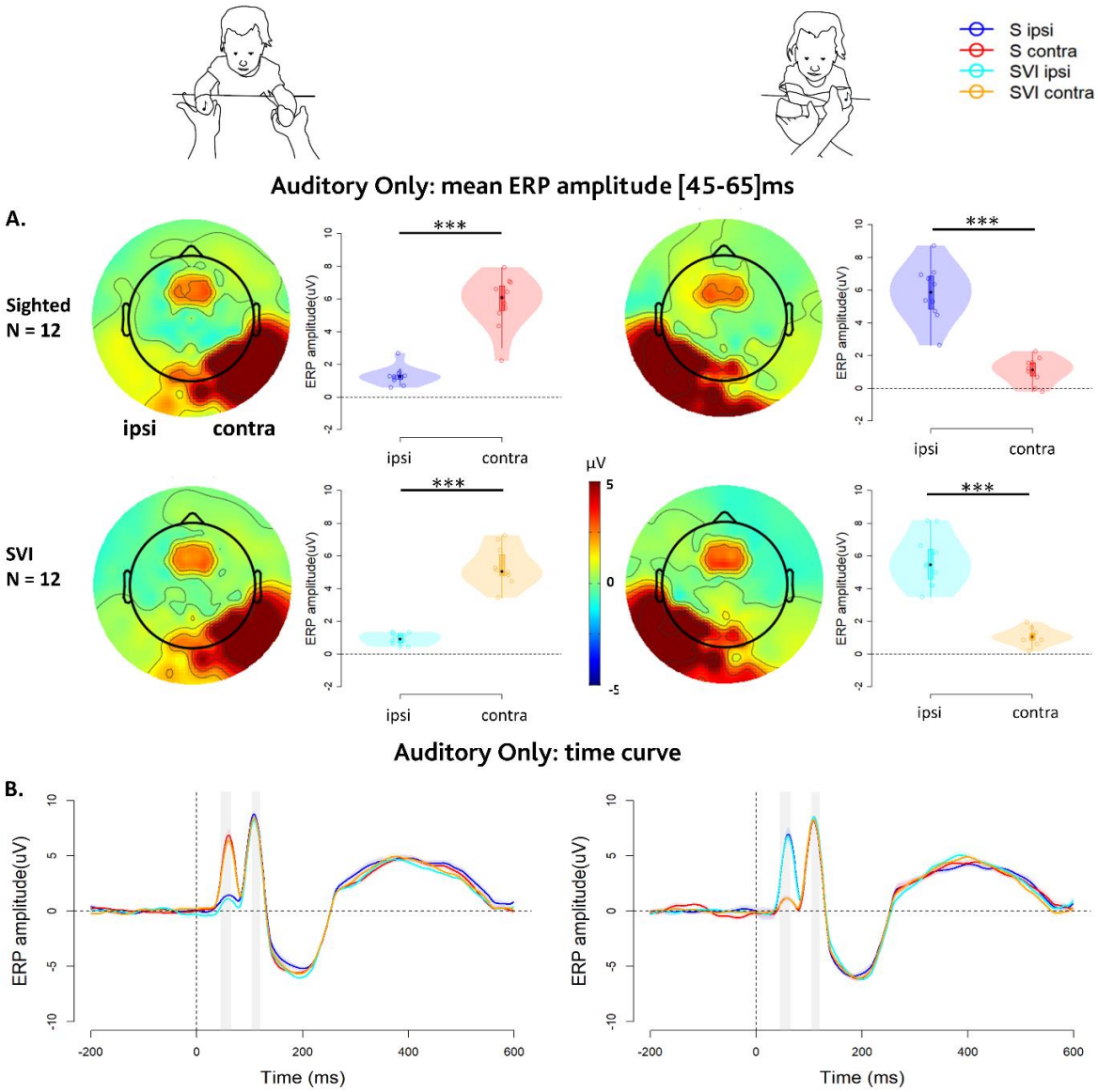

Figure 3.3. ERP results of Auditory only condition. *(A) represent results for the [45-65]ms time window. For each group (row) and posture (column), I report, on the left, the topography distribution and, on the right, the single-subjects ERP amplitude in the temporo-posterior region ipsilateral and contralateral to the stimulated hand. The horizontal dashed line points out 0 amplitude. The stars represent the significant P values (*=P<0.5, **= P<0.01, ***= P<0.001) after the Bonferroni correction. (B) represents the ERP curve during uncrossed and crossed postures, respectively, in sighted (left, S) and severely visually impaired (right, SVI). The horizontal and vertical dashed lines point out 0 amplitude and t=0, respectively. The shadowed areas highlight the considered time windows.*

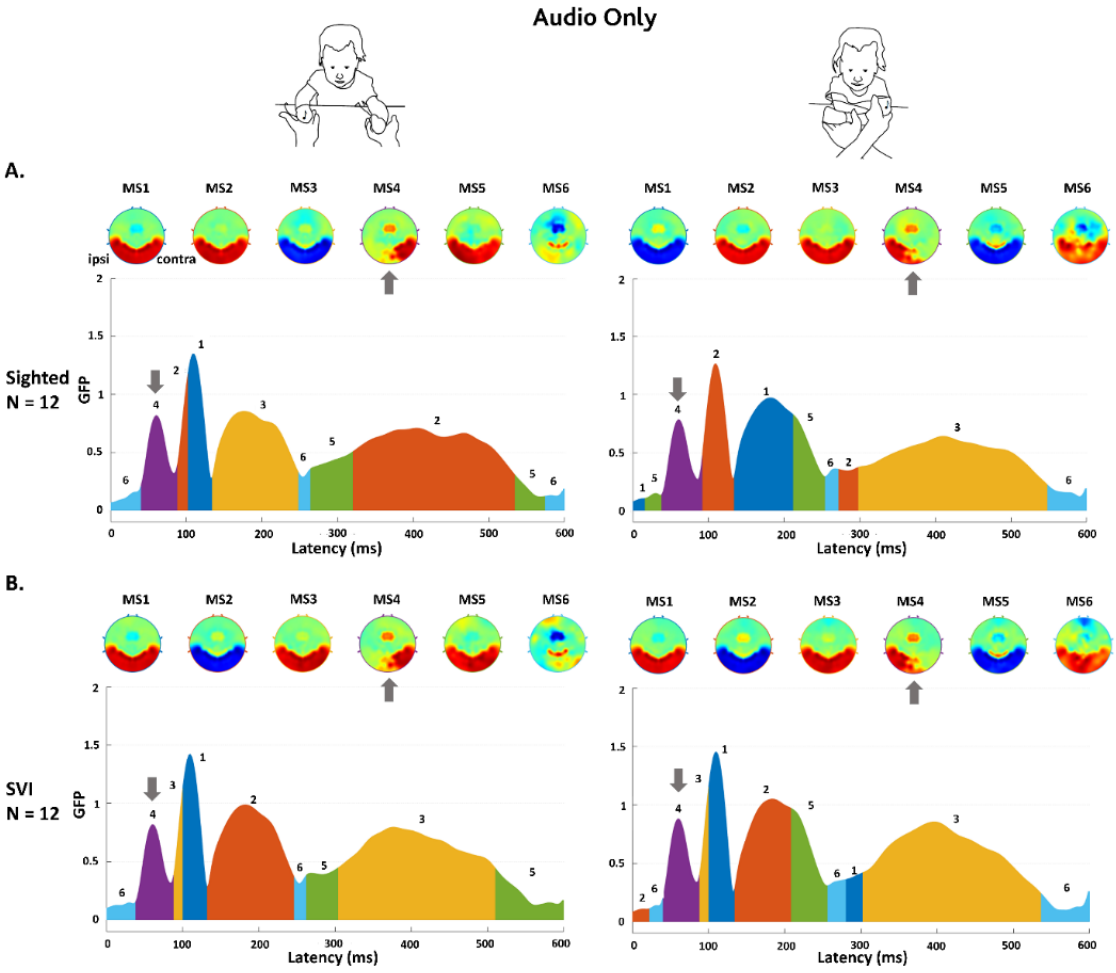

Figure 3.4. Microstates of auditory localization. *For each group (row) and posture (column), the results of the microstate decomposition analysis are as follows: for each subplot on the top, I report the topographic map of each microstate. At the bottom, I report the corresponding microstates' Global Field Power (GFP) and temporal segmentation.*

Considering the association with behavioral responses, the ERP amplitude (described explicitly for each posture) positively correlates with the accuracy of correct answers (see Table 3.4). Figure 3.4 specifically shows this correlation and the results of MVPA.

Auditory localization ERP – behavioral results in the [45-65]ms time widow

	Posture uncrossed				**Posture crossed**			
Linear regression analysis								
	S		**SVI**		**S**		**SVI**	
	R^2	**p**	**R^2**	**p**	**R^2**	**p**	**R^2**	**p**
Ipsi - Accuracy*ERP mean	-	-	-	-	0.828	<0.001*	0.971	<0.001*
Contra - Accuracy*ERP mean	0.858	<0.001*	0.858	<0.001*	-	-	-	-
GLMMs	***accuracy ~ laterality * group * Erp_mean + (1|subject)***				***accuracy ~ laterality * group * Erp_mean + (1|subject)***			
	χ^2(df)		**P**		**χ^2(df)**		**P**	
laterality	1.715(1)		0.19		2.706(1)		0.1	
group	0.102(1)		0.749		0.296(1)		0.586	
ERP mean	16(1)		<0.001*		7.852(1)		0.005*	
laterality:group	0.032(1)		0.858		0.67(1)		0.413	
laterality:erp_mean	13.07(1)		<0.001*		13.8(1)		<0.001*	
group:erp_mean	0.134		0.716		0.146(1)		0.703	
laterality:group:erp_mean	0.321		0.571		0.155(1)		0.694	
Post hoc								
Comparisons for laterality	**Ipsi**		**Contra**		**Ipsi**		**Contra**	
	Z	**p**	**Z**	**p**	**Z**	**p**	**Z**	**p**
S-SVI contrast	0.456	0.649	-0.493	0.622	0.32	0.749	-0.445	0.656
Comparisons for group	**S**		**SVI**		**S**		**SVI**	
	Z	**p**	**Z**	**p**	**Z**	**p**	**Z**	**p**
Ipsi-Contra contrast	-2.568	0.01*	-2.604	0.009*	2.616	0.009*	2.653	0.008*

Table 3.4. Auditory localization ERP-behavioral results. *Statistics of the linear regression and GLMM for each time window and posture evaluate the association between behavioral results and ERP amplitude.*

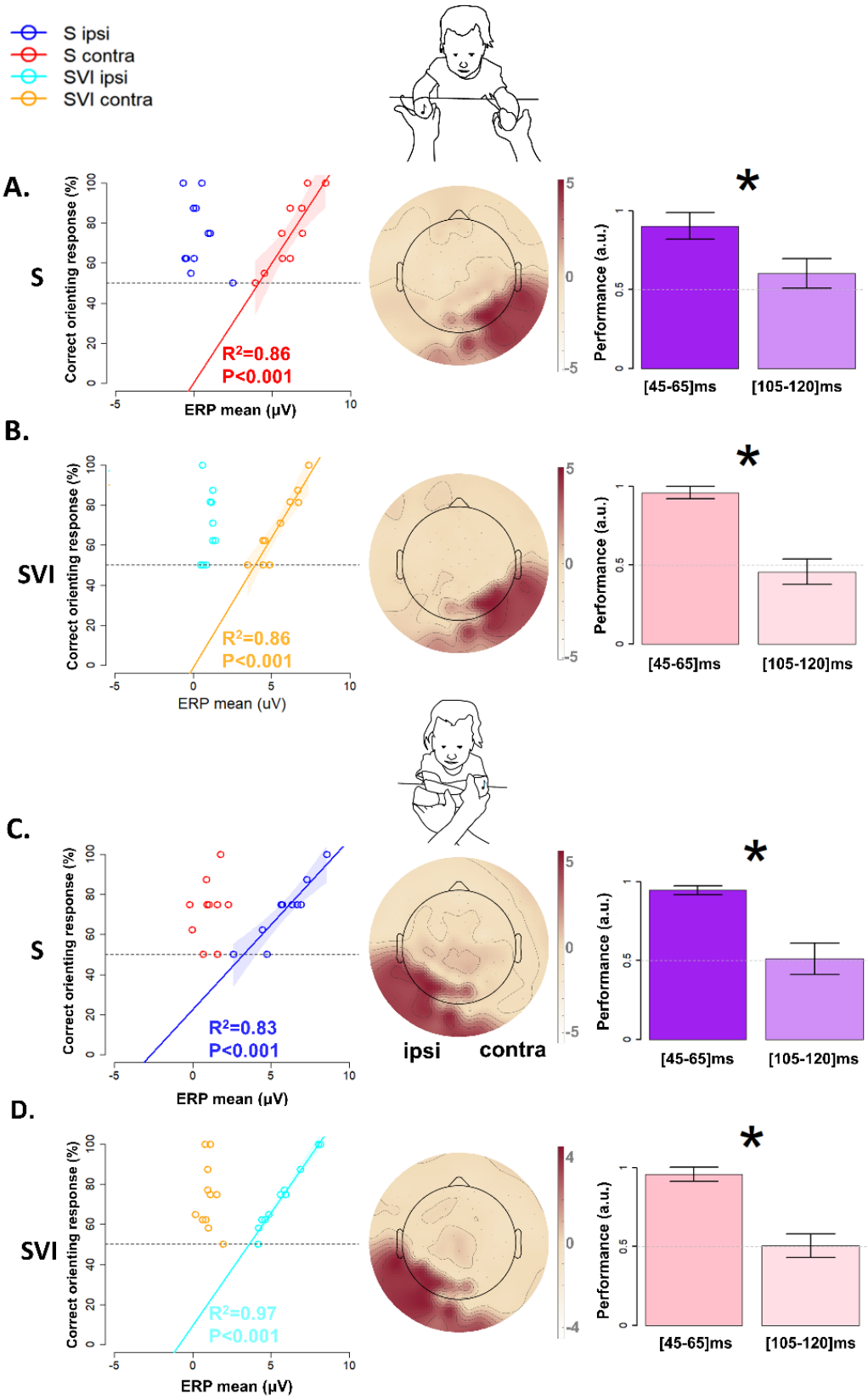
S ipsi
S contra
SVI ipsi
SVI contra
A.
S
Correct orienting response (%)
R²=0.86
P<0.001
ERP mean (µV)
Performance (a.u.)
[45-65]ms
[105-120]ms
B.
SVI
Correct orienting response (%)
R²=0.86
P<0.001
ERP mean (uV)
Performance (a.u.)
[45-65]ms
[105-120]ms
C.
S
Correct orienting response (%)
R²=0.83
P<0.001
ERP mean (µV)
ipsi
contra
Performance (a.u.)
[45-65]ms
[105-120]ms
D.
SVI
Correct orienting response (%)
R²=0.97
P<0.001
ERP mean (µV)
Performance (a.u.)
[45-65]ms
[105-120]ms

Figure 3.5. Auditory localization ERP-behavioral results in the [45-65]ms time window. *For each Group (row) and Posture (column), the results of linear regression of orienting accuracy to ERP amplitudes (leftmost) and MVPA classifying multivariate EEG against the accuracy of the response (middle and rightmost) are reported. The maps represent the feature weight distribution over the scalp during the selected time window, with red and white colors respectively, indicating positive and negative associations with orienting performance. The rightmost subplot represents the decoding performance of the classifier (mean and SD) within the time windows. Stars indicate a significant t-test between time windows (P<0.05 after Bonferroni correction).*

Finally, Figure 3.5 shows the contralateral and ipsilateral ERSP response to auditory localization. The localization of the auditory stimuli strongly modulates the high frequencies in alpha and beta bands in the first sensory processing stages. No significant differences are found between S and SVI infants. Only a main effect of posture is evident early in time, underlying the specificity of the first milliseconds in activating the contralateral area to the stimulation.

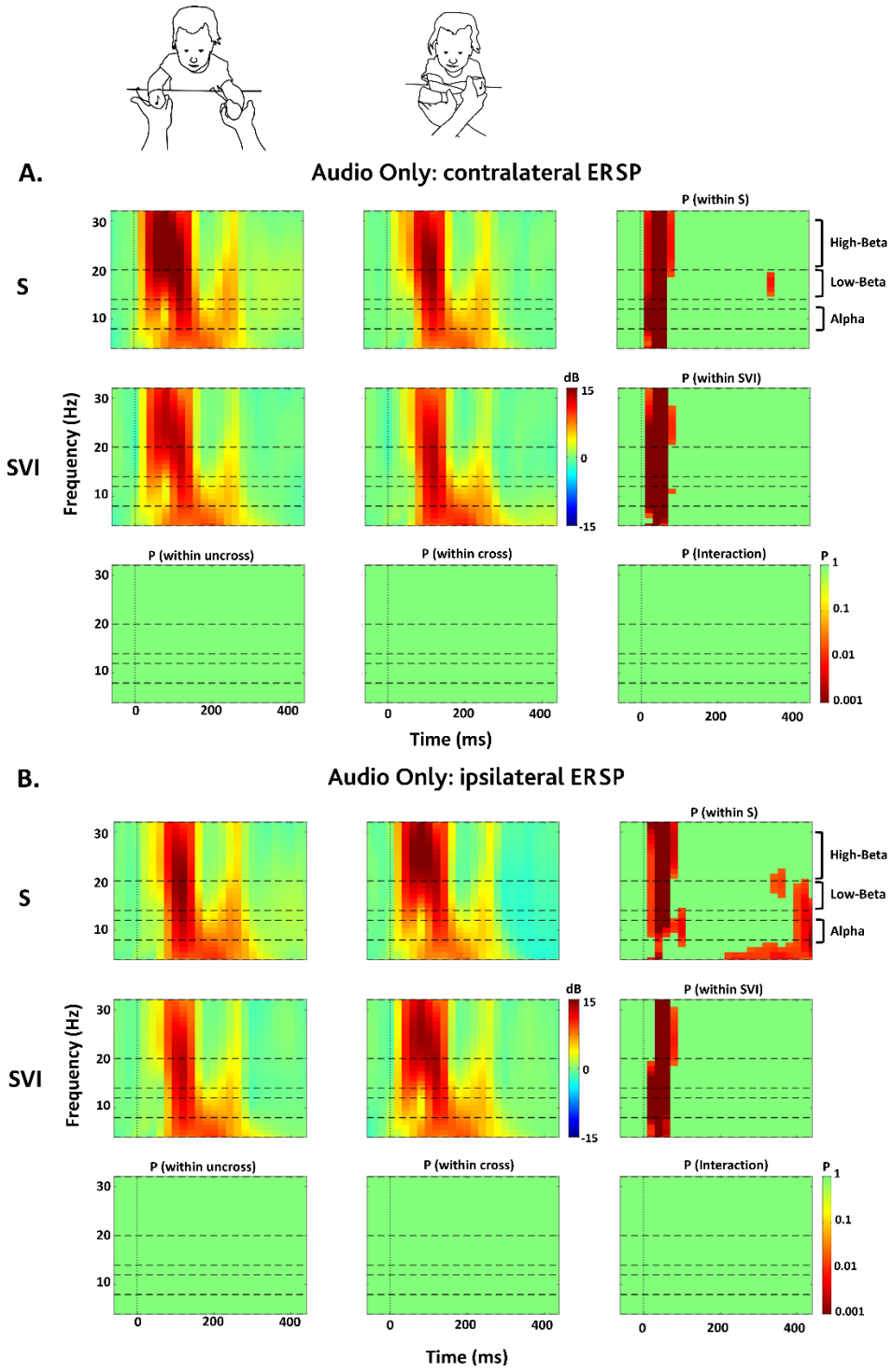

Figure 3.6. ERSP elicited by stimuli during the auditory localization task. *For each group (row) and posture (column), the results of the ERSP analysis are in the temporo-posterior area. Each subplot reports ERSP (dB) as a function of time (ms, x-axis) and frequencies (Hz, y-axis). Vertical dotted lines represent t=0 (stimulus onset), while horizontal dashed lines represent frequency bands of interest. Figure (A) shows the contralateral response. Figure (B) shows the ipsilateral response. The last row and column represent the significant results after the false discovery rate (FDR) correction for multiple comparisons.*

Tactile localization

No difference is observed between the S and SVI infants in the uncrossed-hand posture. Both groups exhibit a distinct centro-parietal positivity response contralateral to the stimulated hand during two-time windows, specifically [45-65]ms and [105-120]ms, associated with early somatosensory processing. However, during the crossed-hand posture, the specificity of these two time windows becomes apparent, along with the difference between S and SVI infants. While the early time window remains similar to the uncrossed posture in both groups, an evident ipsilateral centro-parietal positivity emerges in the [105-120]ms time window, but only in sighted infants, surpassing the contralateral response (see Table 3.5 and Figure 3.5). Figure 3.7 illustrates the findings of microstates analysis.

Tactile localization ERP results

Time window	[45-65]ms							
	Posture uncrossed				Posture crossed			
Linear models of the ERP mean	*Erp_mean ~ laterality * group + (1|subject)*				*Erp_mean ~ laterality * group + (1|subject)*			
	χ^2(df)		**P**		**χ^2(df)**		**P**	
laterality	206.4(1)		<0.001*		297.6(1)		<0.001*	
group	0.017(1)		0.898		4.991(1)		0.025*	
laterality:group	2.019(1)		0.155		11.82(1)		<0.001*	
Post hoc								
Comparisons for laterality	**Ipsi**		**Contra**		**Ipsi**		**Contra**	
	t(df)	p	t(df)	p	t(df)	p	t(df)	p
S-SVI contrast	-	-	-	-	3.868(46)	<0.001*	-0.353(46)	0.726
Comparisons for group	**S**		**SVI**		**S**		**SVI**	
	t(df)	p	t(df)	p	t(df)	p	t(df)	p
Ipsi-contra contrast	-10.86(223)	<0.001*	-9.517(223)	<0.001*	-9.214(246)	<0.001*	-14.98(246)	<0.001*
Time window	[105-120]ms							
	Posture uncrossed				Posture crossed			
Linear models of the ERP mean	*Erp_mean ~ laterality * group + (1|subject)*				*Erp_mean ~ laterality * group + (1|subject)*			
	χ^2(df)		**P**		**χ^2(df)**		**P**	
laterality	110.3(1)		<0.001*		2.623(1)		0.105	
group	0.417(1)		0.518		74.11(1)		<0.001*	
laterality:group	4.015(1)		0.045*		39.43(1)		<0.001*	
Post hoc								
Comparisons for laterality	**Ipsi**		**Contra**		**Ipsi**		**Contra**	
	t(df)	**p**	**t(df)**	**p**	**t(df)**	**p**	**t(df)**	**p**
S-SVI contrast	1.863(64)	0.067	-0.955(64)	0.343	10.48(65)	<0.001*	1.64(65)	0.106
Comparisons for group	**S**		**SVI**		**S**		**SVI**	
	t(df)	**p**	**t(df)**	**p**	**t(df)**	**p**	**t(df)**	**p**
Ipsi-contra contrast	-5.714(223)	<0.001*	-9.034(223)	<0.001*	3.501(247)	<0.001*	-5.458(255)	<0.001*

Table 3.5. ERP results of Tactile only condition. *Statistics of the LMM for each time window and posture evaluate the effects of laterality and group on ERP amplitude.*

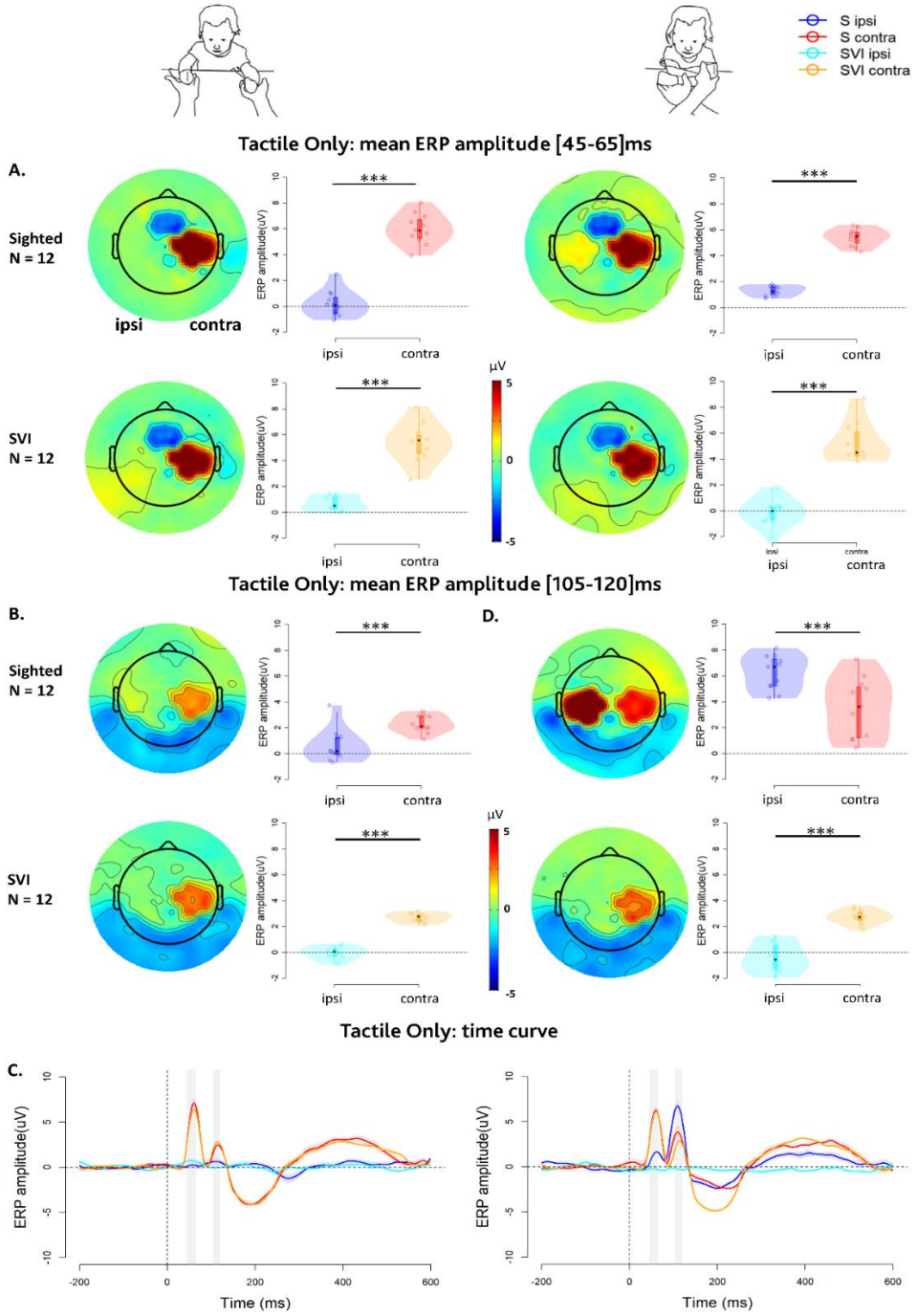

Figure 3.7. ERP results of Tactile only condition. *(A) and (B) represent results for the [45-65]ms and [105-120]ms time windows, respectively. For each group (row) and posture (column), I report, on the left, the topography distribution and, on the right, the single-subjects ERP amplitude in the centro-parietal region ipsilateral and contralateral to the stimulated hand. The stars represent significant P values (*=P<0.5, **= P<0.01, ***= P<0.001) after the Bonferroni correction. (C) represents the ERP curve during uncrossed and crossed postures in sighted (S) and severely visually impaired (SVI). The horizontal and vertical dashed lines point out 0 amplitude and t=0. The shadowed areas highlight the considered time windows.*

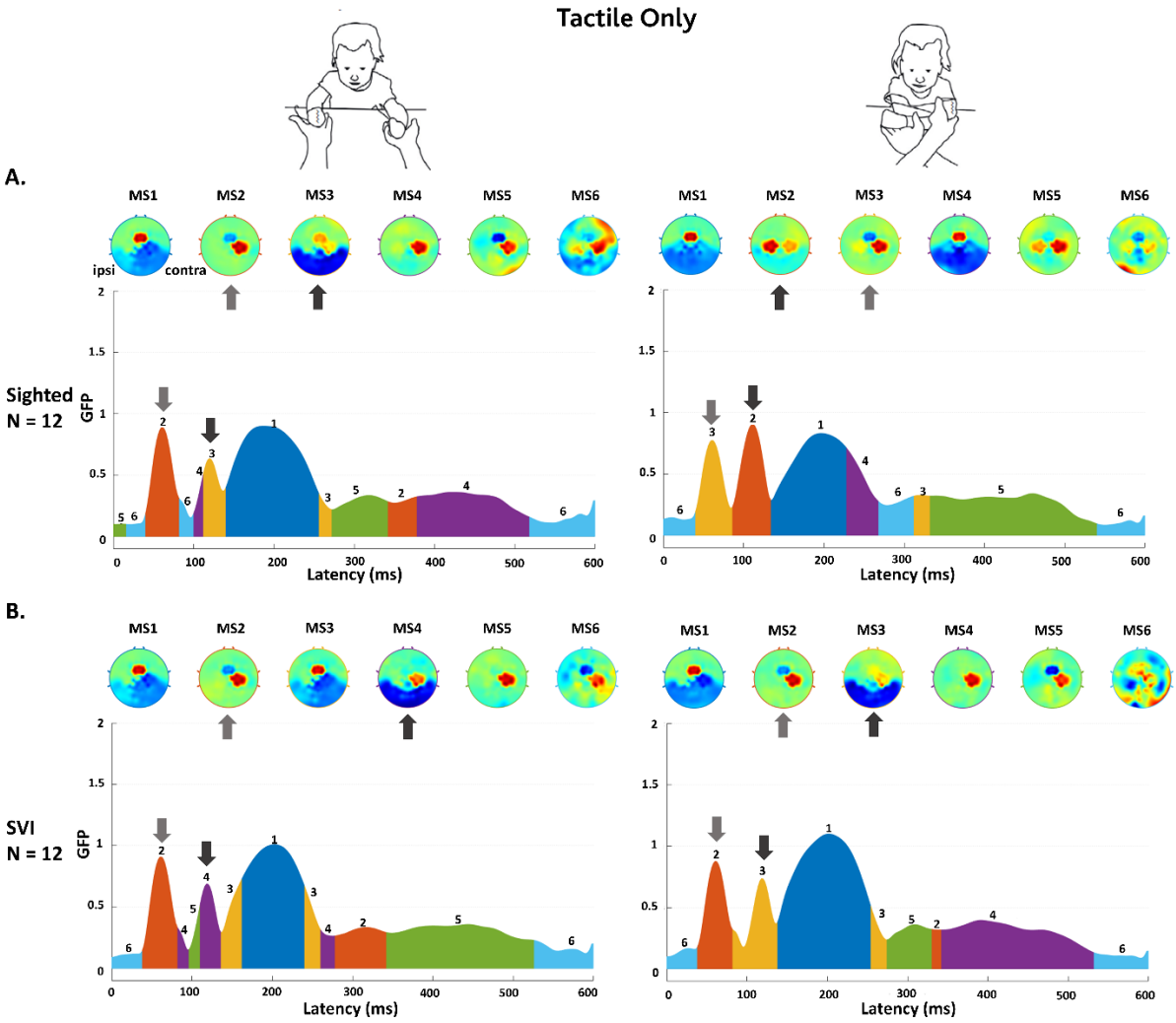

Figure 3.8. Microstates of tactile localization. *For each group (row) and posture (column), the results of the microstate decomposition analysis are as follows: for each subplot on the top, I report the topographic map of each microstate. At the bottom, I report the corresponding microstates' Global Field Power (GFP) and temporal segmentation.*

Considering the correlation with behavioral responses, during the uncrossed-hand posture, a positive relationship between the average ERP of the contralateral centro-parietal response and accuracy in the early time window is found for both S infants, R^2=0.71, p<0.001, and SVI infants, R^2=0.92, p<0.001. However, while both groups display centro-parietal positivity contralateral to the stimulated hand during the crossed-hand posture, a significant correlation between ERP mean, and accuracy is only observed in SVI children, with R^2=0.93, p<0.001. Conversely, S infants exhibit a distinct dual association in the [105-120]ms time window: ipsilateral centro-parietal positivity correlates negatively with behavioral outcomes, with R^2=0.72, p<0.001, whereas contralateral response continues to positively correlate with behavioral outcomes, with R^2=0.90, p<0.001. These results are summarized in Table 3.6 for the early time window and Table 3.7 for the late time window. Figure 3.8 specifically depicts this correlation and the outcomes of MVPA.

Tactile localization and remapping ERP – behavioral results

Time window	[45-65]ms							
	Posture uncrossed				Posture crossed			
Linear regression analysis								
	S		**SVI**		**S**		**SVI**	
	R^2	**p**	**R^2**	**p**	**R^2**	**p**	**R^2**	**p**
Ipsi - Accuracy*ERP mean	-	-	-	-	-	-	-	-
Contra - Accuracy*ERP mean	0.712	<0.001*	0.918	<0.001*	-	-	0.929	<0.001*
Generalized linear mixed models	*accuracy ~ *laterality * group * erp_mean + (1|subject)*				*accuracy ~ laterality * group * erp_mean + (1|subject)*			
	χ^2(df)		**P**		**χ^2(df)**		**P**	
laterality	5.004(1)		0.025*		0.405(1)		0.525	
group	0.349(1)		0.554		9.455(1)		0.002*	
erp_mean	0.172(1)		0.679		7.897(1)		0.005*	
laterality*group	0.419(1)		0.517		0.491(1)		0.483	
laterality*erp_mean	18.02(1)		<0.001*		0.180(1)		0.671	
group*erp_mean	0.481(1)		0.488		1.096(1)		0.295	
laterality:group*erp_mean	0.143(1)		0.705		13.9 (1)		<0.001*	
Post hoc GLMM								
Comparisons for laterality	**Ipsi**		**Contra**		**Ipsi**		**Contra**	
	Z	**p**	**Z**	**p**	**Z**	**p**	**Z**	**p**
S-SVI contrast	-	-	-	-	0.693	0.489	-3.809	<0.001*
Comparisons for group	**S**		**SVI**		**S**		**SVI**	
	Z	**p**	**Z**	**p**	**Z**	**p**	**Z**	**p**
Ipsi-contra contrast	-	-	-	-	1.388	0.181	-3.517	<0.001*

Table 3.6. Tactile localization ERP-behavioral result in [45-65]ms time windows. *Statistics of the linear regression and GLMM for each time window and posture evaluate the association between behavioral results and ERP amplitude.*

Tactile localization and remapping ERP – behavioral results

Time window	[105-120]ms							
	Posture uncrossed				Posture crossed			
Linear regression analysis								
	S		**SVI**		**S**		**SVI**	
	R^2	**p**	**R^2**	**p**	**R^2**	**p**	**R^2**	**p**
Ipsi - Accuracy*ERP mean	-	-	-	-	0.717	<0.001*	-	-
Contra - Accuracy*ERP mean	-	-	-	-	0.899	<0.001*	-	-
Generalized linear mixed models	*accuracy ~ laterality * group * erp_mean + (1|subject)*				*accuracy ~ laterality * group * erp_mean + (1|subject)*			
	χ^2(df)		**P**		**χ^2(df)**		**P**	
laterality	0.001(1)		0.999		0.001(1)		0.971	
group	0.362(1)		0.547		1.857(1)		0.173	
erp_mean	2.572(1)		0.109		0.218(1)		0.641	
laterality*group	0.003(1)		0.955		0.028(1)		0.868	
laterality*erp_mean	0.69(1)		0.406		3.383(1)		0.066	
group*erp_mean	2.112(1)		0.146		0.202(1)		0.653	
laterality:group*erp_mean	0.003(1)		0959		14.53(1)		<0.001*	
Post hoc GLMM								
Comparisons for laterality	**Ipsi**		**Contra**		**Ipsi**		**Contra**	
	Z	**p**	**Z**	**p**	**Z**	**p**	**Z**	**p**
S-SVI contrast	-	-	-	-	-3.143	0.002*	2.829	0.005*
Comparisons for group	**S**		**SVI**		**S**		**SVI**	
	Z	**p**	**Z**	**p**	**Z**	**p**	**Z**	**p**
Ipsi-contra contrast	-	-	-	-	-4.066	<0.001*	-1.279	0.2

Table 3.7. Tactile localization ERP-behavioral result in [105-120]ms time windows. *Statistics of the linear regression and GLMM for each time window and posture evaluate the association between behavioral results and ERP amplitude.*

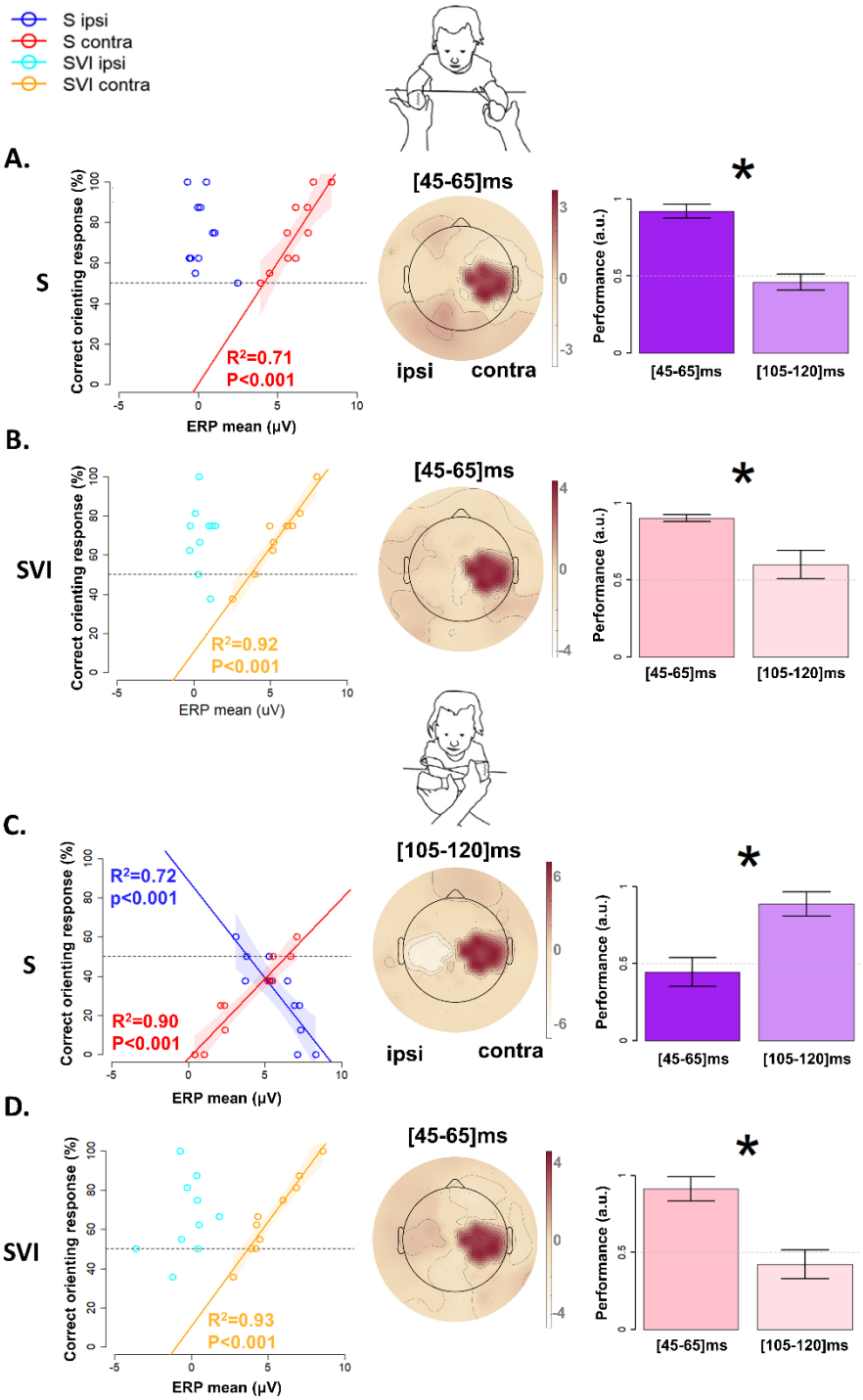

Figure 3.9. Tactile localization ERP-behavioral results. *For each Group (row) and Posture (column), the results of linear regression of orienting accuracy to ERP amplitudes (leftmost) and MVPA classifying multivariate EEG against the accuracy of the response (middle and rightmost) are reported. The maps represent the feature weight distribution over the scalp during the selected time window, with red and white colors indicating positive and negative associations with orienting performance. The rightmost subplot represents the decoding performance of the classifier (mean and SD) within the time windows. Stars indicate a significant t-test between time windows (P<0.05 after Bonferroni correction).*

Finally, Figure 3.9 shows the contralateral and ipsilateral ERSP response to tactile localization. The somatosensory stimuli seem to strongly modulate the high frequencies in alpha and beta bands contralateral to the stimulation in the first sensory processing stages. A significant difference is found between S and SVI infants only in the crossed-hand posture, which mainly involves alpha and low-beta activity. In agreement with previous results, an ipsilateral response is evident only in the crossed-hand posture in sighted infants, with a similar modulation of high frequencies, also shown in the contralateral response.

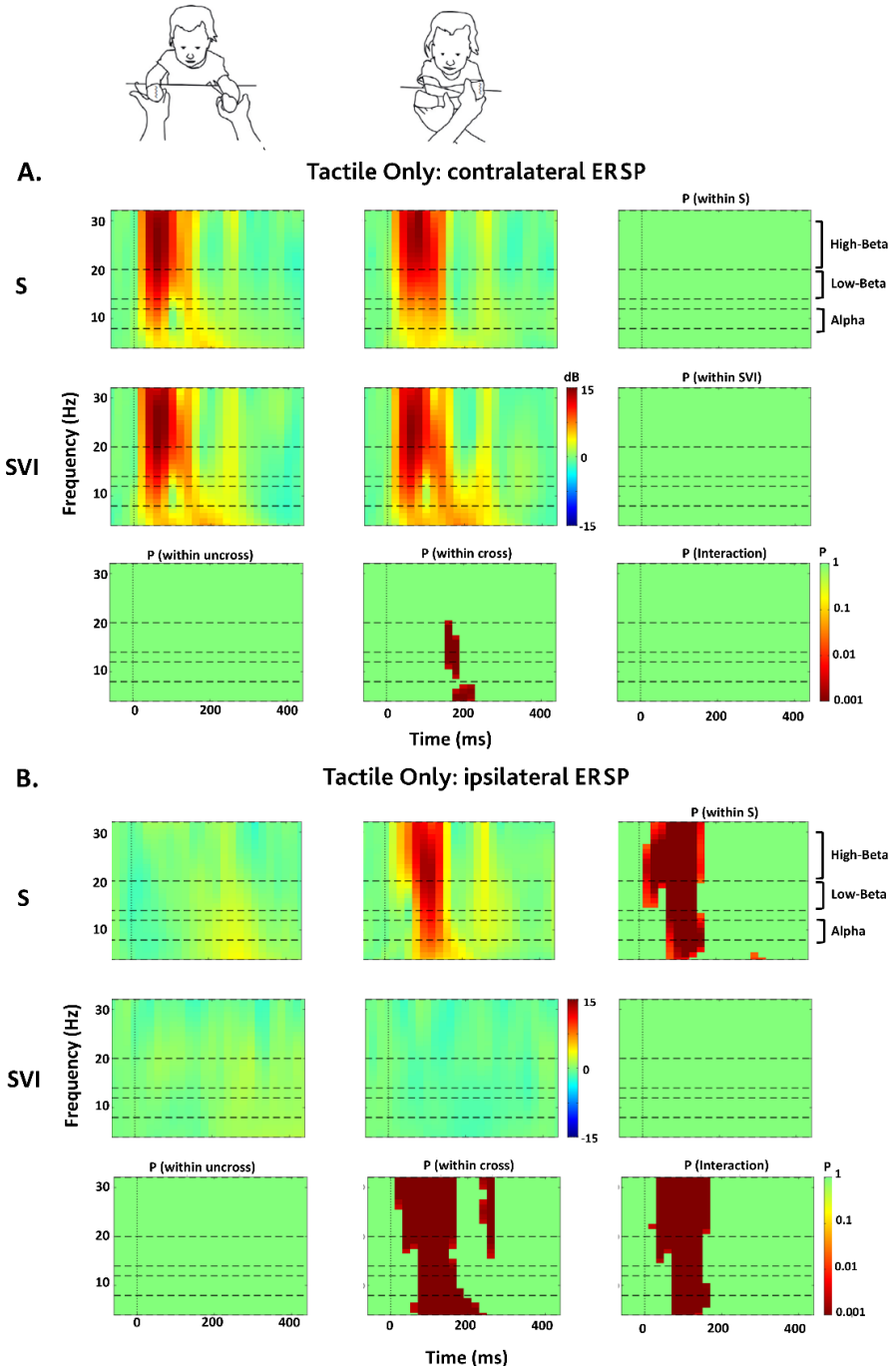

Figure 3.10. ERSP elicited by stimulus during tactile localization. *For each group (row) and posture (column), the results of the ERSP analysis were in the centro-parietal area. Each subplot reports ERSP (dB) as a function of time (ms, x-axis) and frequencies (Hz, y-axis). Vertical dotted lines represent t=0 (stimulus onset), while horizontal dashed lines represent frequency bands of interest. Figure (A) shows the contralateral response. Figure (B) shows the ipsilateral response. The last row and column represent the significant results after the false discovery rate (FDR) correction for multiple comparisons.*

3.1.3 Discussion of results

This study underscores how vision shapes the development of tactile brain processes during early childhood while auditory processes remain unaffected. In both uncrossed and crossed-hand postures, an early tactile ERP response is observed on the central area contralateral to the stimulated hand. However, only SVI infants show a correlation between this contralateral response and their behavioral orienting responses in the crossed-hand posture. Conversely, the later tactile response, occurring both ipsilaterally and contralaterally to the stimulated hand during the crossed-hand posture, was evident only in S infants and correlated with their behavioral response. These findings highlight a specific temporal hierarchy in somatosensory processing influenced by vision during early life stages.

Cortical processing of tactile perception begins in the primary somatosensory cortex (SI). It later extends to higher-order cortical areas, including the secondary somatosensory cortices (SII), the posterior parietal cortex, and the frontal cortices (Allison et al., 1992, 1989; Hämäläinen et al., 1990). These higher-order cortical areas continuously provide feedback to SI and other upstream components of the network to refine tactile information (Uppal et al., 2023). The involvement of SII reflects a remapping step in somatosensory processing, potentially influenced by feedback from the posterior parietal cortex (Buchholz et al., 2011; Macaluso et al., 2000; Schubert et al., 2008).

During uncrossed-hand posture, both S and SVI infants exhibit expected neural responses at the two critical early time windows, [45-65]ms and [105-120]ms, suggesting similar early tactile perception, as well as in the auditory domain. In terms of spectral activity, alpha and beta frequency bands are modulated. Behavioral responses are associated with the early time window, supporting its role in sensory processing (Brandwein et al., 2013; Russo et al., 2010). In this condition, the second time window merely reaffirms the localization of stimuli. In crossed-hand posture, a distinct temporal hierarchy emerges in tactile processing, shedding light on the influence of visual experience on touch-remapping abilities. Both groups initially show contralateral positivity, but S infants also exhibit ipsilateral activation early on, suggesting an early influence of spatial reference frames. Later, S infants demonstrate somatosensory remapping in the centro-parietal region, correlating with behavioral outcomes, while SVI infants do not, which is consistent with behavioral differences. The remapping process mainly modulates alpha and low-beta activity, helping to elucidate neural mechanisms of remapping even further. Specifically, alpha/beta

oscillations might provide a gating role, inhibiting parts of the brain that are irrelevant to processing and channeling processing elsewhere (Jensen and Mazaheri, 2010). I can speculate that sighted infants process somatosensory input first anatomically but then remap touch to external space, inhibiting contralateral processing with a contralateral alpha burst to allow high-frequencies band processing of somatosensory stimulus properties in ipsilateral SI/SII. Furthermore, this step seems to be supported by reduced activity in the posterior parietal cortex, whose feedback allows effective somatosensory remapping (Soto-Faraco and Azañón, 2013).

Overall, visually impaired infants process tactile events differently, relying on a body-centered spatial reference system. In contrast, sighted infants integrate tactile information into an external reference frame, indicating a two-step processing mechanism already apparent in brain responses. The results of this study provide important points of discussion about the brain mechanisms and the role of early visual experience during the processing of sensory and spatial information, which will be thoroughly examined in the overarching discussion outlined in Chapter 5. In the following study, I show preliminary results on the effect of sleep on sensory processing.

3.2 Exp.2: Sleep influence on sensory localization in visually impaired and sighed infants

The difficulties blind children face in shifting towards external coordinates, as discussed in the previous experiment, seem to stem from tactile information having more weight, typically linked to the body, than acoustic information, already oriented to the external environment (Gori et al., 2021). This starkly contrasts the behavior of sighted children, who tend to place higher importance on external auditory signals. This disparity in sensory perception suggests that blind children interpret sensory experiences differently, with profound implications for how these experiences are consolidated during sleep. Indeed, during sleep, the brain processes information acquired during wakefulness, encompassing the consolidation of multisensory experiences into long-term memories (Latchoumane et al., 2017; Tomé et al., 2022). Specifically, NREM sleep seems to have a central role in the synaptic plasticity mechanisms associated with memory formation, frequently linked with the occurrence of sleep spindles and slow waves (Miyamoto, 2023; Rothschild, 2019).

Therefore, I hypothesize that tactile information is more extensively consolidated during sleep in blind children, whereas auditory information takes precedence in the case of sighted children. Additionally, I propose that this effect might be more pronounced in sighted children due to their higher spindle activity compared to blind children. This consolidation effect could be measured by comparing the modulation of alpha activity in response to sensory stimuli between the post-sleep and pre-sleep stimulation phases. This modulation

typically manifests as a decrease compared to the baseline alpha activity (Fujioka et al., 2011; Shen et al., 2021). Measuring spectral activity instead of evoked potentials can offer further insights. Firstly, it can help determine if there's any correlation between the activity of sleep spindles and alpha activity. Secondly, it can help assess whether the lack of difference in alpha activity during the early years of life persists even when exposed to sensory stimuli.

Based on these hypotheses, I conducted a preliminary study involving 7 sighted and 7 visually impaired infants (0-3 years). I measured the modulation of pre- and post-sleep alpha activity in response to both an audio stimulus and a tactile stimulus presented to their hands - using the same caterpillar device (Gori et al.; 2019) and the positioning technique adopted in the experiment previously described in Section 3.1.

3.2.1 Methods

Participants

The simultaneous recordings of video and EEG (video-EEG) of 14 infants (7 S and 7 VI), aged between 5 to 35 months (mean age S= 1.23, mean age VI= 1.16) were collected during audio and tactile stimulations before and after a 50-minute nap possibility. None of the children had a history of prenatal infections, distress during delivery, genetic syndromes, or metabolic disorders. All the participants in this study presented with good general health status. All VI infants were exclusively affected by congenital disorders of the peripheral visual system (i.e., involving pre-chiasmatic structures). Cerebral visual impairment was excluded based on anamnesis, clinical and instrumental visual function assessment, and neurological examination. According to the statistical t-test, with $\alpha = 0.05$ and power = 0.80, 10 participants are needed to achieve a significant result if a large effect size ($d = 1.37$) is expected, as shown in a previous study (Campus et al., 2021).

Data acquisition and preprocessing

The experimental procedure, summarized in Figure 3.10, was as follows: The infants, accompanied by their parents/legal guardians, arrived at the EEG Lab of the Mondino Hospital between 13:00 and 13:30. After a thorough explanation of the protocol, the parents/legal guardians signed the informed consent form, according to the Declaration of Helsinki. Subsequently, the EEG montage was applied. The EEG recording started with a period of baseline brain activity at rest, lasting for at least one minute. Then, the stimulation protocol was initiated. This protocol involved presenting two sensory stimuli, tactile and auditory, to the infant's hands (adopting the same device and positioning explained in the previous experiment), each lasting for 30 seconds, resulting in a total stimulation time of two minutes. The auditory and vibrotactile stimuli were delivered separately to the infant's palms using custom-built stimulators (Gori et al., 2019). Stimulus-linked signals were sent to a visual stimulator behind the infant to signal stimulus onset and offset via the video recording.

The onset and offset signals were marked on the EEG trace during the offline preprocessing. During the next retention period, the participant lay down for a 50-minute sleep opportunity in a bed placed in a darkened and silent room. At the awakening, after 1 minute of well-represented awake EEG activity, the stimulation protocol was provided for the retest.

Brain electrical activity continuously recorded a 512 Hz sampling frequency using a Nicolet vEEG 5.94 system with 21 electrodes. The physical reference was placed in an intermediate position between Fpz and Fz. The light was switched off for the entire registration period, and an infra-red double camera recorded both the infant and the visual stimulator. In a later scoring phase, based on the EEG and video recording, the periods in which subjects were moving or falling asleep were excluded from the analysis, and the signal onset and offset were marked on the EEG trace.

Then, the EEG recordings were filtered between 0.1 and 100 Hz. Transient high-amplitude artifacts were removed using ASR. Data were then referenced to the average. For increasing statistical power, separately for each group and sensory modality, the electrode montage was swapped for conditions with stimuli presented on the right hand, allowing for the identification of contralateral or ipsilateral responses relative to the stimulated hand. With the cleaned swapped data of each subject, the power spectral density (PSD) expressed in uV2/Hz was computed for each stimulation condition and baseline both during pre and post-phases, applying the *spectopo* function of EEGLAB, which returns a PSD estimate via Welch's method using sliding time windows with a duration of 2 seconds and an overlap of one second.

Finally, continuous spectral activity from 0.5 to 13Hz was considered. The spectral activity was normalized by computing the relative spectral power, which measures the ratio of the absolute spectral power to the total power in the signal, to make the spectral activity comparable among participants. Then, the alpha peak for each participant was calculated. A three-stage approach was adopted to estimate background activity's peak frequency. First, the peak in the raw spectrum was searched for. Second, the peak in the spectrum after it was detrended using an exponential decay function was searched for. Toward this purpose, the logarithm of the power spectral density (PSD) at different frequencies was considered and fitted a linear regression model: log(PSD) = A + B•Frequency. In this way, the PSD using coefficients A and B estimated by the regression was computed, PSDest = exp(A) •exp(B•Frequency), and the peak in the detrended PSD PSDdetrend = PSD-PSDest was searched for. Both in the raw and detrended spectrum, the *findpeaks* function of the *pracma* package (Borchers, 2019) for R was used to automatically identify peaks in the background. Third, automatic peak estimates from stages one and two were compared, and where they differed (most times they matched), the most reliable peak position was selected by visual inspection. Analyses were performed considering both alpha peak frequency and peak amplitude.

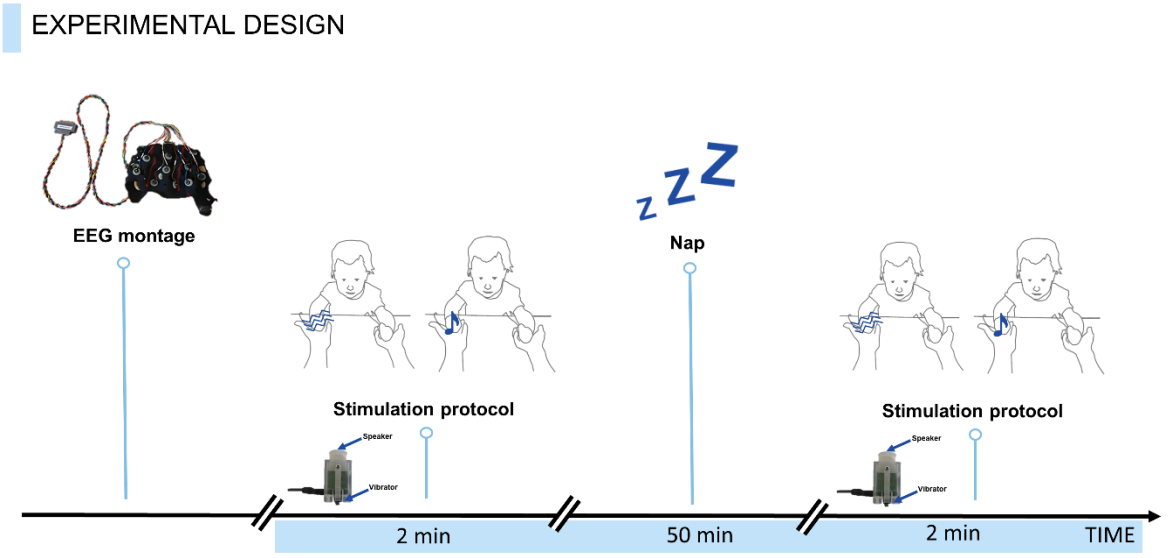

Figure 3.11. Experimental Design. *Representation of the temporal sequence of the experimental design.*

Statistical analysis

The electrode montage of the conditions with stimuli provided on the right hand was swapped separately for each group, posture and sensory modality to perform an analysis related to the physical characteristics of the stimuli, as well as to increase statistical power. Therefore, the response contralateral or ipsilateral to the stimulated hand was considered. Statistical analyses were then performed separately for each ROI: central right, i.e., contralateral (C4); central left, i.e., ipsilateral (C3); temporal right, i.e., contralateral (T4, T6); and temporal left, i.e., ipsilateral (T3, T5). Linear Mixed Models (LMMs) were fitted using the *lmer* function of the *lme4* package (Bates et al., 2015). The predictors were evaluated using Type III Wald $\chi 2$ tests, as implemented in the *Anova* function of the *car* package (Fox and Weisberg, 2018). According to Wilkinson's notation (Wilkinson and Rogers, 1973), the model fitted for each Roi and condition (audio/tactile) are:

Alpha peak frequency (during stimulation) ~ group(VI/S) session (pre/post)* Alpha peak frequency (baseline) + (1|participant)*

Alpha peak amplitude (during stimulation) ~ group(VI/S) session (pre/post)* Alpha peak amplitude (baseline) + (1|participant)*

The planned contrasts were further investigated, fitting the *lm* function for each condition and group separately.

3.2.2 Results

Preliminary results show that unisensory audio and tactile conditions involved the temporal-posterior and central areas, respectively, contralateral to the stimulated hand (see Figure 3.11). As per alpha peak frequency, a significant interaction between group, session, and alpha peak baseline is found for both audio ($\chi2(1) = 5.75$, $p=0.02$) and tactile ($\chi2(1) = 4.37$, $p=0.04$) conditions. Specifically, post-hoc analysis shows that differences between groups involve only the Post session for both audio ($F(1) = 10.24$, $p=0.02$) and tactile ($F(1) = 9.05$, $p=0.02$) conditions. When considering group differences, a specific modulation seems to emerge in the groups for different sensory stimuli: for the VI group, a significant frequency modulation seems to characterize tactile condition ($F(1) = 16.14$, $p=0.007$); in turn, for the S group, a trend for frequency modulation occurs for audio condition ($F(1) = 4.31$, $p=0.07$).

Furthermore, for alpha peak amplitude, a significant interaction emerges in the tactile condition ($\chi2(1) = 7.91$, $p=0.005$) and a trend in the audio condition $\chi2(1) = 3.86$, $p=0.05$). Post-hoc comparisons for tactile condition show results similar to those from peak frequency analysis with differences between groups only in the Post session ($F(1) = 18.12$, $p=0.005$) and specifically driven by the VI group ($F(1) = 14.27$, $p=0.009$).

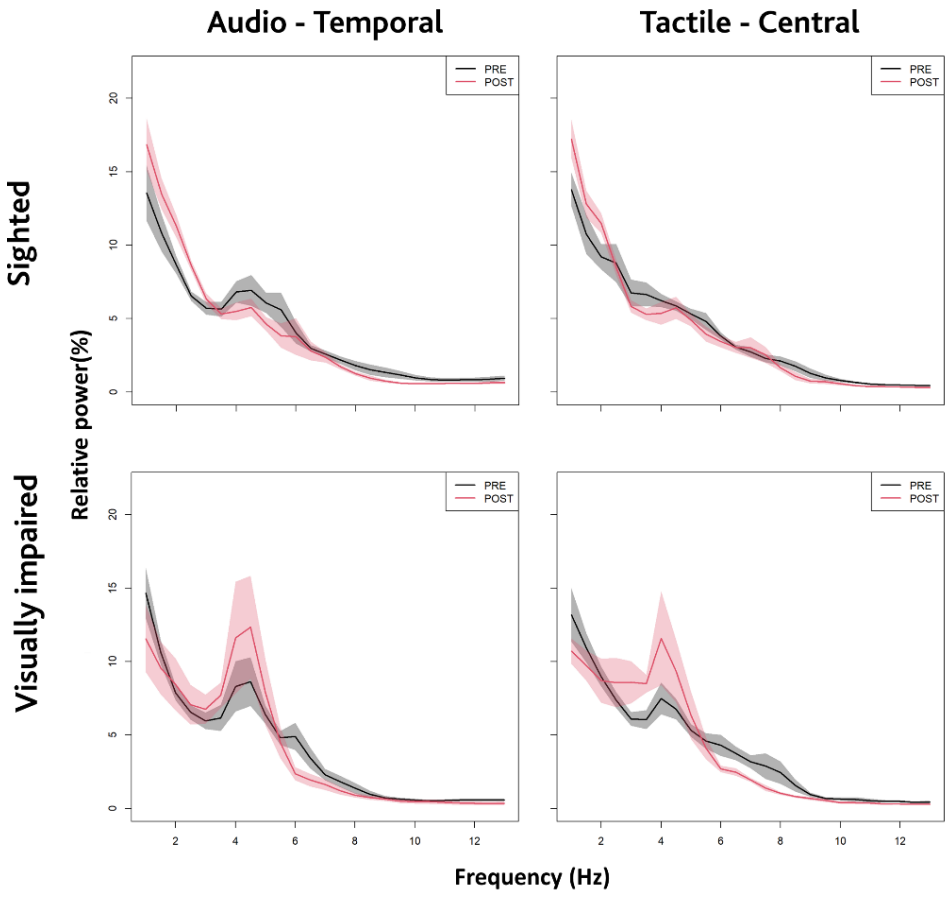

Figure 3.12. Audio and tactile spectral curve. *Each plot shows the spectral curve, calculated as the relative PSDs (%) vs the frequencies (Hz), for Pre and Post sessions. Rows represent groups, and columns represent conditions. For each condition, the plot refers to the specific relative ROI contralateral to the stimulated hand, respectively temporal right (T4, T6) for audio and central right (C4) for tactile sensory stimulations.*

3.2.3 Discussion of results

Although preliminary, these results seem to support the hypothesis, indicating that sleep promotes the strengthening of tactile responses over auditory ones in visually impaired infants. In contrast, the reverse is observed in sighted participants. These differences likely stem from the varying importance of auditory and tactile stimuli in blind versus sighted children. Consolidated during sleep, the heightened emphasis on tactile information may underlie structural and functional reorganizations within the neural structures following congenital visual deprivation (Blumberg et al., 2022; Lin et al., 2022). Indeed, visual deprivation induces plastic changes in the thalamocortical network, which plays a crucial role in information consolidation during sleep. Further insights on the role of the thalamocortical network in developing brain rhythm and sensory neurodevelopment will be largely discussed in Chapter 5. Future analyses will aim to elucidate the relationship between these observed effects and the microstructure of sleep. Additionally, I will explore the correlation between sleep features (e.g., spindles) and alpha activity to better understand the underlying mechanisms at play.

Chapter 4

Multisensory Technology for infants

Using the senses beyond sight in various interventions and assessments has shown significant benefits for populations lacking sight, as well as for the general population. However, multisensory interventions that combine visual, acoustic, tactile, proprioceptive, and motor cues are not commonly utilized. This limitation often stems from the lack of available technologies; many are still in the prototype phase and not yet on the market (Ben Porquis et al., 2017; Bertonati et al., 2020; Morelli et al., 2023; Ringland et al., 2014; Setti et al., 2022). Moreover, these technologies are rarely suitable for children. These challenges often extend to technologies used to assess spatial and multisensory abilities in children and individuals with visual impairments (Bertonati et al., 2023; Gori et al., 2019; Schiatti et al., 2020). The assessment tools should overcome more hurdles, reflecting the broader complexities of developing solutions for individuals with visual impairments. In addition, these tools are rarely validated for use during electroencephalographic recordings. The importance of validating devices during neuroimaging recordings opens up some reflections regarding the reliability and reproducibility of the results. This underscores the need to develop new technologies in this field, maximizing the potential of engagement and inclusivity offered by multisensoriality. In the next section, I present a new technological solution for investigating multisensory skills in infants during EEG recordings (section 4.1).

4.1 Dr-MUSIC: DRagons for MUltisensory Stimulation in Infants and Children

As extensively reported in Chapter 1, the early years of life are crucial for developing neural processing underpinning multisensory integration (MSI). During this time, our brains are inundated with sensory input from the external environment, which our peripheral cells capture and transmit to the brain for processing. However, at birth, our brains are not fully equipped to integrate signals from different senses, requiring learning and development to manage redundant information and perceive a coherent word. In some clinical conditions, the lack of one sense impacts how the external environment is perceived, such as blindness and deafness. Congenital disorders can compromise the ability to integrate multisensory information and perceive space, as in visual system disorders (Röder, 2012), and time, as in hearing system impairments (Scurry et al., 2020).

In this context, I introduce Dr-MUSIC, a novel technological solution designed to assess the early stages of MSI mechanisms during EEG recordings. To date, no technological devices provide specific multimodal stimulation with EEG-compatible timing and an attractive design for children. Dr-MUSIC comprises a couple of chubby dragons that can simultaneously provide uni-, bi-, or tri-modal information. To the best of our knowledge, only few solutions can provide up to tri-modal stimulations in a unique device (Gori et al., 2019; Schiatti et al., 2020), but without the possibility to customize the features of the stimulation. In this device, the color and the intensity of the light, the sequence and the intensity of vibration, and the type of sound can be modified, catering to various practical needs, as well as the duration of the stimulation. The amusing design enhances usability in young participants, and the possibility of changing the stimulation's characteristics makes it attractive even in infants with sensory impairments.

Therefore, Dr-MUSIC provides an effective, innovative system for investigating cross-modal and multisensory development in infants and children in a more natural and engaging environment during EEG recordings. It enables simulations of scenarios where information from one sense may be irrelevant or even conflict with another. Indeed, detecting and filtering out these oddball stimulations in these situations is crucial in developing efficient functioning.

I conduct a high-density EEG compatibility testing during an audio-tactile oddball task with sighted adults to validate its effectiveness. Then, I replicate the same task in a couple of toddlers, confirming its usability in young children.

4.1.2 Methods

Implementation of the device

Here, I briefly present the system's design from a mechanical and electronic point of view.

Mechanical Design

The device's mechanical design was developed using the PTC Creo Parametric 8.0 CAD platform, blending traditional parametric feature-based methods with free-form modeling for the external surfaces. Opting for a chubby dragon shape with a friendly appearance was a deliberate choice to make the device appealing to young participants while concealing the electronics in a compact form factor. The final design, depicted in Figure 4.1, incorporates all electronics onto a central support part, with the outer cover attached to it via two screws at the base. This design feature enables easy separation of the outer covers from the internal electronics, simplifying modifications to the external shape if needed based on user testing feedback. The dragons' tails also serve as guided wire exits for the electronics wiring. The covers were produced using additive manufacturing (AM, also known as 3d printing), specifically with a 3D Systems PRO SLS 6100 selective laser sintering (SLS) machine, using white Polyamide 12 (PA12 - Nylon) as the material. Leveraging AM in device development offers significant cost and time savings, facilitating design iterations and enhancing overall efficiency.

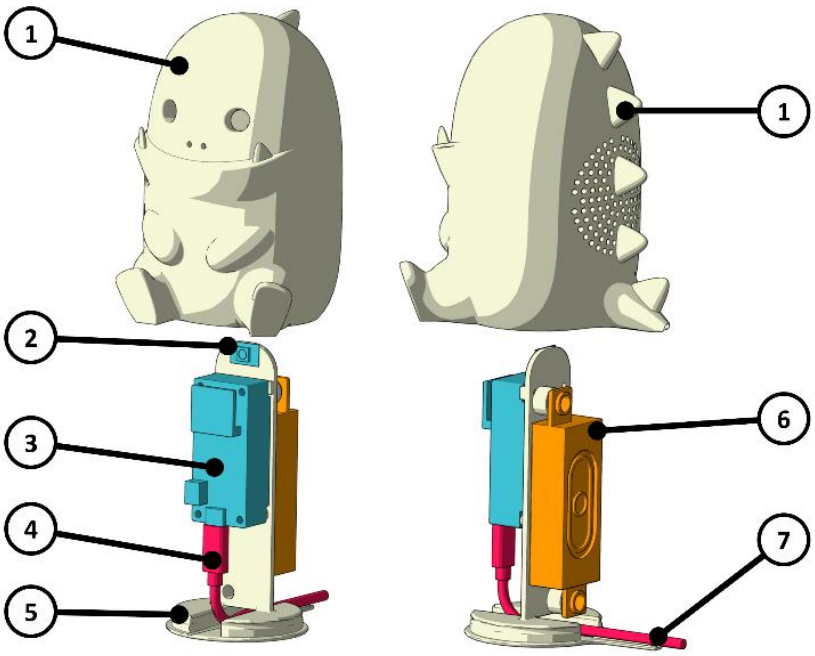

Figure 4.1. CAD view of the device. *The figure shows an exploded view of the device and its components: the outer shell (1), the LED (2), the electronic boards stack (3), the USB cable (4), the support structure (5), the loudspeaker (6) and the wire exit (7).*

Electronic and Firmware Design

Figure 4.2 presents the electronic block scheme of Dr-MUSIC, along with a high-level overview of the software functionality. The system was designed using commercially available Adafruit/Arduino development boards to facilitate implementation and enable rapid prototyping toward a fully engineered solution. It serves as a programmable multisensory output generator capable of producing audio, visual, and vibrotactile outputs. The main unit, Adafruit Feather M0, manages communication with a personal computer (PC) via a Virtual COM port emulated using a USB physical layer. This way, the user can implement high-level software using any development environment that can read and write a Universal Asynchronous Receive and Transmit (UART) interface, such as Matlab (as shown in the figure) or, alternatively, Python. Besides handling communication, the main unit interacts with peripherals to deliver multisensory outputs with accurate timing. Programmable audio outputs are facilitated by an Adafruit Music Maker module, which interfaces with the Feather M0 via a Synchronous Peripheral Interface (SPI). The module drives a miniature speaker with 8Ω impedance, capable of delivering 1W power. It supports microSD for storing audio data in PCM Wave or compressed MP3 formats. Vibrotactile feedback is achieved using an Inter-Integrated Circuit (I2C) vibrotactile driver DRV2605, offering various default vibrotactile profiles or asynchronous duty cycling vibration based on commands from the main unit. This setup utilized a 12kRPM DC Vibromotor compatible with the standard 3.3V regulated voltage in the main unit. Additionally, an RGB LED directly interfaced with the Feather M0 microcontroller was included to provide visual stimulation.

Dr-MUSIC requires the capability to swiftly deliver multisensory feedback, with a focus on audio signals. Given the availability of three stimulus types (audio, visual, and vibrotactile), the software ideally enables all hybrid combinations, allowing a single command from the PC to trigger diverse output types (e.g., audio/tactile, tactile/visual, visual/audio). To achieve this, specific commands for triggering multiple events without transmitting multiple serial commands have been devised, ensuring event jitter remains below 1ms. The internal microcontroller can execute multiple tasks faster than subsequent transmissions on the USB bus. To maintain simplicity in parsing incoming messages from the PC, a 16-bit integer-based transmission has been opted for. This approach offers a flexible and fast solution compared to more complex signaling schemes, facilitating real-time operation through fast decoding (shift and comparisons). Multisensory commands utilize the low byte (C7–C0), while the higher byte's most significant bits are reserved for implementing 64 color values with the RGB LED. Bits marked with X are unused in this context but could be leveraged to expand the device's functionalities in the future.

The trigger functionality in Dr-MUSIC is organized based on the incoming command value *i*. Commands in the 200–299 integer range are designated for audio stimulation. Within this range, there are 5 possible cases: 200 stops all sounds, while 201–205 play specific Wave files stored in the SD memory of the Music Maker. Integer values below 127 and

within the 300–399 range are dedicated to tactile stimulation. For i < 127, continuous tactile stimulation is emitted, with intensity proportional to *i*. When *i* equals 300, tactile stimulation ceases, while values 301–304 trigger specific tactile sequences. The range 500–599 is reserved for visual sequences, with the high-byte part triggering one of 64 possible colors. Additionally, ranges 500–599 and 600–699 are implemented to enable simultaneous audio/tactile and audio/visual multimodal stimulation. Notably, including a fallback command to halt stimulation (e.g., 200 or 300) is advisable to preempt potential issues in high-level software control, especially during initial development stages, thus obviating the need for power cycling to reset the device's state. Firmware development was carried out using the Arduino Integrated Design Environment (IDE) in C++, employing a bare metal approach to ensure maximum responsiveness following the command's reception. Upon peripheral initialization at power-on reset, the main loop waits for a new integer input to be decoded. If this occurs, it implements a selection on its value to call back the specific methods to access the peripheral buses and set the desired stimulation sequence.

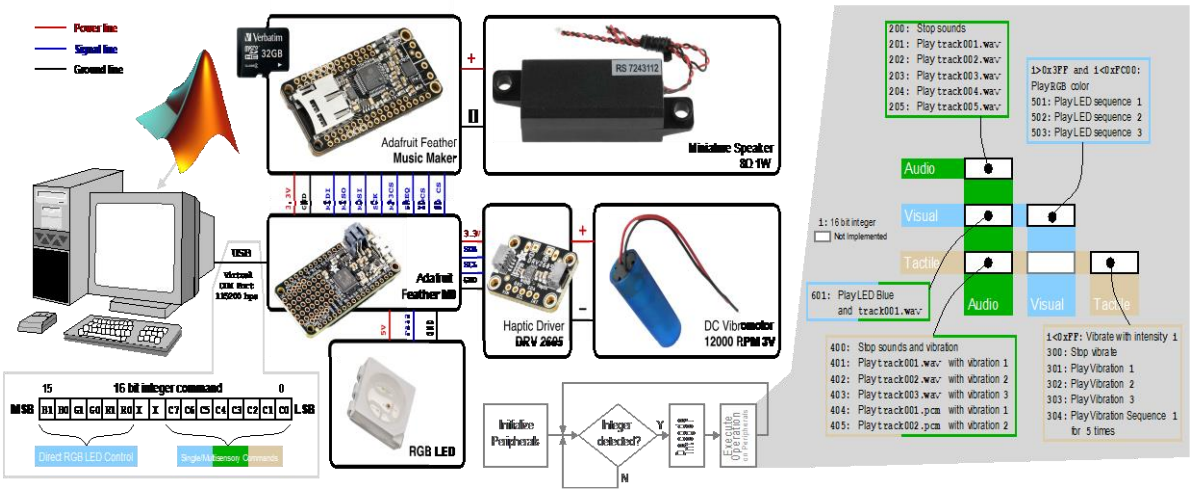

Figure 4.2. Block scheme device. *Block scheme of Dr-MUSIC with details on the components used and the scheme of the internal firmware implementation. The device can perform accurate multisensory stimulation thanks to integer-based dedicated commands.*

Experimental Protocol

Two experiments were conducted to assess the performance of our device using an audio-tactile oddball paradigm. In the first experiment, 8 adults (average age 30.74 years ± 5.44, 4 females) were recruited. Subsequently, the device's functionality was evaluated in a second experiment on two twin toddlers (age 35 months, with 1 female). All participants were recruited from local contacts in Genoa. The study received approval from the local ethics committee (ASL3 Genovese), and all participants or their guardians provided written informed consent in accordance with the principles of the Declaration of Helsinki.

Data acquisition and preprocessing

EEG data were collected using the EGI (Electrical Geodesics, Inc.) system with 129 electrodes, referencing the Cz electrode, and sampled at 1000 Hz. Before placement, participants' head sizes were measured to ensure proper positioning of the EGI net. The net was placed on their heads using sponges soaked in a salt-water solution. Participants were seated comfortably with the Dr-MUSIC device positioned in front of them, holding a small dragon for tactile stimulation in their right hand (see Figure 4.3A). As a common practice adopted in similar EEG experiments (Kadlaskar et al., 2021), to keep the participants more relaxed/compliant and to reduce movements, during the experiment, they watched a silent movie (Shaun the Sheep) while passively engaging in an audio-tactile oddball task. This task included 70% standard audio stimuli (750 Hz beep sound, command 201), 10% oddball audio stimuli (blazer sound, command 202), 10% oddball tactile stimuli (middle-intensity vibration, command 100), and 10% oddball audio-tactile stimuli (a combination of audio and tactile oddball stimuli, command 503). All stimuli lasted for 250 ms (see Figure 4.3B). A total of 600 trials were presented randomly, with at least one standard stimulus preceding every oddball stimulus. Throughout the experiment, participants were instructed to remain still and focus on the movie while ignoring stimuli from the Dr-MUSIC device. An experimenter, trained to monitor participant responses, was seated behind them.

The EEG signal was processed using custom scripts that integrated the EEGLAB (Delorme and Makeig, 2004) and Fieldtrip (Oostenveld et al., 2011) toolboxes. The continuous EEG signals were initially filtered between 1 and 45 Hz (zero-phase Butterworth filter, fourth order), followed by down sampling to 500 Hz. Artifact subspace reconstruction (ASR) was then applied to remove high-amplitude artifacts (Mullen et al., 2013). The data were segmented into epochs spanning from -1000 ms to 1000 ms after stimulus onset. Independent component analysis (ICA) was subsequently employed to further clean the EEG data, with artefactual components identified and removed based on manual inspection of topography, latency, amplitude, and trial distribution. Any previously removed noisy channels were interpolated, and the data were referenced to the average of the left and right mastoids (E57 and E100 electrodes). Finally, event-related potentials (ERPs) were derived by reducing epochs to a range of -200 ms before and 500 ms after stimulus onset, with a baseline correction of 200 ms before the stimulus onset applied.

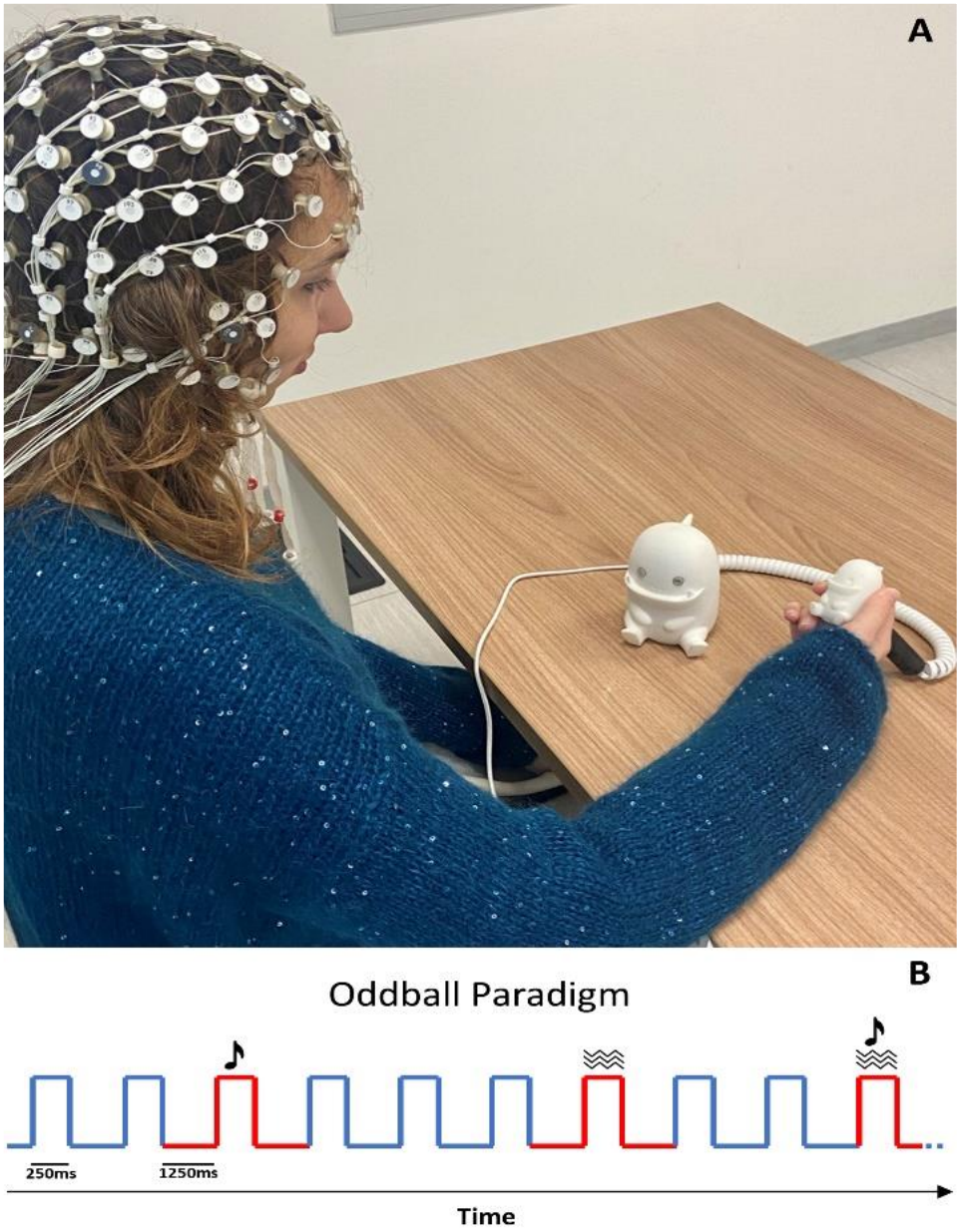

Figure 4.3. Experimental procedure of the audio-tactile oddball task. *(A) The figure shows an adult participant during EEG recording. (B) A representation of paradigm sequence.*

Statistical analysis

Two analyses were conducted to assess the efficacy of the Dr-MUSIC device in exploring multisensory and attentional mechanisms. Firstly, attentional mechanisms were examined within each group's grand averages by contrasting standard and oddball sounds. Secondly, the multisensory effect on attentional processes in our oddball stimuli was investigated using the additive criterion model (Mercier et al., 2013; Senkowski et al., 2007; Stein, 1998). This model defines the MSI effect as the non-linear summation of responses to multisensory

stimuli (AT), which differs from the sum of responses to unisensory stimuli (A+T); these effects can be supra- or sub-additive. Two-tailed cluster-based permutation t-tests were utilized to examine these processes across all channels (Maris and Oostenveld, 2007) and within the time window of 0 to 500 ms post-stimulus onset, employing 1000 random permutations. This non-parametric method enables multiple comparison testing across various channels and time points without assuming specific time windows or scalp locations where differences may arise. Additionally, this approach has been validated to maintain a correct type 1 family-wise error rate (FWER), even with small sample sizes (Pernet et al., 2015).

4.1.3 Results

This study validates the Dr-Music device in 8 adults and 2 toddlers during an EEG audio-tactile oddball task.

Audio-tactile Oddball in Adults

How auditory, tactile, and audio-tactile oddball stimuli modulate event-related potentials (ERPs) in adult participants was examined. The first analysis assessed attentional processing by comparing responses to oddball and standard sounds. The cluster permutation analysis on ERPs reveals a significant negative cluster ($p < 0.001$), indicating differences between standard and oddball stimuli responses. As shown in Figure 4.4A, This cluster spans from 258 ms to 392 ms over frontocentral channels, consistent with previous literature where rare sounds elicit changes in ERP responses during this time window (Tomé et al., 2015). Specifically, the N2 (250-300 ms) and P3 (300-400 ms) components are implicated in this attentional process. The oddball sound induces mismatch negativity (MMN) within the P2 component, represented by a negative peak following the N2 (Tomé et al., 2015). In the second analysis, the influence of multisensory integration (MSI) on attentional processing was explored by applying the additive model ($A+T \neq AT$) to assess interactions between unimodal and multimodal oddball stimuli. The cluster permutation analysis reveals a significant negative cluster ($p < 0.001$) between 144 ms and 212 ms over frontocentral channels, indicating a non-linear interaction between unimodal and audio-tactile stimuli within the N1 component (150-200 ms). This finding suggests the presence of the MSI effect, which was sub-additive, consistent with prior MSI research (Bernasconi et al., 2011; De Meo et al., 2015; Mercier et al., 2013).

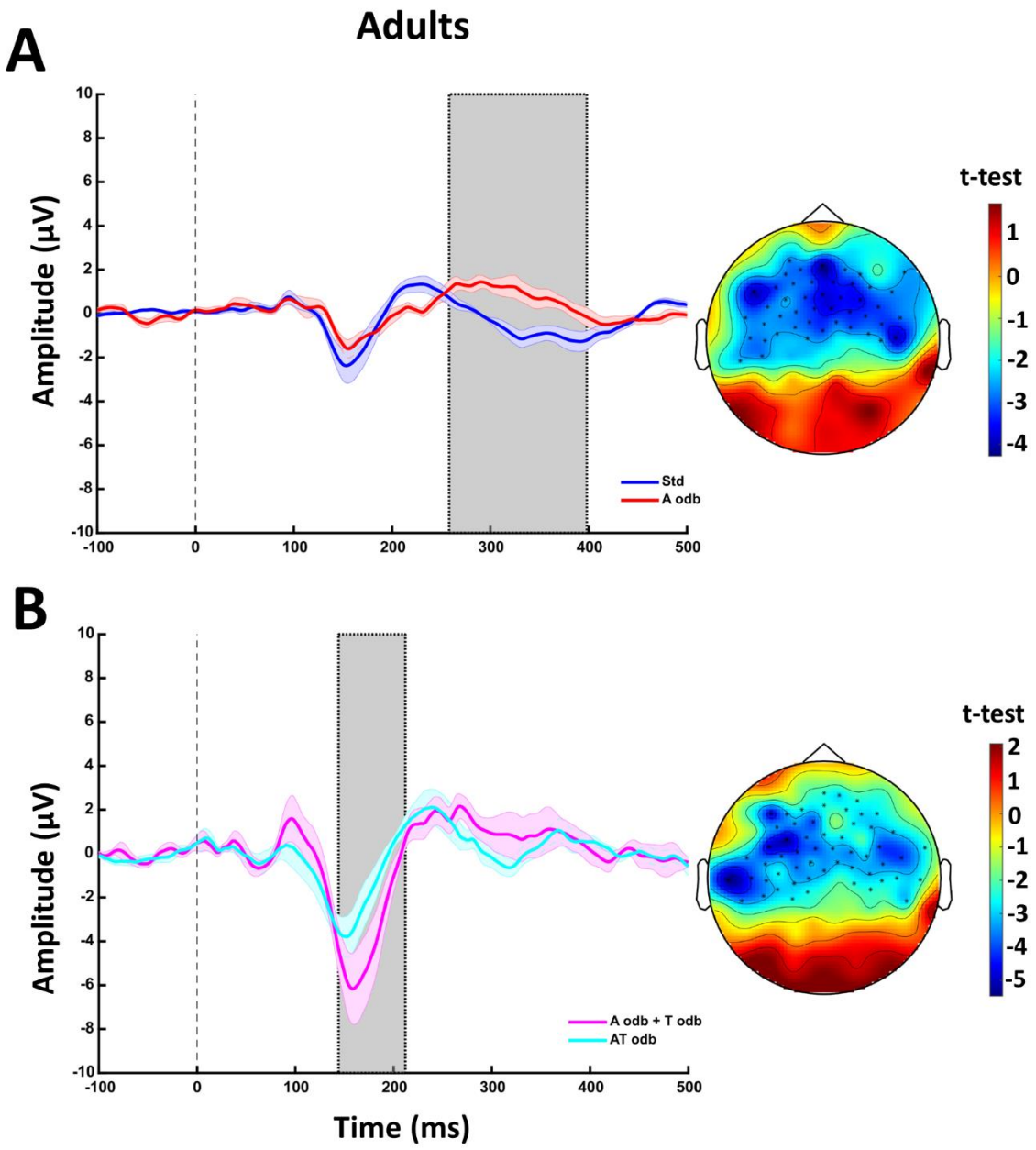

Figure 4.4. ERP results in the adult's experiment. *(A) shows the ERPs of the standard (blue) and oddball sound (red). (B) shows the ERPs in the additive model, comparing the auditory + tactile oddball stimuli (magenta) with the audio-tactile oddball (cyan). The ERPs are averaged across central electrodes. The shade bands represent the SE. The light grey areas highlight the time windows of the significant differences between the conditions. The maps represent the topographical distribution of the significant t-values in the comparison of the two conditions; the crosses represent the electrodes included in the significant negative clusters.*

Audio-tactile Oddball in Toddlers

In this second experiment, I assessed the usability of the audio-tactile oddball paradigm using Dr-MUSIC in young children and evaluated the toddlers' engagement during the session. The children actively interacted with the device throughout the approximately 40-

minute experiment, holding the small dragon in their hands. The EEG analysis reveals a negative cluster ($p < 0.001$) between 298 ms and 318 ms over central channels (Figure 4.5), indicating the presence of attentional-orienting processing in the mismatch negativity (MMN) domain, consistent with findings in similar studies (Choudhury and Benasich, 2011). Notably, no significant clusters are observed when examining the additive model in uni- and multi-modal oddball stimuli. The absence of a multisensory integration (MSI) effect aligns with the understanding that this process develops in later stages (Brandwein et al., 2013). However, further investigations with larger participant groups will be essential to validate and extend these findings.

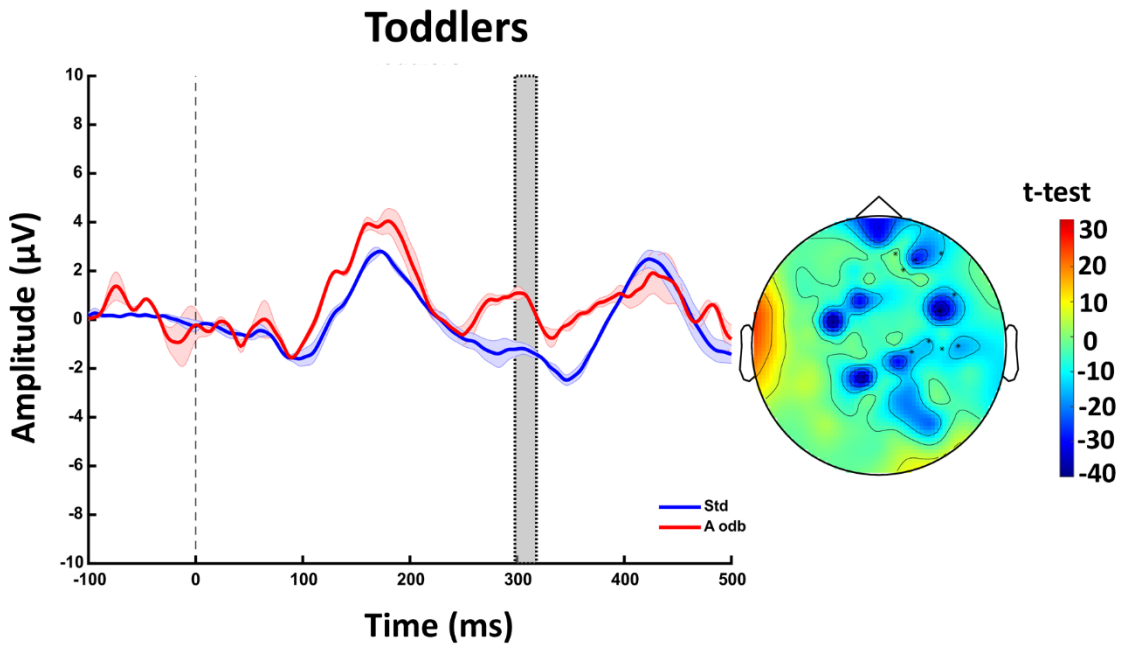

Figure 4.5. ERP results in the toddler's experiment. *The figure shows the ERPs' standard (blue) and oddball sound (red). The ERPs are averaged across central electrodes. The shade bands represent the SE. The light grey areas highlight the time windows of the significant differences between the conditions. The maps represent the topographical distribution of the significant t-values in comparing the two conditions; the crosses represent the electrodes included in the significant negative clusters.*

4.1.4 Discussion of results

This study presents a novel and efficient technological solution for investigating cross-modal and multisensory development during high-density EEG recordings in young individuals. The experiments successfully validated the applicability of Dr-MUSIC in EEG recordings with both adult and toddler participants, effectively capturing changes in brain activity in response to unattended oddball stimuli, consistent with existing literature. Additionally, I observe an audio-tactile multisensory integration (MSI) effect in the N1 domain among

adults but not in children, underscoring the significance of exploring the neural mechanisms underlying MSI during brain development to delineate the developmental milestones critical for optimal multisensory processing. Moving forward, I plan to employ our system in both typically developing children and those with sensory and neurodevelopmental disorders. The ultimate goal is to identify the onset of developmental deviations in MSI abilities, informing the design of early intervention strategies.

Notably, ensuring the accuracy and reliability of neuroimaging recordings is paramount in neuroscientific research. Validating devices during EEG data acquisition plays a crucial role in enhancing the reliability of results. By validating these devices, researchers can mitigate potential sources of error or interference. Increasing the reliability of data acquisition and analysis is critical to detecting early differences in brain and cognitive development. Although my new device still has to pass many tests to advance and be considered a medical device, it is important to underline the importance of initial validation during the acquisition of brain activity. Indeed, as a member of the "reliability working group" for EEG studies of the "RESPECT 4 Neurodevelopment" network (https://respect4neurodevelopment.com/activities/another-activity/) it is my duty to underline that to obtain reliable and reproducible results, responsible behavior, and validation strategies should be applied at all levels of a research study starting from the device used. This allows us to advance technologically to obtain increasingly scalable and customizable devices. In this way, it will be possible to ensure that neurotechnology can be used in different labs, clinics, or homes and can be tailored to individual children's needs and characteristics. Further observations will be discussed in Chapter 5.

The reported data have been partially extracted and adapted from: *Bollini A*[†]*, Vitali H*[†]*, Crepaldi M, Parmiggiani A, Campus C, Lorini C, Gori M. Dr-MUSIC: An Effective Device for Investigating Multisensory Mechanisms during Development with EEG recordings (2023). Annu Int Conf IEEE Eng Med Biol Soc.* Figures were reprinted with permission © 2021 IEEE.

Chapter 5

General discussion

The overall aim of the current Ph.D. project is to investigate how the lack of one sense, as in the case of blindness, affects the neural mechanisms and multisensory skills development in early life and specify the role of sleep in constructing a multisensory representation of the world. To this end, the project involves different studies that compare the development of neural mechanisms between blind and sighted children. After a general introduction to brain development and the complexity of the multisensory world (Chapter 1), I illustrate the evolution of neural mechanisms in childhood during waking and sleeping stages (Chapter 2) and during spatial multisensory tasks in infancy (Chapter 3). Subsequently, I report a possible technological solution to investigate these processes in early life better (Chapter 4). Neurophysiological differences between blind and sighted children could be interpreted from a broader perspective of a different brain development, specifically related to thalamocortical activity.

5.1 The thalamocortical network in blindness

In Chapter 2, I investigate the development of brain oscillations during waking and sleeping stages and how blind children deviate from the typical developmental trajectory. During wakefulness, the development of alpha activity appears to be one of the primary processes impacted by blindness (see section 2.1). Specifically, alpha activity appears to progress similarly in blind and sighted children in their early life, indicating that visual deprivation may alter or partially suppress the neural processes underpinning alpha activity later in childhood. This divergence is most noticeable between the ages of 3 and 6, a critical period for social interactions, spatial exploration, and the development of executive functions (Bollini et al., 2023; Cappagli et al., 2019, 2017; Houwen et al., 2009, 2007; Sabbagh et al., 2009). Indeed, when I consider the associations with motor dysfunctions, starting from this period, lower alpha activity in blind children heightens the likelihood of both motor

coordination impairment and hypotonia. This supports the hypothesis that a perceptual deficit resulting from a lack of vision can reduce a person's capacity to interact with their external environment, potentially negatively affecting motor development. Notably, the differences in alpha activity between blind and sighted children, as well as the correlations with motor disfunction indices, first emerge in the alpha1 sub-band, followed by alpha2. This evidence suggests that visual deprivation primarily impacts low-level attention-related neural processes and only later alters high-level processes related to semantics and memory.

In terms of the underlying neural mechanisms involved in the maturation of alpha activity, I present in Chapter 1 that alpha waves primarily originate from the thalamocortical network (Andersen and Andersson, 1968; Andersson and Manson, 1971) and/or cortico-cortical connections (Pfurtscheller and Lopes da Silva, 1999). However, which of the two networks is specifically affected by blindness is not fully clear, as well as if the reduced occipital alpha power in blind children may result from attenuated inhibitory circuits (Sherman and Spear, 1982) and/or from the atrophy of structures involved in the rhythm's generation. On one side, the lateral geniculate nuclei (LGN) are known to be atrophied following blindness in animals (Berman, 1991; Rakic et al., 1991) and humans (Breitenseher et al., 1998). Conversely, an alteration of the neural connections involved in the cortico-cortical network is observed in cases of early visual deprivation (Sherman and Spear, 1982). Specifically, pyramid cells of cortex layer V exhibit intrinsic rhythm-generating properties capable of producing synchronous alpha waves (Pfurtscheller and Lopes da Silva, 1999). Interestingly, the pyramidal cells in layer V of the primary visual cortex maintain strong connections to the superior colliculi (SC), which plays an essential role in controlling eye movements (Wenzhi and Yang, 2009) and multisensory integration (Stein and Meredith, 1993). In animals, direct visual input to the SC decreases significantly after congenital visual deprivation (Vidyasagar, 1978).

Although the results presented here cannot fully elucidate these complex alterations in neural structures, understanding how the development of alpha activity deviates in blind children may shed light on these processes. First, alpha activity seems to develop similarly in both blind and sighted children but diverges notably later on. This finding suggests that a degenerative process over time, such as atrophy of involved structures or a reduction in neural inputs to the visual cortex, may be at play rather than an early alteration in the formation of pyramidal cells. Second, both the shift to faster frequencies in brain activity and the variations in alpha power with development reflect the maturation of neural networks. As we grow, the relative alpha power increases, mirroring structural changes in thalamocortical connectivity, while the overall alpha oscillatory power decreases due to synaptic pruning processes (Cragg et al., 2011; Mcsweeney et al., 2023; Tröndle et al., 2022; Whitford et al., 2007). Considering that I specifically investigated the relative alpha power, an absence of its maturation in blind children suggests that developmental processes in the thalamocortical connectivity may be altered. While recent research indicates that an alteration of aperiodic brain activity in congenitally blind adults that persists after sight

restoration is linked to an altered excitatory/inhibitory (E/I) balance in the cortical network due to a deficit in the functioning of inhibitory interneurons, it is possible that this mechanism only partially involves the reduced grow of alpha activity (Ossandón et al., 2023). Indeed, an early disruption in thalamocortical activity could first affect alpha activity's growth, with subsequent potential repercussions on the excitatory/inhibitory (E/I) balance.

The findings from my sleep study further bolster the evidence of how blindness can affect the development of thalamocortical pathways (see section 2.2). Indeed, sleep spindles, known to mirror the activity of those pathways (Fernandez and Lüthi, 2020), demonstrate an aberrant maturation in blind children, suggesting that vision plays a crucial role in the proper development of spindle generators. Specifically, the generation of spindles is attributed to the thalamus (Morison and Bassett, 1945; Timofeev and Steriade, 1996). Within the thalamus, spindles originate through activating cells in the reticular thalamic nucleus (RTN), which triggers inhibitory currents in thalamocortical (TC) neurons. This inhibition leads to a rebound effect in TC neurons, further stimulating the RTN (Bal et al., 1995). Cortical neurons are stimulated in synchrony by thalamocortical neurons, generating cortical field potential spindles. However, the cortical network does not merely passively mirror thalamic spindles; instead, it actively initiates spindle onset, especially during slow oscillations, and also plays a significant role in their termination (Bazhenov et al., 2001; Bonjean et al., 2011; Contreras and Steriade, 1996).

While this model is still valid, it does not fully elucidate the mechanisms underlying sleep spindles, particularly the distinction between slow and fast spindles (Timofeev and Chauvette, 2013). Indeed, these two types are linked to different generators. Whereas the traditional thalamocortical mechanism effectively explains the neural process behind fast spindles, it falls short in elucidating the generation of slow spindles (Ayoub et al., 2013; Timofeev and Chauvette, 2013). Other mechanisms in the thalamocortical circuits, or probably in the intra-cortical connections, might be responsible for slow spindle generation. The specific impact of blindness on the development of fast spindles highlights its effect on sensorimotor processing during sleep and the involvement of the thalamocortical network. Notably, differences between blind and sighted infants in high-sigma and high-beta power emerge from my data as early as three years of age and are correlated with visual impairment indices. This finding suggests that deviations in brain structure development between sighted and blind children manifest earlier during sleep than during wakefulness, consistent with the fact that sleep constitutes a significant portion of an infant's hours. Moreover, the early association with perceptual indices and the later association with motor functions validate the hypothesis that alterations in perceptual abilities could precede subsequent motor difficulties observed in blind children.

Therefore, the sleep study findings support the notion that compromised thalamocortical maturation may represent the earliest neurophysiological mechanism affected, potentially leading to future impairments. An impairment in high-frequency spindles' mechanisms could

also explain why children with blindness start with a slower spindle frequency. It is plausible to speculate that the slower spindle frequency observed in blind children in their early years may be linked to processes occurring in their first six months of life, which were not considered in my study. Previous research has indicated that during the first months of life, there is a rise in spindle frequency followed by later decreases (D'Atri et al., 2018; Kwon et al., 2023; Louis et al., 1992). This increase is likely attributed to enhancing synaptic connections related to thalamocortical connectivity. A slower spindle frequency observed as early as 6 months of age in blind children may be associated with an early disruption of this mechanism.

Overall, both an impairment in alpha activity and sleep spindle development in blindness might be linked to abnormalities in thalamocortical activity. Given that the thalamus plays a central role in transmitting sensory information to the cortex, how could altering these connections affect multisensory processing? Let's step back and consider what occurs after birth to promote sensory neurodevelopment. Recently, a conceptual framework has been proposed to integrate prevalent theories on sensory neural development and their connection to waking and sleeping states (Blumberg et al., 2022).

5.2 State-dependent modulation of sensory neurodevelopment

The most common framework for understanding sensory neurodevelopment focuses on spontaneous and intrinsic activity in the sensory periphery or downstream neural structures (Martini et al., 2021). For instance, spontaneous bursts of activity in the retina, cochlea, or limbs are believed to shape the development of the visual, auditory, and somatosensory cortex (Meng et al., 2021). Therefore, the reliable transmission of sensory signals underscores the crucial role of the periphery in directing and organizing inputs to the developing brain, which is essential for forming an integrated functional system between the brain and body.

However, animal studies on the visual system showed that the intrinsic activity within the primary visual cortex and the lateral geniculate nucleus (LGN) of the thalamus, along with interactions between these structures, also play a significant role in the scalping of the sensory pathway (Weliky and Katz, 1999). When peripheral information is removed, all LGN activity is initially lost, with activity levels gradually recovering over time (Chiu and Weliky, 2001; Weliky and Katz, 1999). However, the restored LGN activity does not revert to its original spatiotemporal pattern but reorganizes into a new pattern. This recovery process of LGN activity following the deprivation of peripheral inputs may reflect a form of homeostatic plasticity akin to what occurs in other systems when neural input is experimentally altered (Turrigiano and Nelson, 2004). Furthermore, the inactivation of LGN

results in a significant reduction (about 90%) in primary visual area activity (Smith et al., 2018). Beyond the visual system, studies investigating the whisker somatosensory system in mice also reveal the critical role of thalamic activity in the development of cortical somatotopy. In the whisker system, mechanoreceptors that transduce whisker movement transmit somatosensory input across the brainstem to the ventral posteromedial thalamic nucleus (VPM), which then relays this input to the corresponding whisker representation area in the primary somatosensory cortex. In adults, the arrangement of whiskers on the snout is represented by anatomical shapes and functional maps in VPM and somatosensory cortex. However, the initial development of functional maps in the cortex relies on patterned inputs originating from the fetal VPM (Antón-bolaños et al., 2019).

In summary, research into the development of the visual and somatosensory systems reveals a complex interplay of activity among the sensory periphery, thalamus, and cortex, which collectively contribute to the optimal development of these sensory systems. Building upon the insights provided in Chapter 1, it is conceivable that this intricate interconnection may also influence the maturation of alpha activity observed during developmental stages. Alterations in activity patterns at these levels can result in aberrant developmental outcomes. Importantly, sensory neurodevelopment is not solely influenced by waking activity but is also shaped and refined through activity occurring during sleep, highlighting the crucial role of sleep in neural plasticity and development.

During sleep, an extended neural network is activated, favoring brain plasticity (Brzosko et al., 2019; Jones, 2020). Sleep-dependent neuromodulation promotes local effects on specific sensory systems and global effects on overall nervous system function. Both REM and NREM sleep stages seem to contribute to sensory plasticity. Synaptic pruning, a crucial process in early neural development, contributes to modeling neural circuits during sleep, although the exact mechanism by which stable circuits are defined remains incompletely understood. In the first months of life, REM sleep enhances functional connectivity in distant sensorimotor structures through synchronous oscillatory activities, such as hippocampal theta rhythm. This rhythm is closely linked to neural plasticity (Boyce et al., 2016; Puentes-Mestril et al., 2019). Early in life, it first emerges as short bursts in response to contractions (Mohns and Blumberg, 2008). Moreover, contractions also trigger spindle activation in the somatosensory cortex of neonatal rats and premature human infants (Khazipov et al., 2004; Milh et al., 2007). Spindle bursts, characterized by short thalamocortical oscillations with a dominant frequency of 15 Hz, have been observed in sensory and motor cortical regions in response to sensory inputs (Hanganu et al., 2006; Tiriac et al., 2022). The period of prominent spindle production also overlaps with a period in which whisker somatotopic maps are refined in mice (Mitrukhina et al., 2015), while in mammals, these spindle bursts, also known as delta brushes in human infants, are recognized features of early cortical development (Murata and Colonnese, 2019).

Although spindle bursts play a crucial role in early cortical development, their significance diminishes rapidly. In human newborns, spindle bursts vanish by the end of the

first postnatal month (Whitehead et al., 2018). Subsequently, another thalamocortical oscillation emerges during non-REM sleep, known as sleep spindles, characterized by a similar dominant frequency (12–15 Hz) as spindle bursts but with specific associations with NREM sleep (Sokoloff et al., 2021; Wakai and Lutter, 2016). Sleep spindles are strongly linked to neural plasticity, including sensorimotor and visual plasticity, across development and throughout the lifespan of humans and rodents (Fernandez and Lüthi, 2020; Menicucci et al., 2022). Additionally, limb contractions in human infants are not exclusive to REM sleep; they also occur during NREM sleep, starting around 3 months of age (Sokoloff et al., 2021). Furthermore, NREM sleep becomes increasingly abundant in sleep spindles around this age, particularly in the sensorimotor cortex. Notably, arm and leg contractions during NREM sleep synchronize with sleep spindles. Besides the previously understood contractions during REM sleep, there's another noteworthy occurrence: contractions coincide with the NREM sleep component, fostering plasticity. This discovery unveils a novel type of sleep-dependent sensorimotor plasticity that emerges after some months of life.

Indeed, a more articulated system may emerge that incorporates the sleep-mediated reprocessing of multisensory and sensorimotor memories acquired during wakefulness. Studies on songbirds show that they can learn their distinct songs through a sophisticated process of memorization and sensorimotor learning facilitated by NREM sleep. Juvenile birds initially produce highly variable vocalizations, then memorize a song model provided by an adult "tutor," and gradually refine their singing performance by comparing auditory feedback with the memorized model. During this period of sensorimotor learning, neural activity during sleep plays a pivotal role (Giret, 2019). Similarly, NREM sleep facilitates the learning and imprinting visual characteristics of biologically relevant stimuli in newly hatched chicks (Jackson et al., 2008). Hence, in both songbirds and chicks, sleep serves as a crucial context for sensorimotor and visual system plasticity, respectively. Sleep-dependent learning and memory processes can enhance developmental neural plasticity, facilitating the functional integration of the brain and body (Rasch and Born, 2013). Although the mechanisms by which salient multisensory experiences are consolidated into long-term memories are not completely clarified, it is well established that a hippocampus-thalamus-cortex circuit is involved in this function, coordinating synaptic plasticity timescales during NREM sleep (Latchoumane et al., 2017; Tomé et al., 2022). The activity of this network at the cortical level appears associated with both sleep spindles and slow waves (Miyamoto, 2023; Rothschild, 2019).

5.3 The role of vision for sensory neurodevelopment

Overall, the evidence outlined in the previous subchapter highlights the pivotal role of the thalamocortical axis in developing sensory systems, with its activity during sleep fostering

their shaping, possibly incorporating sensory memories from everyday experiences. However, the specific mechanisms through which sleep facilitates this plasticity remain largely unknown. To shed light on these mechanisms in the context of this thesis, I conducted a preliminary study based on the hypothesis that NREM sleep activity could accentuate the sensory disparities observed in sighted children compared to blind infants during the early years of life.

Sighted children appear to prioritize auditory over tactile information when localizing stimuli, whereas blind children exhibit the opposite behavior (Gori et al., 2021). This preference for tactile over auditory spatial information in blind children may stem from the absence of vision, resulting in a more limited sensory framework for orienting to distant stimuli. Moreover, some aspects of spatial perception in visual deprivation may arise indirectly from multisensory differences rather than solely from the absence of vision. The bias towards responding to tactile rather than auditory stimuli could also lead to more reliance on body-centered coordinates and features. Thus, this differential weighting of sensory modalities could contribute to the challenges faced by blind children in remapping information within internal and external spatial coordinates, as discussed in section 3.1. Indeed, the ability to remap stimuli on the external reference frame emerges from the interplay between our senses and environmental interactions and requires several years to develop (Röder et al., 2014; Ruggiero et al., 2016). Specifically, the maturation of the visual system favors the shift from body to external coordinates to represent the space (Bremner et al., 2013). The absence of visual experience seems to prioritize bodily stimuli (i.e., tactile perception) and maintain a body-centered reference system as a default.

As previously explained, NREM sleep reinforces the most salient sensory information relevant to waking experiences. Visual information may be paramount in sighted individuals, while tactile information assumes greater importance in blind infants. However, in the absence of vision, sighted children may prioritize acoustic information during sleep, as they are already oriented towards interacting with the external environment. Therefore, synaptic pruning processes during sleep may strengthen tactile information in the blind and acoustic information in the sighted, reflecting their respective sensorial salience in daily experiences. To validate this hypothesis and deepen our understanding of the role of sleep in sensory plasticity, I conducted a preliminary study investigating the modulation of pre- and post-sleep alpha activity in response to both an audio stimulus and a tactile stimulus presented to the infant's hand (see section 3.2.). The preliminary findings support my hypothesis, suggesting that in visually impaired infants, sleep enhances tactile responses more than auditory ones, while the opposite occurs in sighted infants. These disparities likely arise from the differing significance of auditory and tactile stimuli in blind versus sighted children. The increased emphasis on tactile information, reinforced during sleep, might drive structural and functional changes within the thalamocortical network following congenital visual deprivation (Lin et al., 2022). Indeed, such deprivation induces plastic changes in this network. Specifically, the visual thalamus exhibits smaller volume in blind children than in

sighted ones, though it increases with experience. Conversely, the somatosensory thalamus shows a larger volume in blind children, tending to decrease with age. These changes could be associated with reallocating visual thalamic function to process tactile information with experience. Indeed, a cross-sensory reorganization is also evident in thalamocortical connections, with visual deprivation impacting the development of functional connections between the somatosensory thalamus and "visual" cortical regions. In childhood, blind children demonstrate weaker connectivity compared to sighted children, yet synchronization between structures increases in blind adults, leading to heightened connectivity. These results align with animal studies showing that congenital enucleation in rodents prompts the visual cortex to receive input from thalamic nuclei associated with somatosensory and auditory cortices (Chabot et al., 2007; Karlen et al., 2006). However, further analyses exploring the relationship between sleep microstructure and responses to sensory stimulation while awake could elucidate the role of thalamocortical connections in sensory information consolidation.

5.4 Concluding remarks and technological perspectives

The current thesis aims to investigate how blindness affects the brain and sensory development, highlighting significant alterations in congenital visual deprivation, which leads to deviations from typical developmental trajectories. These alterations do not only affect wakefulness but also deeply involve sleep, suggesting a common underlying mechanism. I propose the thalamocortical network as a possible mediator of these alterations. Indeed, these structures during sleep are implicated in consolidating salient experiences, reflecting the blind child's tendency to prioritize tactile over auditory information, contrasting with the sighted child. The observed sensory differences in blind children elucidate certain behavioral traits. Firstly, the bias for tactile over auditory stimuli may result in a heightened reliance on body-centered coordinates (Gori et al., 2021; Rigato et al., 2014). This could compromise the ability to perceive limb position in space and correctly remap sensory information into a broader external reference frame. Secondly, the lack of visual input from birth and the increased emphasis on tactile information may limit blind children's spatial exploration of their bodies, thereby reducing interaction with the external environment. This behavior affects spatial perception and diminishes opportunities for social interaction with peers (Bollini et al., 2023; Cappagli et al., 2019, 2017). Lastly, diminished environmental interaction may contribute to motor impairment over time (Cappagli et al., 2019; Esposito et al., 2021; Houwen et al., 2009, 2007). My findings suggest that mechanisms governing brain oscillations during wakefulness and sleep could contribute to these effects. Recent evidence indicates that spindles not only reflect thalamocortical activity but also actively participate in thalamocortical network maturation (Schoch et al.,

2021; Sokoloff et al., 2021), hypothesizing a reciprocal cause-and-effect relationship between the maturation of the spindles and our sensorimotor skills.

These findings not only hold significant importance from a neuroscientific perspective, shedding light on the functional changes in the brain during development and in cases of visual deprivation, but they also offer intriguing insights into technological advancements. Technology plays a dual role in this domain. On one side, it provides tools for assessing functions and understanding the underlying brain mechanisms behind behavior. On the other side, comprehension of aberrant brain functions can spur technological innovations to improve some behaviors and potentially induce plastic changes at the brain level. This thesis focused on developing technology that favors a deeper understanding of the brain mechanisms in children during EEG recordings. However, the implications of the results extend beyond academic research. They may have many repercussions for rehabilitation strategies following sensory loss. First, they may have repercussions in terms of timing interventions. Indeed, multiple sensitive periods were identified here for optimal brain development. Furthermore, these findings suggest new therapeutic possibilities by considering both waking and sleeping periods as potential intervention windows. For instance, future technologies could explore multisensory stimulations during sleep as part of rehabilitative programs to enhance impaired abilities in visually impaired children. This innovative approach holds promise for improving outcomes in sensory rehabilitation and fostering neuroplasticity in affected individuals. Finally, the technology I have developed provides a tool to assess and validate rehabilitation processes mediated by intervention training. This enables us to evaluate behavioral aspects and uncover neural correlates, thereby gaining deeper insights into the mechanisms targeted by rehabilitation interventions. This integrated approach, cyclically bridging basic science, technological development, and rehabilitation, epitomizes what is known as "responsible technology."

Scientific Production

Papers

- **Published**

  Vitali H, Campus C, De Giorgis V, Signorini S, Morelli F, Fasce M, Gori M. Sensorimotor Oscillations in Human Infants During an Innate Rhythmic Movement (2024). *Brain Sciences*

  Vitali H, Campus C, Signorini S, De Giorgis V, Morelli F, Varesio C, Pasca L, Sammartano A, Gori M. Blindness affects the developmental trajectory of the sleeping brain (2024). *Neuroimage.*

  Bollini A†, **Vitali** H†, Crepaldi M, Parmiggiani A, Campus C, Lorini C, Gori M. Dr-MUSIC: An Effective Device for Investigating Multisensory Mechanisms during Development with EEG recordings (2023). *Annu Int Conf IEEE Eng Med Biol Soc (EMBC).*

  Setti W†, **Vitali** H†, Campus C, Picinali L, Gori M. Audio-Corsi: a novel system to evaluate audio-spatial memory skills (2023). *Annu Int Conf IEEE Eng Med Biol Soc (EMBC).*

  Vitali H, Campus C, De Giorgis V, Signorini S, Gori M. The vision of dreams: from ontogeny to dream engineering in blindness (2022). *Review. J Clin Sleep Med*.

  Campus C, Signorini S, **Vitali** H, De Giorgis V, Papalia G, Morelli F, Gori M. Sensitive period for the plasticity of alpha activity in humans (2021). *Dev Cogn Neurosci.*

- **Under review, submitted or in preparation**

  Gori M†, **Vitali** H†, *et al.* Visual experience drives the neural construction of a two-stage spatial processing in infancy. *Under review*

  †Authors contributed equally to this work.

Conferences

- **Talks**

Vitali H, Gori M, *et al.* The absence of vision in infants impairs the somatosensory body remapping (2024). 68° Congresso Nazionale SINC Società Italiana di Neurofisiologia Clinica, Genova. Oral presentation

Vitali H. Sleep technologist in research activities (2023). World Sleep Congress, Rio de Janeiro. Invited Talk

Vitali H, Campus C, Signorini S, De Giorgis V, Morelli F, Varesio C, Pasca L, Sammartano A, Gori M. NREM nap differences in children with and without visual impairment: the role of fast sleep spindles (2023). World Sleep Congress, Rio de Janeiro. Oral presentation

Vitali H, Campus C, Signorini S, De Giorgis V, Gori M. Brain activity development in visually impaired children during waking and sleep stages (2023). VISION, Denver. Invited Talk.

Vitali H, Campus C, Signorini S, De Giorgis V, Gori M. The development of cortical activity during waking and sleep stages in children with and without visual impairment (2023). 67° Congresso Nazionale SINC Società Italiana di Neurofisiologia Clinica, Bergamo. Oral presentation. **Winner: Young Technician Communication Challenge**

Vitali H, Campus C, Signorini S, De Giorgis V, Gori M. The development of cortical activity during wake and sleep stages in children with and without visual impairment (2022). International Multisensory Research Forum, Ulm. Oral presentation.

Vitali H, Campus C, De Giorgis V, Signorini S, Morelli F, Fasce M, Gori M. Is non-nutritive sucking a tool for blind infants to map space? an EEG study (2021). 8th International Conference on Spatial Cognition, online. Oral presentation.

- **Posters**

Vitali H, Bollini A, Campus C, Gori M. Cross modal attention through the three sensory modalities in human adults: an EEG study (2024). Cognitive Neuroscience Society, Toronto.

Vitali H, Campus C, De Giorgis V, Signorini S, Papalia G, Fasce M, Morelli F, Gori M. Nap modulation of cross-sensory audio-tactile skills in visually impaired and sighed infants: an EEG study (2023). European Sleep Research Society, online.

Vitali H, Campus C, Signorini S, De Giorgis V, Morelli F, Varesio C, Pasca L, Sammartano A, Gori M. NREM nap differences in children with and without visual impairment: the role of fast sleep spindles (2023). World Sleep Congress, Rio de Janeiro. **Winner: New Investigation Award**

Vitali H, Campus C, De Giorgis V, Signorini S, Papalia G, Fasce M, Morelli F, Gori M. Nap modulation of cross-sensory audio-tactile skills in visually impaired and sighed infants: an EEG study (2023). European Sleep Research Society, online.

Vitali H, Campus C, Signorini S, De Giorgis V, Morelli F, Fasce M, Gori M. Sensorimotor brain oscillations in human toddlers (2022). Federation of European Neuroscience Societies Forum, Paris.

Vitali H, Campus C, De Giorgis V, Signorini S, Morelli F, Varesio C, Gori M. Sleep Architecture Development in Blind and Sighted Children (2022). World sleep congress, Rome.

Vitali H, Campus C, Signorini S, De Giorgis V, Morelli F, Papalia G, Fasce M, Gori M. EEG spectral activity and its association with sensory-motor coordination in blind and sighted children (2021). Society of Neuroscience Annual Meeting, online.

Vitali H, Campus C, Signorini S, De Giorgis V, Morelli F, Papalia G, Fasce M, Gori M. How the lack of vision affects the development of alpha activity in the earliest stages of life (2021). 43rd European Conference on Visual Perception, online.

References

Adhikari, S., van Nispen, R.M.A., Poudel, M., van Rens, F., Elsman, E.B.M., van der Werf, Y.D., van Rens, G.H.M.B., 2023. Sleep Patterns in Children With Blindness: A Comparison With Normally Sighted Peers. Invest. Ophthalmol. Vis. Sci. 64, 46. https://doi.org/10.1167/iovs.64.14.46

Akiyama, Y., Parmelee Jr., A.H., Flescher, J., 1964. The Electroencephalogram in Visually Handicapped Children. J Pediatr 65, 233–242. https://doi.org/10.1016/s0022-3476(64)80525-4

Alais, D., Burr, D., 2004. The Ventriloquist Effect Results from Near-Optimal Bimodal Integration. Curr. Biol. 14, 257–262. https://doi.org/https://doi.org/10.1016/j.cub.2004.01.029

Allison, T., McCarthy, G., Wood, C.C., 1992. The relationship between human long-latency somatosensory evoked potentials recorded from the cortical surface and from the scalp. Electroencephalogr. Clin. Neurophysiol. 84, 301–314. https://doi.org/10.1016/0168-5597(92)90082-m

Allison, T., McCarthy, G., Wood, C.C., Darcey, T.M., Spencer, D.D., Williamson, P.D., 1989. Human cortical potentials evoked by stimulation of the median nerve. I. Cytoarchitectonic areas generating short-latency activity. J. Neurophysiol. 62, 694–710. https://doi.org/10.1152/jn.1989.62.3.694

Amadeo, M.B., Störmer, V.S., Campus, C., Gori, M., 2019. Peripheral sounds elicit stronger activity in contralateral occipital cortex in blind than sighted individuals. Sci. Rep. 9, 1–10. https://doi.org/10.1038/s41598-019-48079-3

Amedi, A., Jacobson, G., Hendler, T., Malach, R., Zohary, E., 2002. Convergence of visual and tactile shape processing in the human lateral occipital complex. Cereb. Cortex 12, 1202–1212. https://doi.org/10.1093/cercor/12.11.1202

Amedi, A., Stern, W.M., Camprodon, J.A., Bermpohl, F., Merabet, L., Rotman, S., Hemond, C., Meijer, P., Pascual-Leone, A., 2007. Shape conveyed by visual-to-auditory sensory substitution activates the lateral occipital complex. Nat. Neurosci. 10, 687–689. https://doi.org/10.1038/nn1912

Andersen, P, Andersson, S.A., 1968. Physiological Basis of the Alpha Rhythm, Neuroscience series. Appleton-Century-Crofts.

Andersen, Per, Andersson, S.A., 1968. Physiological basis of the alpha rhythm. Plenum Publishing Corporation.

Anderson, A.J., Perone, S., 2018. Developmental change in the resting state electroencephalogram: insights into cognition and the brain. Brain Cogn. 126, 40–52.

Anderson, K.L., Ding, M., 2011. Attentional modulation of the somatosensory mu rhythm. Neuroscience 180, 165–180. https://doi.org/10.1016/j.neuroscience.2011.02.004

Anderson, P.W., Zahorik, P., 2014. Auditory/visual distance estimation: accuracy and variability. Front. Psychol. 5, 1097. https://doi.org/10.3389/fpsyg.2014.01097

Andersson, S.A., Manson, J.R., 1971. Rhythmic activity in the thalamus of the unanaesthetized decorticate cat. Electroencephalogr. Clin. Neurophysiol. 31, 21–34. https://doi.org/https://doi.org/10.1016/0013-4694(71)90286-0

Angelini, L., Comani, S., Tamburro, G., Lionetti, F., Spinelli, M., Zappasodi, F., Fasolo, M., Aureli, T., 2023. Alpha and theta brain activity in 9- - old infants during a live referential gaze paradigm 1–12. https://doi.org/10.1111/psyp.14198

Antón-bolaños, N., Sempere-ferràndez, A., Guillamón-Vivancos, T., Martini, F.J., Pérez-Saiz, L., Gezelius, H., Filipchuk, A., Valdeolmillos, M., López-bendito, G., 2019. Functional Cortical Maps in Mice. Science (80-.). 990, 987–990.

Atkinson, J., 2002. The Developing Visual Brain. Oxford University Press UK.

Aton, S.J., Broussard, C., Dumoulin, M., Seibt, J., Watson, A., Coleman, T., Frank, M.G., 2013. Visual experience and subsequent sleep induce sequential plastic changes in putative inhibitory and excitatory cortical neurons. Proc. Natl. Acad. Sci. U. S. A. 110, 3101–3106. https://doi.org/10.1073/pnas.1208093110

Aton, S.J., Seibt, J., Dumoulin, M., Jha, S.K., Steinmetz, N., Coleman, T., Naidoo, N., Frank, M.G., 2009. Mechanisms of sleep-dependent consolidation of cortical plasticity. Neuron 61, 454–466. https://doi.org/10.1016/j.neuron.2009.01.007

Aubin, S., Gacon, C., Jennum, P., Ptito, M., Kupers, R., 2016. Altered sleep–wake patterns in blindness: a combined actigraphy and psychometric study. Sleep Med. https://doi.org/10.1016/j.sleep.2016.07.021

Averkin, R.G., Szemenyei, V., Bordé, S., Tamás, G., 2016. Identified Cellular Correlates of Neocortical Ripple and High-Gamma Oscillations during Spindles of Natural Sleep. Neuron 92, 916–928. https://doi.org/10.1016/j.neuron.2016.09.032

Ayoub, A., Aumann, D., Hörschelmann, A., Kouchekmanesch, A., Paul, P., Born, J., Marshall, L., 2013. Differential effects on fast and slow spindle activity, and the sleep slow oscillation in humans with carbamazepine and flunarizine to antagonize voltage-dependent Na+ and Ca2+ channel activity. Sleep 36, 905–911. https://doi.org/10.5665/sleep.2722

Azañón, E., Camacho, K., Soto-faraco, S., 2010a. Tactile remapping beyond space 31, 1858–1867. https://doi.org/10.1111/j.1460-9568.2010.07233.x

Azañón, E., Longo, M.R., Soto-Faraco, S., Haggard, P., 2010b. The posterior parietal cortex remaps touch into external space. Curr. Biol. 20, 1304–1309.

https://doi.org/10.1016/j.cub.2010.05.063

Azañón, E., Soto-Faraco, S., 2008. Changing Reference Frames during the Encoding of Tactile Events. Curr. Biol. 18, 1044–1049. https://doi.org/10.1016/j.cub.2008.06.045

Babiloni, C., Frisoni, G.B., Pievani, M., Vecchio, F., Lizio, R., Buttiglione, M., Geroldi, C., Fracassi, C., Eusebi, F., Ferri, R., Rossini, P.M., 2009. Hippocampal volume and cortical sources of EEG alpha rhythms in mild cognitive impairment and Alzheimer disease. Neuroimage 44, 123–135. https://doi.org/10.1016/j.neuroimage.2008.08.005

Bahrick, L.E., 2001. Increasing Specificity in Perceptual Development: Infants' Detection of Nested Levels of Multimodal Stimulation. J. Exp. Child Psychol. 79, 253–270. https://doi.org/https://doi.org/10.1006/jecp.2000.2588

Bahrick, L.E., Lickliter, R., Flom, R., 2004. Intersensory Redundancy Guides the Development of Selective Attention , Perception , and Cognition in Infancy. Curr. Dir. Psychol. Sci. 13, 99–102.

Bal, T., von Krosigk, M., McCormick, D.A., 1995. Role of the ferret perigeniculate nucleus in the generation of synchronized oscillations in vitro. J. Physiol. 483 (Pt 3, 665–685. https://doi.org/10.1113/jphysiol.1995.sp020613

Barakat, M., Doyon, J., Debas, K., Vandewalle, G., Morin, A., Poirier, G., Martin, N., Lafortune, M., Karni, A., Ungerleider, L.G., Benali, H., Carrier, J., 2011. Fast and slow spindle involvement in the consolidation of a new motor sequence. Behav. Brain Res. 217, 117–121. https://doi.org/10.1016/j.bbr.2010.10.019

Başar-Eroglu, C., Kolev, V., Ritter, B., Aksu, F., Başar, E., 1994. EEG, auditory evoked potentials and evoked rhythmicities in three-year-old children. Int. J. Neurosci. 75, 239–255. https://doi.org/10.3109/00207459408986307

Başar, E., 2012. A review of alpha activity in integrative brain function: Fundamental physiology, sensory coding, cognition and pathology. Int. J. Psychophysiol. 86, 1–24. https://doi.org/https://doi.org/10.1016/j.ijpsycho.2012.07.002

Basar, E., Bullock, T.H., 1992. Induced Rhythms in the Brain, in: Brain Dynamics.

Başar, E., Schürmann, M., 1994. Functional aspects of evoked alpha and theta responses in humans and cats. Occipital recordings in "cross modality" experiments. Biol. Cybern. 72, 175–183. https://doi.org/10.1007/BF00205981

Başar, E., Yordanova, J., Kolev, V., Başar-Eroglu, C., 1997. Is the alpha rhythm a control parameter for brain responses? Biol. Cybern. 76, 471–480. https://doi.org/10.1007/s004220050360

Bates, D., Mächler, M., Bolker, B., Walker, S., 2015. Fitting Linear Mixed-Effects Models Using lme4. J. Stat. Softw. 67, 1–48. https://doi.org/10.18637/jss.v067.i01

Bazanova, O.M., Vernon, D., 2014. Interpreting EEG alpha activity. Neurosci. Biobehav. Rev. 44, 94–110. https://doi.org/10.1016/j.neubiorev.2013.05.007

Bazhenov, M., Sejnowski, T.J., Steriade, M., Timofeev, I., 2001. Contribution of intrinsic and synaptic factors in the desynchronization of thalamic oscillatory activity. Thalamus Relat. Syst. 1, 53–69. https://doi.org/DOI: 10.1017/S1472928801000048

Beauchamp, M.S., 2005. See me, hear me, touch me: multisensory integration in lateral occipital-temporal cortex. Curr. Opin. Neurobiol. 15, 145–153. https://doi.org/10.1016/j.conb.2005.03.011

Bell, M.A., Cuevas, K., 2012. Using EEG to Study Cognitive Development: Issues and Practices. J. Cogn. Dev. Off. J. Cogn. Dev. Soc. 13, 281–294. https://doi.org/10.1080/15248372.2012.691143

Ben Porquis, L., Finocchietti, S., Zini, G., Cappagli, G., Gori, M., Baud-Bovy, G., 2017. ABBI: A wearable device for improving spatial cognition in visually-impaired children, in: 2017 IEEE Biomedical Circuits and Systems Conference (BioCAS). pp. 1–4. https://doi.org/10.1109/BIOCAS.2017.8325128

Berchicci, M., Zhang, T., Romero, L., Peters, A., Annett, R., Teuscher, U., Bertollo, M., Okada, Y., Stephen, J., Comani, S., 2011. Development of mu rhythm in infants and preschool children. Dev. Neurosci. 33, 130–143. https://doi.org/10.1159/000329095

Berman, N.E.J., 1991. Alterations of visual cortical connections in cats following early removal of retinal input. Dev. Brain Res. https://doi.org/10.1016/0165-3806(91)90076-U

Bernardi, G., Siclari, F., Handjaras, G., Riedner, B.A., Tononi, G., 2018. Local and Widespread Slow Waves in Stable NREM Sleep: Evidence for Distinct Regulation Mechanisms. Front. Hum. Neurosci. 12, 248. https://doi.org/10.3389/fnhum.2018.00248

Bernasconi, F., Manuel, A.L., Murray, M.M., Spierer, L., 2011. Pre-stimulus beta oscillations within left posterior sylvian regions impact auditory temporal order judgment accuracy. Int. J. Psychophysiol. 79, 244–248. https://doi.org/10.1016/j.ijpsycho.2010.10.017

Berry, R., Quan, S., Abreu, A., Bibbs, M., DelRosso, L., Harding, S., Mao, M., Plante, D., Pressman, M., Troester, M., Vaughn, B., 2020. The AASM Manual for the Scoring of Sleep and Associated Events: Rules, Terminology and Technical Specifications, Version 2. ed. Darien, IL: America Accademy of Sleep Medicine, Darien, IL.

Bertelson, P., Aschersleben, G., 2003. Temporal ventriloquism: crossmodal interaction on the time dimension. 1. Evidence from auditory-visual temporal order judgment. Int. J. Psychophysiol. Off. J. Int. Organ. Psychophysiol. 50, 147–155. https://doi.org/10.1016/s0167-8760(03)00130-2

Bertonati, G., Casado-Palacios, M., Crepaldi, M., Parmiggiani, A., Maviglia, A., Torazza, D., Campus, C., Gori, M., 2023. MultiTab: A Novel Portable Device to Evaluate Multisensory Skills(). Annu. Int. Conf. IEEE Eng. Med. Biol. Soc. IEEE Eng. Med. Biol. Soc. Annu. Int. Conf. 2023, 1–4. https://doi.org/10.1109/EMBC40787.2023.10341048

Bertonati, G., Tonelli, A., Cuturi, L.F., Setti, W., Gori, M., 2020. Assessment of spatial reasoning in blind individuals using a haptic version of the Kohs Block Design Test. Curr. Res. Behav. Sci. 1, 100004. https://doi.org/10.1016/j.crbeha.2020.100004

Birbaumer, N., 1971. Das Elektro-encephalogramm bei Blindgeborenen. Huber.

Blumberg, M.S., Dooley, J.C., Tiriac, A., 2022. Sleep, plasticity, and sensory neurodevelopment. Neuron 110, 3230–3242. https://doi.org/10.1016/j.neuron.2022.08.005

Bollini, A., Cocchi, E., Salvagno, V., Gori, M., 2023. The causal role of vision in the development of spatial coordinates: Evidence from visually impaired children. J. Exp. Psychol. Hum. Percept. Perform. https://doi.org/10.1037/xhp0001122

Bolognini, N., Rasi, F., Coccia, M., Làdavas, E., 2005. Visual search improvement in hemianopic patients after audio-visual stimulation. Brain 128, 2830–2842. https://doi.org/10.1093/brain/awh656

Bonjean, M., Baker, T., Lemieux, M., Timofeev, I., Sejnowski, T., Bazhenov, M., 2011. Corticothalamic Feedback Controls Sleep Spindle Duration In Vivo. J. Neurosci. 31, 9124–9134. https://doi.org/10.1523/JNEUROSCI.0077-11.2011

Borchers, H.W., 2019. pracma: Practical Numerical Math Functions.

Botvinick, M., Cohen, J., 1998. Rubber hands 'feel' touch that eyes see. Nature 391, 756. https://doi.org/10.1038/35784

Boyce, R., Glasgow, S.D., Williams, S., Adamantidis, A., 2016. Causal evidence for the role of REM sleep theta rhythm in contextual memory consolidation. Science 352, 812–816. https://doi.org/10.1126/science.aad5252

Brandwein, A.B., Foxe, J.J., Butler, J.S., Russo, N.N., Altschuler, T.S., Gomes, H., Molholm, S., 2013. The development of multisensory integration in high-functioning autism: High-density electrical mapping and psychophysical measures reveal impairments in the processing of audiovisual inputs. Cereb. Cortex 23, 1329–1341. https://doi.org/10.1093/cercor/bhs109

Brandwein, A.B., Foxe, J.J., Russo, N.N., Altschuler, T.S., Gomes, H., Molholm, S., 2011. The development of audiovisual multisensory integration across childhood and early adolescence: A high-density electrical mapping study. Cereb. Cortex 21, 1042–1055. https://doi.org/10.1093/cercor/bhq170

Braun, A.R., Balkin, T.J., Wesensten, N.J., Carson, R.E., Varga, M., Baldwin, P., Selbie, S., Belenky, G., Herscovitch, P., 1997. Regional cerebral blood flow throughout the sleep-wake cycle. An H215O PET study. Brain 120, 1173–1197. https://doi.org/10.1093/brain/120.7.1173

Breitenseher, M., Uhl, F., Prayer Wimberger, D., Deecke, L., Trattnig, S., Kramer, J., 1998. Morphological dissociation between visual pathways and cortex: MRI of visually-deprived patients with congenital peripheral blindness. Neuroradiology. https://doi.org/10.1007/s002340050616

Bremmer, F., Schlack, A., Shah, N.J., Zafiris, O., Kubischik, M., Hoffmann, K., Zilles, K., Fink, G.R., 2001. Polymodal motion processing in posterior parietal and premotor cortex: a human fMRI study strongly implies equivalencies between humans and monkeys. Neuron 29, 287–296. https://doi.org/10.1016/s0896-6273(01)00198-2

Bremner, A.J., Hill, E.L., Pratt, M., Rigato, S., Spence, C., 2013. Bodily Illusions in Young Children: Developmental Change in Visual and Proprioceptive Contributions to

Perceived Hand Position. PLoS One 8, 1–6. https://doi.org/10.1371/journal.pone.0051887

Bremner, A.J., Spence, C., 2017. The Development of Tactile Perception. Adv. Child Dev. Behav. 52, 227–268. https://doi.org/10.1016/bs.acdb.2016.12.002

Brett-Green, B.A., Miller, L.J., Gavin, W.J., Davies, P.L., 2008. Multisensory integration in children: A preliminary ERP study. Brain Res. 1242, 283–290. https://doi.org/10.1016/j.brainres.2008.03.090

Britz, J., Van De Ville, D., Michel, C.M., 2010. BOLD correlates of EEG topography reveal rapid resting-state network dynamics. Neuroimage 52, 1162–70. https://doi.org/10.1016/j.neuroimage.2010.02.052

Brown, A.M., Dobson, V., Maier, J., 1987. Visual acuity of human infants at scotopic, mesopic and photopic luminances. Vision Res. 27, 1845–1858. https://doi.org/10.1016/0042-6989(87)90113-1

Brzosko, Z., Mierau, S.B., Paulsen, O., 2019. Neuromodulation of Spike-Timing-Dependent Plasticity: Past, Present, and Future. Neuron 103, 563–581. https://doi.org/10.1016/j.neuron.2019.05.041

Buchholz, V.N., Jensen, O., Medendorp, W.P., 2013. Parietal oscillations code nonvisual reach targets relative to gaze and body. J. Neurosci. 33, 3492–3499. https://doi.org/10.1523/JNEUROSCI.3208-12.2013

Buchholz, V.N., Jensen, O., Medendorp, W.P., 2011. Multiple Reference Frames in Cortical Oscillatory Activity during Tactile Remapping for Saccades 31, 16864–16871. https://doi.org/10.1523/JNEUROSCI.3404-11.2011

Buchmann, A., Ringli, M., Kurth, S., Schaerer, M., Geiger, A., Jenni, O.G., Huber, R., 2011. EEG Sleep Slow-Wave Activity as a Mirror of Cortical Maturation. Cereb. Cortex 21, 607–615. https://doi.org/10.1093/cercor/bhq129

Bushara, K.O., Weeks, R.A., Ishii, K., Catalan, M.J., Tian, B., Rauschecker, J.P., Hallett, M., 1999. Modality-specific frontal and parietal areas for auditory and visual spatial localization in humans. Nat. Neurosci. 2, 759–766. https://doi.org/10.1038/11239

Buzsáki, G., Watson, B.O., 2012. Brain rhythms and neural syntax: implications for efficient coding of cognitive content and neuropsychiatric disease. Dialogues Clin. Neurosci. 14, 345–367. https://doi.org/10.31887/DCNS.2012.14.4/gbuzsaki

Calvert, G.A., Brammer, M.J., Bullmore, E.T., Campbell, R., Iversen, S.D., David, A.S., 1999. Response amplification in sensory-specific cortices during crossmodal binding. Neuroreport 10, 2619–2623. https://doi.org/10.1097/00001756-199908200-00033

Calvert, G.A., Bullmore, E.T., Brammer, M.J., Campbell, R., Williams, S.C., McGuire, P.K., Woodruff, P.W., Iversen, S.D., David, A.S., 1997. Activation of auditory cortex during silent lipreading. Science 276, 593–596. https://doi.org/10.1126/science.276.5312.593

Campbell, I.G., Feinberg, I., 2016. Maturational Patterns of Sigma Frequency Power Across Childhood and Adolescence: A Longitudinal Study. Sleep 39, 193–201.

https://doi.org/10.5665/sleep.5346

Campbell, I.G., Feinberg, I., 2009. Longitudinal trajectories of non-rapid eye movement delta and theta EEG as indicators of adolescent brain maturation. Proc. Natl. Acad. Sci. U. S. A. 106, 5177–5180. https://doi.org/10.1073/pnas.0812947106

Campus, C., Sandini, G., Amadeo, M.B., Gori, M., 2019. Stronger responses in the visual cortex of sighted compared to blind individuals during auditory space representation. Sci. Rep. 9, 1935. https://doi.org/10.1038/s41598-018-37821-y

Campus, C., Signorini, S., Vitali, H., De Giorgis, V., Papalia, G., Morelli, F., Gori, M., 2021. Sensitive period for the plasticity of alpha activity in humans. Dev. Cogn. Neurosci. 49, 100965. https://doi.org/10.1016/j.dcn.2021.100965

Cappagli, G., Cocchi, E., Gori, M., 2017. Auditory and proprioceptive spatial impairments in blind children and adults. Dev. Sci. 20. https://doi.org/10.1111/desc.12374

Cappagli, G., Finocchietti, S., Cocchi, E., Giammari, G., Zumiani, R., Cuppone, A.V., Baud-Bovy, G., Gori, M., 2019. Audio motor training improves mobility and spatial cognition in visually impaired children. Sci. Rep. 9, 1–9. https://doi.org/10.1038/s41598-019-39981-x

Cappe, C., Thut, G., Romei, V., Murray, M.M., 2010. Auditory-visual multisensory interactions in humans: timing, topography, directionality, and sources. J. Neurosci. Off. J. Soc. Neurosci. 30, 12572–12580. https://doi.org/10.1523/JNEUROSCI.1099-10.2010

Castelnovo, A., Lividini, A., Riedner, B.A., Avvenuti, G., Jones, S.G., Miano, S., Tononi, G., Manconi, M., Bernardi, G., 2023. Origin, synchronization, and propagation of sleep slow waves in children. Neuroimage 274, 120133. https://doi.org/10.1016/j.neuroimage.2023.120133

Cattaneo, Z., Vecchi, T., Cornoldi, C., Mammarella, I., Bonino, D., Ricciardi, E., Pietrini, P., 2008. Imagery and spatial processes in blindness and visual impairment. Neurosci. Biobehav. Rev. 32, 1346–1360. https://doi.org/10.1016/j.neubiorev.2008.05.002

Cecchetti, L., Ricciardi, E., Handjaras, G., Kupers, R., Ptito, M., Pietrini, P., 2016. Congenital blindness affects diencephalic but not mesencephalic structures in the human brain. Brain Struct. Funct. 221, 1465–1480. https://doi.org/10.1007/s00429-014-0984-5

Chabot, N., Robert, S., Tremblay, R., Miceli, D., Boire, D., Bronchti, G., 2007. Audition differently activates the visual system in neonatally enucleated mice compared with anophthalmic mutants. Eur. J. Neurosci. 26, 2334–2348. https://doi.org/10.1111/j.1460-9568.2007.05854.x

Chanauria, N., Bharmauria, V., Bachatene, L., Cattan, S., Rouat, J., Molotchnikoff, S., 2019. Sound Induces Change in Orientation Preference of V1 Neurons: Audio-Visual Cross-Influence. Neuroscience 404, 48–61. https://doi.org/10.1016/j.neuroscience.2019.01.039

Chang, C.Y., Hsu, S.H., Pion-Tonachini, L., Jung, T.P., 2018. Evaluation of Artifact Subspace Reconstruction for Automatic EEG Artifact Removal. Proc. Annu. Int.

Conf. IEEE Eng. Med. Biol. Soc. EMBS 2018-July, 1242–1245. https://doi.org/10.1109/EMBC.2018.8512547

Chatburn, A., Coussens, S., Lushington, K., Kennedy, D., Baumert, M., Kohler, M., 2013. Sleep spindle activity and cognitive performance in healthy children. Sleep 36, 237–243. https://doi.org/10.5665/sleep.2380

Ching, S., Cimenser, A., Purdon, P.L., Brown, E.N., Kopell, N.J., 2010. Thalamocortical model for a propofol-induced α -rhythm associated with loss of consciousness. https://doi.org/10.1073/pnas.1017069108

Chiu, C., Weliky, M., 2001. Spontaneous Activity in Developing Ferret Visual Cortex In Vivo J. Neurosci. 21, 8906 LP – 8914. https://doi.org/10.1523/JNEUROSCI.21-22-08906.2001

Choudhury, N., Benasich, A.A., 2011. Maturation of auditory evoked potentials from 6 to 48 months: Prediction to 3 and 4 year language and cognitive abilities. Clin. Neurophysiol. 122, 320–338. https://doi.org/10.1016/J.CLINPH.2010.05.035

Cirelli, C., 2013. Sleep and synaptic changes. Curr. Opin. Neurobiol. 23, 841–846. https://doi.org/10.1016/j.conb.2013.04.001

Clemens, Z., Fabó, D., Halász, P., 2005. Overnight verbal memory retention correlates with the number of sleep spindles. Neuroscience 132, 529–535. https://doi.org/10.1016/j.neuroscience.2005.01.011

Clemens, Z., Mölle, M., Eross, L., Jakus, R., Rásonyi, G., Halász, P., Born, J., 2011. Fine-tuned coupling between human parahippocampal ripples and sleep spindles. Eur. J. Neurosci. 33, 511–520. https://doi.org/10.1111/j.1460-9568.2010.07505.x

Cohen, J., Boshes, L.D., Snider, R.S., 1961. Electroencephalographic changes following retrolental fibroplasia. Electroencephalogr. Clin. Neurophysiol. 13, 914–922.

Collignon, O., Champoux, F., Voss, P., Lepore, F., 2011. Sensory rehabilitation in the plastic brain. Prog. Brain Res. 191, 211–231. https://doi.org/10.1016/B978-0-444-53752-2.00003-5

Collignon, O., Dormal, G., Albouy, G., Vandewalle, G., Voss, P., Phillips, C., Lepore, F., 2013. Impact of blindness onset on the functional organization and the connectivity of the occipital cortex. Brain 136, 2769–2783. https://doi.org/10.1093/brain/awt176

Collignon, O., Voss, P., Lassonde, M., Lepore, F., 2009. Cross-modal plasticity for the spatial processing of sounds in visually deprived subjects. Exp. Brain Res. 192, 343–358. https://doi.org/10.1007/s00221-008-1553-z

Contreras, D., Steriade, M., 1996. Spindle oscillation in cats: the role of corticothalamic feedback in a thalamically generated rhythm. J. Physiol. 490 (Pt 1, 159–179. https://doi.org/10.1113/jphysiol.1996.sp021133

Cragg, L., Kovacevic, N., McIntosh, A.R., Poulsen, C., Martinu, K., Leonard, G., Paus, T., 2011. Maturation of EEG power spectra in early adolescence: a longitudinal study. Dev. Sci. 14, 935–943. https://doi.org/10.1111/j.1467-7687.2010.01031.x

Cuevas, K., Cannon, E.N., Yoo, K., Fox, N.A., 2014. The Infant EEG Mu Rhythm:

Methodological Considerations and Best Practices. Dev. Rev. 34, 26–43. https://doi.org/10.1016/j.dr.2013.12.001

D'Atri, A., Novelli, L., Ferrara, M., Bruni, O., De Gennaro, L., 2018. Different maturational changes of fast and slow sleep spindles in the first four years of life. Sleep Med. 42, 73–82. https://doi.org/10.1016/j.sleep.2017.11.1138

Dale, N., Sakkalou, E., O'Reilly, M., Springall, C., De Haan, M., Salt, A., 2017. Functional vision and cognition in infants with congenital disorders of the peripheral visual system. Dev. Med. Child Neurol. https://doi.org/10.1111/dmcn.13429

Dale, N., Sonksen, P., 2002. Developmental outcome, including setback, in young children with severe visual impairment. Dev. Med. Child Neurol. https://doi.org/10.1017/S0012162201002651

Dall'Orso, S., Steinweg, J., Allievi, A.G., Edwards, A.D., Burdet, E., Arichi, T., 2018. Somatotopic Mapping of the Developing Sensorimotor Cortex in the Preterm Human Brain. Cereb. Cortex 28, 2507–2515. https://doi.org/10.1093/cercor/bhy050

De Meo, R., Murray, M.M., Clarke, S., Matusz, P.J., 2015. Top-down control and early multisensory processes: Chicken vs. egg. Front. Integr. Neurosci. 9, 1–6. https://doi.org/10.3389/fnint.2015.00017

Del Viva, M.M., Igliozzi, R., Tancredi, R., Brizzolara, D., 2006. Spatial and motion integration in children with autism. Vision Res. 46, 1242–1252. https://doi.org/10.1016/j.visres.2005.10.018

Delorme, A., Makeig, S., 2004. EEGLAB: an open source toolbox for analysis of single-trial EEG dynamics including independent component analysis. J. Neurosci. Methods 134, 9–21. https://doi.org/10.1016/j.jneumeth.2003.10.009

Dirks, C., Grünewald, D., Young, P., Heidbreder, A., 2019. Pilot study to investigate sleep disorders in the blind and persons with relevant visual impairment. Ophthalmologe. https://doi.org/10.1007/s00347-018-0723-z

Doppelmayr, M., Klimesch, W., Stadler, W., Pöllhuber, D., Heine, C., 2002. EEG alpha power and intelligence. Intelligence. https://doi.org/10.1016/s0160-2896(01)00101-5

Dormal, G., Collignon, O., 2011. Functional selectivity in sensory-deprived cortices. J. Neurophysiol. 105, 2627–2630. https://doi.org/10.1152/jn.00109.2011

Doucette, M.R., Kurth, S., Chevalier, N., Munakata, Y., LeBourgeois, M.K., 2015. Topography of Slow Sigma Power during Sleep is Associated with Processing Speed in Preschool Children. Brain Sci. 5, 494–508. https://doi.org/10.3390/brainsci5040494

Drasgow, F., 2004. Polychoric and Polyserial Correlations, in: Encyclopedia of Statistical Sciences. John Wiley & Sons, Ltd. https://doi.org/https://doi.org/10.1002/0471667196.ess2014

Drew, A.R., Meltzoff, A.N., Marshall, P.J., Drew, A.R., 2018. Interpersonal Influences on Body Representations in the Infant Brain 9, 1–12. https://doi.org/10.3389/fpsyg.2018.02601

Dwyer, P., Takarae, Y., Zadeh, I., Rivera, S.M., Saron, C.D., 2022. Multisensory

integration and interactions across vision, hearing, and somatosensation in autism spectrum development and typical development. Neuropsychologia 175, 108340. https://doi.org/10.1016/j.neuropsychologia.2022.108340

Eardley, A.F., van Velzen, J., 2011. Event-related potential evidence for the use of external coordinates in the preparation of tactile attention by the early blind. Eur. J. Neurosci. https://doi.org/10.1111/j.1460-9568.2011.07672.x

Eimer, M., Forster, B., Fieger, A., Harbich, S., 2004. Effects of hand posture on preparatory control processes and sensory modulations in tactile-spatial attention. Clin. Neurophysiol. 115, 596–608. https://doi.org/https://doi.org/10.1016/j.clinph.2003.10.015

Eisermann, M., Kaminska, A., Moutard, M.L., Soufflet, C., Plouin, P., 2013. Normal EEG in childhood: From neonates to adolescents. Neurophysiol. Clin. 43, 35–65. https://doi.org/10.1016/j.neucli.2012.09.091

Elbert, T., Sterr, A., Rockstroh, B., Pantev, C., Mu, M.M., 2002. Expansion of the Tonotopic Area in the Auditory Cortex of the Blind 22, 1–4.

Ellemberg, D., Lewis, T.L., Dirks, M., Maurer, D., Ledgeway, T., Guillemot, J.-P., Lepore, F., 2004. Putting order into the development of sensitivity to global motion. Vision Res. 44, 2403–2411. https://doi.org/10.1016/j.visres.2004.05.006

Enge, S., Kaloud, H., Lechner, H., 1973. EEG-Untersuchungen bei blinden und sehschwachen Kindern. Padiatr. Padol. 8, 175–180.

Ernst, M.O., Banks, M.S., 2002. Humans integrate visual and haptic information in a statistically optimal fashion. Nature 415, 429–433. https://doi.org/10.1038/415429a

Esposito, D., Bollini, A., Gori, M., 2021. Early Blindness Limits the Head-Trunk Coordination Development for Horizontal Reorientation. Front. Hum. Neurosci. 15, 699312. https://doi.org/10.3389/fnhum.2021.699312

Fabio, C., Salemme, R., Farnè, A., Miller, L.E., 2024. Alpha oscillations reflect similar mapping mechanisms for localizing touch on hands and tools. iScience 109092. https://doi.org/10.1016/j.isci.2024.109092

Faivre, N., Arzi, A., Lunghi, C., Salomon, R., 2017. Consciousness is more than meets the eye : a call for a multisensory study of subjective experience † 1–8. https://doi.org/10.1093/nc/nix003

Falchier, A., Clavagnier, S., Barone, P., Kennedy, H., 2002. Anatomical evidence of multimodal integration in primate striate cortex. J. Neurosci. Off. J. Soc. Neurosci. 22, 5749–5759. https://doi.org/10.1523/JNEUROSCI.22-13-05749.2002

Fazzi, E., Signorini, S.G., Uggetti, C., Bianchi, P.E., Lanners, J., Lanzi, G., 2005. Towards improved clinical characterization of leber congenital amaurosis: Neurological and systemic findings. Am. J. Med. Genet. https://doi.org/10.1002/ajmg.a.30301

Fazzi, E., Zaccagnino, M., Gahagan, S., Capsoni, C., Signorini, S., Ariaudo, G., Lanners, J., Orcesi, S., 2008. Sleep disturbances in visually impaired toddlers. Brain Dev. 30, 572–578. https://doi.org/10.1016/j.braindev.2008.01.008

Feinberg, I., Campbell, I.G., 2010. Sleep EEG changes during adolescence: an index of a fundamental brain reorganization. Brain Cogn. 72, 56–65. https://doi.org/10.1016/j.bandc.2009.09.008

Fernandez, L.M.J., Lüthi, A., 2020. Sleep spindles: Mechanisms and functions. Physiol. Rev. 100, 805–868. https://doi.org/10.1152/physrev.00042.2018

Finocchietti, S., Cappagli, G., Gori, M., 2015. Encoding audio motion: spatial impairment in early blind individuals. Front. Psychol. 6, 1357. https://doi.org/10.3389/fpsyg.2015.01357

Flanagan, J.R., Beltzner, M.A., 2000. Independence of perceptual and sensorimotor predictions in the size-weight illusion. Nat. Neurosci. 3, 737–741. https://doi.org/10.1038/76701

Fogel, S.M., Smith, C.T., 2011. The function of the sleep spindle: a physiological index of intelligence and a mechanism for sleep-dependent memory consolidation. Neurosci. Biobehav. Rev. 35, 1154–1165. https://doi.org/10.1016/j.neubiorev.2010.12.003

Fort, A., Delpuech, C., Pernier, J., Giard, M.H., 2002. Early auditory-visual interactions in human cortex during nonredundant target identification. Brain Res. Cogn. Brain Res. 14, 20–30. https://doi.org/10.1016/s0926-6410(02)00058-7

Fortin, M., Voss, P., Lord, C., Lassonde, M., Pruessner, J., Saint-Amour, D., Rainville, C., Lepore, F., 2008. Wayfinding in the blind: Larger hippocampal volume and supranormal spatial navigation. Brain 131, 2995–3005. https://doi.org/10.1093/brain/awn250

Fox, J., Weisberg, S., 2018. An R companion to applied regression. Sage publications.

Foxe, J.J., Morocz, I.A., Murray, M.M., Higgins, B.A., Javitt, D.C., Schroeder, C.E., 2000. Multisensory auditory-somatosensory interactions in early cortical processing revealed by high-density electrical mapping. Brain Res. Cogn. Brain Res. 10, 77–83. https://doi.org/10.1016/s0926-6410(00)00024-0

Foxe, J.J., Schroeder, C.E., 2005. The case for feedforward multisensory convergence during early cortical processing. Neuroreport 16, 419–423. https://doi.org/10.1097/00001756-200504040-00001

Foxe, J.J., Wylie, G.R., Martinez, A., Schroeder, C.E., Javitt, D.C., Guilfoyle, D., Ritter, W., Murray, M.M., 2002. Auditory-somatosensory multisensory processing in auditory association cortex: an fMRI study. J. Neurophysiol. 88, 540–543. https://doi.org/10.1152/jn.2002.88.1.540

Frank, M.G., Issa, N.P., Stryker, M.P., 2001. Sleep Enhances Plasticity in the Developing Visual Cortex. Neuron 30, 275–287. https://doi.org/10.1016/S0896-6273(01)00279-3

Frasnelli, J., Collignon, O., Voss, P., Lepore, F., 2011. Crossmodal plasticity in sensory loss. Prog. Brain Res. 191, 233–249. https://doi.org/10.1016/B978-0-444-53752-2.00002-3

Freeman, W.J., 2004. Origin, structure, and role of background EEG activity. Part 1. Analytic amplitude. Clin. Neurophysiol. 115, 2077–2088.

https://doi.org/https://doi.org/10.1016/j.clinph.2004.02.029

Freier, L., Cooper, R.P., Mareschal, D., 2017. Preschool children's control of action outcomes. Dev. Sci. 20, 1–13. https://doi.org/10.1111/desc.12354

Fujioka, T., Mourad, N., Trainor, L.J., 2011. Development of auditory-specific brain rhythm in infants 33, 521–529. https://doi.org/10.1111/j.1460-9568.2010.07544.x

Fujioka, T., Ross, B., 2008. Auditory processing indexed by stimulus-induced alpha desynchronization in children. Int. J. Psychophysiol. Off. J. Int. Organ. Psychophysiol. 68, 130–140. https://doi.org/10.1016/j.ijpsycho.2007.12.004

Galland, B.C., Taylor, B.J., Elder, D.E., Herbison, P., 2012. Normal sleep patterns in infants and children: A systematic review of observational studies. Sleep Med. Rev. https://doi.org/10.1016/j.smrv.2011.06.001

Gasser, T., Verleger, R., Bacher, P., Sroka, L., 1988. Development of the EEG of school-age children and adolescents. I. Analysis of band power. Electroencephalogr Clin Neurophysiol 69, 91–99.

Gaudreau, H., Carrier, J., Montplaisir, J., 2001. Age-related modifications of NREM sleep EEG: from childhood to middle age. J. Sleep Res. 10, 165–172. https://doi.org/10.1046/j.1365-2869.2001.00252.x

Geiger, A., Huber, R., Kurth, S., Ringli, M., Jenni, O.G., Achermann, P., 2011. The sleep EEG as a marker of intellectual ability in school age children. Sleep 34, 181–189. https://doi.org/10.1093/sleep/34.2.181

Ghazanfar, A.A., Schroeder, C.E., 2006. Is neocortex essentially multisensory ? 10. https://doi.org/10.1016/j.tics.2006.04.008

Gibson, E.J., Walker, A.S., 1984. Development of knowledge of visual-tactual affordances of substance. Child Dev. 55, 453–460.

Giret, N., 2019. Chapter 26 - The Role of Sleep in Song Learning Processes in Songbird, in: Dringenberg, H.C.B.T.-H. of B.N. (Ed.), Handbook of Sleep Research. Elsevier, pp. 395–410. https://doi.org/https://doi.org/10.1016/B978-0-12-813743-7.00026-8

Gobbelé, R., Schürmann, M., Forss, N., Juottonen, K., Buchner, H., Hari, R., 2003. Activation of the human posterior parietal and temporoparietal cortices during audiotactile interaction. Neuroimage 20, 503–511. https://doi.org/10.1016/s1053-8119(03)00312-4

Goldreich, D., Kanics, I.M., 2003. Tactile acuity is enhanced in blindness. J. Neurosci. 23, 3439–3445. https://doi.org/10.1523/jneurosci.23-08-03439.2003

Gori, M., 2015. Multisensory Integration and Calibration in Children and Adults with and without Sensory and Motor Disabilities. Multisens. Res. 28, 71–99. https://doi.org/10.1163/22134808-00002478

Gori, M., Amadeo, M.B., Campus, C., 2018. Temporal Cues Influence Space Estimations in Visually Impaired Individuals. iScience 6, 319–326. https://doi.org/10.1016/j.isci.2018.07.003

Gori, M., Bollini, A., Maviglia, A., Amadeo, M.B., Tonelli, A., Crepaldi, M., Campus, C.,

2019. MSI Caterpillar: An Effective Multisensory System to Evaluate Spatial Body Representation, in: 2019 IEEE International Symposium on Medical Measurements and Applications (MeMeA). pp. 1–6. https://doi.org/10.1109/MeMeA.2019.8802133

Gori, M., Campus, C., Signorini, S., Rivara, E., Bremner, A.J., 2021. Multisensory spatial perception in visually impaired infants. Curr. Biol. 31, 5093-5101.e5. https://doi.org/10.1016/j.cub.2021.09.011

Gori, M., Del Viva, M., Sandini, G., Burr, D.C., 2008. Young children do not integrate visual and haptic form information. Curr. Biol. 18, 694–698. https://doi.org/10.1016/j.cub.2008.04.036

Gori, M., Giuliana, L., Sandini, G., Burr, D., 2012a. Visual size perception and haptic calibration during development. Dev. Sci. 15, 854–862. https://doi.org/10.1111/j.1467-7687.2012.2012.01183.x

Gori, M., Sandini, G., Burr, D., 2012b. Development of Visuo-Auditory Integration in Space and Time. Front. Integr. Neurosci. 6, 77. https://doi.org/10.3389/fnint.2012.00077

Gori, M., Sandini, G., Martinoli, C., Burr, D., 2010. Poor haptic orientation discrimination in nonsighted children may reflect disruption of cross-sensory calibration. Curr. Biol. 20, 223–225. https://doi.org/10.1016/j.cub.2009.11.069

Gori, M., Sandini, G., Martinoli, C., Burr, D.C., 2014. Impairment of auditory spatial localization in congenitally blind human subjects. Brain 137, 288–293. https://doi.org/10.1093/brain/awt311

Gori, M., Squeri, V., Sciutti, A., Masia, L., Sandini, G., Konczak, J., 2012c. Motor commands in children interfere with their haptic perception of objects. Exp. brain Res. 223, 149–157. https://doi.org/10.1007/s00221-012-3248-8

Gottbield, G., 1972. Development of Species Identification in Birds: An Inquiry into the Prenatal Determinants of Perception. University of Chicago Press, Chicago.

Gougoux, F., Zatorre, R.J., Lassonde, M., Voss, P., Lepore, F., 2005. A functional neuroimaging study of sound localization: Visual cortex activity predicts performance in early-blind individuals. PLoS Biol. 3, 0324–0333. https://doi.org/10.1371/journal.pbio.0030027

Grandchamp, R., Delorme, A., 2011. Single-trial normalization for event-related spectral decomposition reduces sensitivity to noisy trials. Front. Psychol. 2, 236. https://doi.org/10.3389/fpsyg.2011.00236

Grigg-Damberger, M.M., 2017. Ontogeny of Sleep and Its Functions in Infancy, Childhood, and Adolescence, in: Nevšímalová, S., Bruni, O. (Eds.), Sleep Disorders in Children. Springer US, pp. 3–29.

Gruber, R., Wise, M.S., 2016. Sleep Spindle Characteristics in Children with Neurodevelopmental Disorders and Their Relation to Cognition. Neural Plast. 2016, 4724792. https://doi.org/10.1155/2016/4724792

Gruber, R., Wise, M.S., Frenette, S., Knäauper, B., Boom, A., Fontil, L., Carrier, J., 2013.

The association between sleep spindles and IQ in healthy school-age children. Int. J. Psychophysiol. Off. J. Int. Organ. Psychophysiol. 89, 229–240. https://doi.org/10.1016/j.ijpsycho.2013.03.018

Habermann, M., Weusmann, D., Stein, M., Koenig, T., 2018. A student's guide to randomization statistics for multichannel event-related potentials using Ragu. Front. Neurosci. 12, 1–20. https://doi.org/10.3389/fnins.2018.00355

Halassa, M.M., Kastner, S., 2017. Thalamic functions in distributed cognitive control. Nat. Neurosci. 20. https://doi.org/10.1038/s41593-017-0020-1

Hämäläinen, H., Kekoni, J., Sams, M., Reinikainen, K., Näätänen, R., 1990. Human somatosensory evoked potentials to mechanical pulses and vibration: contributions of SI and SII somatosensory cortices to P50 and P100 components. Electroencephalogr. Clin. Neurophysiol. 75, 13–21. https://doi.org/10.1016/0013-4694(90)90148-d

Hanganu, I.L., Ben-Ari, Y., Khazipov, R., 2006. Retinal Waves Trigger Spindle Bursts in the Neonatal Rat Visual Cortex. J. Neurosci. 26, 6728 LP – 6736. https://doi.org/10.1523/JNEUROSCI.0752-06.2006

Hartley, S., Dauvilliers, Y., Quera-Salva, M.A., 2018. Circadian Rhythm Disturbances in the Blind. Curr. Neurol. Neurosci. Rep. 18, 1–8. https://doi.org/10.1007/s11910-018-0876-9

Hayton, J., Marshall, J., Dimitriou, D., 2021. Lights Out: Examining Sleep in Children with Vision Impairment. Brain Sci. 11. https://doi.org/10.3390/brainsci11040421

Heed, T., Azañón, E., 2014. Using time to investigate space: A review of tactile temporal order judgments as a window onto spatial processing in touch. Front. Psychol. 5, 1–16. https://doi.org/10.3389/fpsyg.2014.00076

Heed, T., Buchholz, V.N., Engel, A.K., Röder, B., 2015. Tactile remapping: from coordinate transformation to integration in sensorimotor processing. Trends Cogn. Sci. 19, 251–8. https://doi.org/10.1016/j.tics.2015.03.001

Heed, T., Röder, B., 2010. Common anatomical and external coding for hands and feet in tactile attention: evidence from event-related potentials. J. Cogn. Neurosci. 22, 184–202. https://doi.org/10.1162/jocn.2008.21168

Heimler, B., Striem-Amit, E., Amedi, A., 2015. Origins of task-specific sensory-independent organization in the visual and auditory brain: neuroscience evidence, open questions and clinical implications. Curr. Opin. Neurobiol. 35, 169–177. https://doi.org/10.1016/j.conb.2015.09.001

Hoedlmoser, K., Heib, D.P.J., Roell, J., Peigneux, P., Sadeh, A., Gruber, G., Schabus, M., 2014. Slow sleep spindle activity, declarative memory, and general cognitive abilities in children. Sleep 37, 1501–1512. https://doi.org/10.5665/sleep.4000

Hofstee, M., Huijding, J., Cuevas, K., Deković, M., 2022. Self-regulation and frontal EEG alpha activity during infancy and early childhood : A multilevel meta-analysis 1–17. https://doi.org/10.1111/desc.13298

Houwen, S., Hartman, E., Visscher, C., 2009. Physical activity and motor skills in children

with and without visual impairments. Med. Sci. Sports Exerc. 41, 103–109. https://doi.org/10.1249/MSS.0b013e318183389d

Houwen, S., Visscher, C., Hartman, E., Lemmink, K.A.P.M., 2007. Gross motor skills and sports participation of children with visual impairments. Res. Q. Exerc. Sport 78, 16–23. https://doi.org/10.1080/02701367.2007.10762235

Hughes, S.W., Crunelli, V., 2007. Just a phase they're going through: the complex interaction of intrinsic high-threshold bursting and gap junctions in the generation of thalamic alpha and theta rhythms. Int. J. Psychophysiol. Off. J. Int. Organ. Psychophysiol. 64, 3–17. https://doi.org/10.1016/j.ijpsycho.2006.08.004

Hyde, D.C., Jones, B.L., Porter, C.L., Flom, R., 2010. Visual stimulation enhances auditory processing in 3-month-old infants and adults. Dev. Psychobiol. 52, 181–189. https://doi.org/10.1002/dev.20417

Ingram, D.G., Cruz, J.M., Stahl, E.D., Carr, N.M., Lind, L.J., Keirns, C.C., 2022. Sleep Challenges and Interventions in Children With Visual Impairment. J. Pediatr. Ophthalmol. \& Strabismus 59, 77–86. https://doi.org/10.3928/01913913-20210623-01

Inuggi, A., Pichiecchio, A., Ciacchini, B., Signorini, S., Morelli, F., Gori, M., 2020. Multisystemic Increment of Cortical Thickness in Congenital Blind Children. Cereb. Cortex Commun. 1, 1–11. https://doi.org/10.1093/texcom/tgaa071

Jackson, C., McCabe, B.J., Nicol, A.U., Grout, A.S., Brown, M.W., Horn, G., 2008. Dynamics of a memory trace: effects of sleep on consolidation. Curr. Biol. 18, 393–400. https://doi.org/10.1016/j.cub.2008.01.062

James, K.H., Kersey, A.J., 2018. Dorsal stream function in the young child: an fMRI investigation of visually guided action. Dev. Sci. https://doi.org/10.1111/desc.12546

Jan, J.E., Wong, P.K., 1988. Behaviour of the alpha rhythm in electroencephalograms of visually impaired children. Dev Med Child Neurol 30, 444–450. https://doi.org/10.1111/j.1469-8749.1988.tb04771.x

Jaramillo, V., Schoch, S.F., Markovic, A., Kohler, M., Huber, R., Lustenberger, C., Kurth, S., 2023. An infant sleep electroencephalographic marker of thalamocortical connectivity predicts behavioral outcome in late infancy. Neuroimage 269, 119924. https://doi.org/10.1016/j.neuroimage.2023.119924

Jeavons, P.M., 1964. THE ELECTRO-ENCEPHALOGRAM IN BLIND CHILDREN. Br. J. Ophthalmol. https://doi.org/10.1136/bjo.48.2.83

Jenni, O.G., Borbély, A.A., Achermann, P., 2004. Development of the nocturnal sleep electroencephalogram in human infants. Am. J. Physiol. Regul. Integr. Comp. Physiol. 286, R528-38. https://doi.org/10.1152/ajpregu.00503.2003

Jensen, O., Mazaheri, A., 2010. Shaping functional architecture by oscillatory alpha activity: Gating by inhibition. Front. Hum. Neurosci. 4, 1–8. https://doi.org/10.3389/fnhum.2010.00186

Jiang, W., Jiang, H., Stein, B.E., 2006. Neonatal Cortical Ablation Disrupts Multisensory

Development in Superior Colliculus. J. Neurophysiol. 95, 1380–1396. https://doi.org/10.1152/jn.00880.2005

Jiang, W., Wallace, M.T., Jiang, H., Vaughan, J.W., Stein, B.E., 2001. Two Cortical Areas Mediate Multisensory Integration in Superior Colliculus Neurons. J. Neurophysiol. 85, 506–522. https://doi.org/10.1152/jn.2001.85.2.506

Johnson, C.E., 2000. Children's phoneme identification in reverberation and noise. J. Speech. Lang. Hear. Res. 43, 144–157. https://doi.org/10.1044/jslhr.4301.144

Jones, B.E., 2020. Arousal and sleep circuits. Neuropsychopharmacology 45, 6–20. https://doi.org/10.1038/s41386-019-0444-2

Kadlaskar, G., Bergmann, S., McNally Keehn, R., Seidl, A., Keehn, B., 2021. Electrophysiological Measures of Tactile and Auditory Processing in Children With Autism Spectrum Disorder. Front. Hum. Neurosci. 15. https://doi.org/10.3389/fnhum.2021.729270

Kalauzi, A., Vuckovic, A., Bojić, T., 2012. EEG alpha phase shifts during transition from wakefulness to drowsiness. Int. J. Psychophysiol. 86, 195–205. https://doi.org/10.1016/j.ijpsycho.2012.04.012

Kandel, E.R., Koester, J.D., Mack, S.H., Siegelbaum, S.A., 2021. No Title, in: Principles of Neural Science, 6e. McGraw Hill, New York, NY.

Karlen, S.J., Kahn, D.M., Krubitzer, L., 2006. Early blindness results in abnormal corticocortical and thalamocortical connections. Neuroscience 142, 843–858. https://doi.org/10.1016/j.neuroscience.2006.06.055

Kayser, C., Petkov, C.I., Logothetis, N.K., 2009. Multisensory interactions in primate auditory cortex: fMRI and electrophysiology. Hear. Res. 258, 80–88. https://doi.org/10.1016/j.heares.2009.02.011

Keil, J., Senkowski, D., 2018. Neural Oscillations Orchestrate Multisensory Processing. https://doi.org/10.1177/1073858418755352

Khazipov, R., Sirota, A., Leinekugel, X., Holmes, G.L., Ben-Ari, Y., Buzsáki, G., 2004. Early motor activity drives spindle bursts in the developing somatosensory cortex. Nature 432, 758–761. https://doi.org/10.1038/nature03132

Kim, D., Woo, J.H., Jeong, J., Kim, S., 2023. The sound stimulation method and EEG change analysis for development of digital therapeutics that can stimulate the nervous system: Cortical activation and drug substitution potential. CNS Neurosci. Ther. 29, 402–411. https://doi.org/10.1111/cns.14014

King, A.J., 2014. What happens to your hearing if you are born blind? Brain 137, 6–8. https://doi.org/10.1093/brain/awt346

King, A.J., Carlile, S., 1993. Changes induced in the representation of auditory space in the superior colliculus by rearing ferrets with binocular eyelid suture. Exp. brain Res. 94, 444–455. https://doi.org/10.1007/BF00230202

King, A.J., Walker, K.M.M., 2012. Integrating information from different senses in the auditory cortex 617–625. https://doi.org/10.1007/s00422-012-0502-x

Klimesch, W., 1997. EEG-alpha rhythms and memory processes, in: International Journal of Psychophysiology. https://doi.org/10.1016/S0167-8760(97)00773-3

Klimesch, W., Doppelmayr, M., Pachinger, T., Russegger, H., 1997. Event-related desynchronization in the alpha band and the processing of semantic information. Brain Res. Cogn. Brain Res. 6, 83–94. https://doi.org/10.1016/s0926-6410(97)00018-9

Klimesch, W., Schimke, H., Pfurtscheller, G., 1993. Alpha frequency, cognitive load and memory performance. Brain Topogr. 5, 241–251. https://doi.org/10.1007/BF01128991

Klimesch, W., Schimke, H., Schwaiger, J., 1994. Episodic and semantic memory: an analysis in the EEG theta and alpha band. Electroencephalogr. Clin. Neurophysiol. https://doi.org/10.1016/0013-4694(94)90164-3

Knudsen, E.I., 1998. Capacity for plasticity in the adult owl auditory system expanded by juvenile experience. Science 279, 1531–1533. https://doi.org/10.1126/science.279.5356.1531

Kolarik, A.J., Cirstea, S., Pardhan, S., 2013. Evidence for enhanced discrimination of virtual auditory distance among blind listeners using level and direct-to-reverberant cues. Exp. brain Res. 224, 623–633. https://doi.org/10.1007/s00221-012-3340-0

Kolarik, A.J., Pardhan, S., Cirstea, S., Moore, B.C.J., 2017. Auditory spatial representations of the world are compressed in blind humans. Exp. brain Res. 235, 597–606. https://doi.org/10.1007/s00221-016-4823-1

Kolev, V., Başar-Eroglu, C., Aksu, F., Başar, E., 1994. EEG rhythmicities evoked by visual stimuli in three-year-old children. Int. J. Neurosci. 75, 257–270. https://doi.org/10.3109/00207459408986308

Kovács, I., Kozma, P., Fehér, A., Benedek, G., 1999. Late maturation of visual spatial integration in humans. Proc. Natl. Acad. Sci. U. S. A. 96, 12204–12209. https://doi.org/10.1073/pnas.96.21.12204

Kriegseis, A., Hennighausen, E., Rösler, F., Röder, B., 2006. Reduced EEG alpha activity over parieto-occipital brain areas in congenitally blind adults. Clin. Neurophysiol. 117, 1560–1573. https://doi.org/https://doi.org/10.1016/j.clinph.2006.03.030

Kuehn, E., Pleger, B., 2018. How Visual Body Perception Influences Somatosensory Plasticity. Neural Plast. 2018, 7909684. https://doi.org/10.1155/2018/7909684

Kuhl, P.K., Meltzoff, A.N., 1982. The bimodal perception of speech in infancy. Science 218, 1138–1141. https://doi.org/10.1126/science.7146899

Kujala, T., Huotilainen, M., Sinkkonen, J., Ahonen, A.I., Alho, K., Hämäläinen, M.S., Ilmoniemi, R.J., Kajola, M., Knuutila, J.E., Lavikainen, J., 1995. Visual cortex activation in blind humans during sound discrimination. Neurosci. Lett. 183, 143–146. https://doi.org/10.1016/0304-3940(94)11135-6

Kupers, R., Ptito, M., 2011. Insights from darkness: what the study of blindness has taught us about brain structure and function. Prog. Brain Res. 192, 17–31.

https://doi.org/10.1016/B978-0-444-53355-5.00002-6

Kurdziel, L., Duclos, K., Spencer, R.M.C., 2013. Sleep spindles in midday naps enhance learning in preschool children. Proc. Natl. Acad. Sci. 110, 17267 LP – 17272. https://doi.org/10.1073/pnas.1306418110

Kurth, S., Ringli, M., Geiger, A., LeBourgeois, M., Jenni, O.G., Huber, R., 2010. Mapping of Cortical Activity in the First Two Decades of Life: A High-Density Sleep Electroencephalogram Study. J. Neurosci. 30, 13211–13219. https://doi.org/10.1523/JNEUROSCI.2532-10.2010

Kurth, S., Ringli, M., LeBourgeois, M.K., Geiger, A., Buchmann, A., Jenni, O.G., Huber, R., 2012. Mapping the electrophysiological marker of sleep depth reveals skill maturation in children and adolescents. Neuroimage 63, 959–965. https://doi.org/10.1016/j.neuroimage.2012.03.053

Kwok, E.Y.L., Oram, J., Allman, B.L., Allen, P., 2019. Dynamics of spontaneous alpha activity correlate with language ability in young children. Behav. Brain Res. 359, 56–65. https://doi.org/10.1016/j.bbr.2018.10.024

Kwon, H., Walsh, K.G., Berja, E.D., Manoach, D.S., Eden, U.T., Kramer, M.A., Chu, C.J., 2023. Sleep spindles in the healthy brain from birth through 18 years. Sleep 46. https://doi.org/10.1093/sleep/zsad017

Làdavas, E., Farnè, A., 2004. Visuo-tactile representation of near-the-body space. J. Physiol. Paris 98, 161–170. https://doi.org/10.1016/j.jphysparis.2004.03.007

Latchoumane, C.F. V., Ngo, H.V. V., Born, J., Shin, H.S., 2017. Thalamic Spindles Promote Memory Formation during Sleep through Triple Phase-Locking of Cortical, Thalamic, and Hippocampal Rhythms. Neuron 95, 424-435.e6. https://doi.org/10.1016/j.neuron.2017.06.025

Laurienti, P.J., Wallace, M.T., Maldjian, J.A., Susi, C.M., Stein, B.E., Burdette, J.H., 2003. Cross-modal sensory processing in the anterior cingulate and medial prefrontal cortices. Hum. Brain Mapp. 19, 213–223. https://doi.org/10.1002/hbm.10112

Laventure, S., Pinsard, B., Lungu, O., Carrier, J., Fogel, S., Benali, H., Lina, J.-M., Boutin, A., Doyon, J., 2018. Beyond spindles: interactions between sleep spindles and boundary frequencies during cued reactivation of motor memory representations. Sleep 41. https://doi.org/10.1093/sleep/zsy142

Le Bon, O., 2020. Relationships between REM and NREM in the NREM-REM sleep cycle: a review on competing concepts. Sleep Med. 70, 6–16. https://doi.org/10.1016/j.sleep.2020.02.004

Leed, J.E., Chinn, L.K., Lockman, J.J., 2019. Reaching to the Self: The Development of Infants' Ability to Localize Targets on the Body. Psychol. Sci. 30, 1063–1073. https://doi.org/10.1177/0956797619850168

Leger, D., Guilleminault, C., Santos, C., Paillard, M., 2002. Sleep/wake cycles in the dark: Sleep recorded by polysomnography in 26 totally blind subjects compared to controls. Clin. Neurophysiol. 113, 1607–1614. https://doi.org/10.1016/S1388-2457(02)00221-3

Leger, D., Prevot, E., Philip, P., Yence, C., Labaye, N., Paillard, M., Guilleminault, C., 1999. Sleep disorders in children with blindness. Ann. Neurol. 46, 648–651. https://doi.org/10.1002/1531-8249(199910)46:4<648::aid-ana14>3.0.co;2-x

Leger, D., Stal, V., Quera-Salva, M.A., Guilleminault, C., Paillard, M., 2001. Disorders of wakefulness and sleep in blind patients. Rev. Neurol. (Paris). 157, S135-9.

Legge, G.E., Madison, C., Vaughn, B.N., Cheong, A.M.Y., Miller, J.C., 2008. Retention of high tactile acuity throughout the life span in blindness. Percept. Psychophys. 70, 1471–1488. https://doi.org/10.3758/PP.70.8.1471

Lehtelä, L., Salmelin, R., Hari, R., 1997. Evidence for reactive magnetic 10-Hz rhythm in the human auditory cortex. Neurosci. Lett. 222, 111–114. https://doi.org/10.1016/s0304-3940(97)13361-4

Lehtinen-Railo, S., Juurmaa, J., 1994. Effect of visual experience on locational judgements after perspective change in small-scale space. Scand. J. Psychol. 35, 175–183. https://doi.org/10.1111/j.1467-9450.1994.tb00941.x

Leiter, R.G., 1980. Leiter International Performance Scale, instruction manual. Chicago.

Lenassi, E., Likar, K., Stirn-Kranjc, B., Brecelj, J., 2008. VEP maturation and visual acuity in infants and preschool children. Doc. Ophthalmol. https://doi.org/10.1007/s10633-007-9111-8

Lenth, R. V, 2022. emmeans: Estimated Marginal Means, aka Least-Squares Means.

Lessard, N., Paré, M., Lepore, F., Lassonde, M., 1998. Early-blind human subjects localize sound sources better than sighted subjects. Nature 395, 278–280. https://doi.org/10.1038/26228

Lewkowicz, D.J., Turkewitz, G., 1980. Cross-modal equivalence in early infancy: Auditory-visual intensity matching. Dev. Psychol. 16, 597–607. https://doi.org/10.1037//0012-1649.16.6.597

Ley, P., Bottari, D., Shenoy, B.H., Kekunnaya, R., Röder, B., 2013. Partial recovery of visual-spatial remapping of touch after restoring vision in a congenitally blind man. Neuropsychologia 51, 1119–1123. https://doi.org/10.1016/j.neuropsychologia.2013.03.004

Lin, J., Zhang, L., Guo, R., Jiao, S., Song, X., Feng, S., Wang, K., Li, M., Luo, Y., Han, Z., 2022. The influence of visual deprivation on the development of the thalamocortical network : Evidence from congenitally blind children and adults. Neuroimage 264, 119722. https://doi.org/10.1016/j.neuroimage.2022.119722

Longo, M.R., Azañón, E., Haggard, P., 2010. More than skin deep: body representation beyond primary somatosensory cortex. Neuropsychologia 48, 655–668. https://doi.org/10.1016/j.neuropsychologia.2009.08.022

Loomis, J.M., Klatzky, R.L., Philbeck, J.W., Golledge, R.G., 1998. Assessing auditory distance perception using perceptually directed action. Percept. Psychophys. 60, 966–980. https://doi.org/10.3758/bf03211932

Lopes Da Silva, F.H., 1995. Dynamic of Electrical Activity of the Brain, Networks, and

and Modulating Systems. Neocortical Dyn. Hum. EEG Rhythm. 249–271.

Lopes da Silva, F.H., van Lierop, T.H., Schrijer, C.F., van Leeuwen, W.S., 1973. Organization of thalamic and cortical alpha rhythms: spectra and coherences. Electroencephalogr. Clin. Neurophysiol. 35, 627–639. https://doi.org/10.1016/0013-4694(73)90216-2

Louis, J., Zhang, J.X., Revol, M., Debilly, G., Challamel, M.J., 1992. Ontogenesis of nocturnal organization of sleep spindles: a longitudinal study during the first 6 months of life. Electroencephalogr. Clin. Neurophysiol. 83, 289–296. https://doi.org/https://doi.org/10.1016/0013-4694(92)90088-Y

Luiz, D.M., Foxcroft, C.D., Stewart, R., 2001. The construct validity of the Griffiths Scales of Mental Development. Child. Care. Health Dev. 27, 73–83. https://doi.org/https://doi.org/10.1046/j.1365-2214.2001.00158.x

Lustenberger, C., Maric, A., Dürr, R., Achermann, P., Huber, R., 2012. Triangular Relationship between Sleep Spindle Activity, General Cognitive Ability and the Efficiency of Declarative Learning. PLoS One 7. https://doi.org/10.1371/journal.pone.0049561

Macaluso, E., Frith, C.D., Driver, J., 2000. Modulation of Human Visual Cortex by Crossmodal Spatial Attention 289, 1206–1209.

Maffongelli, L., D'Ausilio, A., Fadiga, L., Daum, M.M., 2019. The ontogenesis of action syntax. Collabra Psychol. https://doi.org/10.1525/collabra.215

Maij, F., Seegelke, C., Medendorp, W.P., Heed, T., 2020. External location of touch is constructed post-hoc based on limb choice. Elife 9, 1–47. https://doi.org/10.7554/ELIFE.57804

Maitre, N.L., Key, A.P., Slaughter, J.C., Yoder, P.J., Neel, M.L., Richard, C., Wallace, M.T., Murray, M.M., 2020. Neonatal Multisensory Processing in Preterm and Term Infants Predicts Sensory Reactivity and Internalizing Tendencies in Early Childhood. Brain Topogr. 33, 586–599. https://doi.org/10.1007/s10548-020-00791-4

Maquet, P., 2010. Understanding non rapid eye movement sleep through neuroimaging. world J. Biol. psychiatry Off. J. World Fed. Soc. Biol. Psychiatry 11 Suppl 1, 9–15. https://doi.org/10.3109/15622971003637736

Maquet, P., Degueldre, C., Delfiore, G., Aerts, J., Péters, J.M., Luxen, A., Franck, G., 1997. Functional neuroanatomy of human slow wave sleep. J. Neurosci. Off. J. Soc. Neurosci. 17, 2807–2812. https://doi.org/10.1523/JNEUROSCI.17-08-02807.1997

Marcuse, L. V, Schneider, M., Mortati, K.A., Donnelly, K.M., Arnedo, V., Grant, A.C., 2008. Quantitative analysis of the EEG posterior-dominant rhythm in healthy adolescents. Clin. Neurophysiol. Off. J. Int. Fed. Clin. Neurophysiol. 119, 1778–1781. https://doi.org/10.1016/j.clinph.2008.02.023

Maris, E., Oostenveld, R., 2007. Nonparametric statistical testing of EEG- and MEG-data. J. Neurosci. Methods. https://doi.org/10.1016/j.jneumeth.2007.03.024

Marshall, P.J., Bar-Haim, Y., Fox, N.A., 2002. Development of the EEG from 5 months to

4 years of age. Clin. Neurophysiol. https://doi.org/10.1016/S1388-2457(02)00163-3

Martini, F.J., Guillamón-Vivancos, T., Moreno-Juan, V., Valdeolmillos, M., López-Bendito, G., 2021. Spontaneous activity in developing thalamic and cortical sensory networks. Neuron 109, 2519–2534. https://doi.org/10.1016/j.neuron.2021.06.026

Marzano, C., Moroni, F., Gorgoni, M., Nobili, L., Ferrara, M., De Gennaro, L., 2013. How we fall asleep: regional and temporal differences in electroencephalographic synchronization at sleep onset. Sleep Med. 14, 1112–1122. https://doi.org/https://doi.org/10.1016/j.sleep.2013.05.021

Mauguière, F., Merlet, I., Forss, N., Vanni, S., Jousmäki, V., Adeleine, P., Hari, R., 1997. Activation of a distributed somatosensory cortical network in the human brain: a dipole modelling study of magnetic fields evoked by median nerve stimulation. Part II: Effects of stimulus rate, attention and stimulus detection. Electroencephalogr. Clin. Neurophysiol. 104, 290–295. https://doi.org/10.1016/s0013-4694(97)00018-7

McClain, I.J., Lustenberger, C., Achermann, P., Lassonde, J.M., Kurth, S., LeBourgeois, M.K., 2016. Developmental Changes in Sleep Spindle Characteristics and Sigma Power across Early Childhood. Neural Plast. 2016, 3670951. https://doi.org/10.1155/2016/3670951

Mcsweeney, M., Morales, S., Valadez, E.A., Buzzell, G.A., Yoder, L., Fifer, W.P., Pini, N., Shuffrey, L.C., Elliott, A.J., Isler, J.R., Fox, N.A., 2023. Age-related trends in aperiodic EEG activity and alpha oscillations during early- to middle-childhood 1–22. https://doi.org/10.1016/j.neuroimage.2023.119925.Age-related

Mecarelli, O., 2019. Electrode Placement Systems and Montages, in: Mecarelli, O. (Ed.), Clinical Electroencephalography. Springer International Publishing, Cham, pp. 35–52. https://doi.org/10.1007/978-3-030-04573-9_4

Meltzoff, A.N., Borton, R.W., 1979. Intermodal matching by human neonates. Nature 282, 403–404. https://doi.org/10.1038/282403a0

Meltzoff, A.N., Saby, J.N., Marshall, P.J., 2019. Neural representations of the body in 60-day-old human infants. Dev. Sci. 22, e12698. https://doi.org/10.1111/desc.12698

Meng, X., Mukherjee, D., Kao, J.P.Y., Kanold, P.O., 2021. Early peripheral activity alters nascent subplate circuits in the auditory cortex. Sci. Adv. 7. https://doi.org/10.1126/sciadv.abc9155

Menicucci, D., Lunghi, C., Zaccaro, A., Morrone, M.C., Gemignani, A., 2022. Mutual interaction between visual homeostatic plasticity and sleep in adult humans. Elife 11, e70633. https://doi.org/10.7554/eLife.70633

Mercier, M.R., Foxe, J.J., Fiebelkorn, I.C., Butler, J.S., Schwartz, T.H., Molholm, S., 2013. Auditory-driven phase reset in visual cortex: Human electrocorticography reveals mechanisms of early multisensory integration. Neuroimage 79, 19–29. https://doi.org/10.1016/j.neuroimage.2013.04.060

Meredith, M.A., Stein, B.E., 1986. Visual, auditory, and somatosensory convergence on cells in superior colliculus results in multisensory integration. J. Neurophysiol. 56, 640–662. https://doi.org/10.1152/jn.1986.56.3.640

Meredith, M.A., Stein, B.E., 1983. Interactions among converging sensory inputs in the superior colliculus. Science 221, 389–391. https://doi.org/10.1126/science.6867718

Meredith, M.A., Wallace, M.T., Clemo, H.R., 2018. Do the Different Sensory Areas Within the Cat Anterior Ectosylvian Sulcal Cortex Collectively Represent a Network Multisensory Hub? Multisens. Res. 31, 793–823. https://doi.org/10.1163/22134808-20181316

Michel, C.M., Koenig, T., 2018. EEG microstates as a tool for studying the temporal dynamics of whole-brain neuronal networks: A review. Neuroimage 180, 577–593. https://doi.org/10.1016/j.neuroimage.2017.11.062

Milh, M., Kaminska, A., Huon, C., Lapillonne, A., Ben-Ari, Y., Khazipov, R., 2007. Rapid cortical oscillations and early motor activity in premature human neonate. Cereb. Cortex 17, 1582–1594. https://doi.org/10.1093/cercor/bhl069

Miller, L., 1992. Diderot Reconsidered: Visual Impairment and Auditory Compensation. J. Vis. Impair. Blind. 86, 206–210. https://doi.org/10.1177/0145482X9208600504

Miskovic, V., Ma, X., Chou, C.A., Fan, M., Owens, M., Sayama, H., Gibb, B.E., 2015. Developmental changes in spontaneous electrocortical activity and network organization from early to late childhood. Neuroimage 118, 237–247. https://doi.org/10.1016/j.neuroimage.2015.06.013

Mitrukhina, O., Suchkov, D., Khazipov, R., Minlebaev, M., 2015. Imprecise Whisker Map in the Neonatal Rat Barrel Cortex. Cereb. Cortex 25, 3458–3467. https://doi.org/10.1093/cercor/bhu169

Mix, K.S., Huttenlocher, J., Levine, S.C., 1996. Do Preschool Children Recognize Auditory-Visual Numerical Correspondences? Child Dev. https://doi.org/10.1111/j.1467-8624.1996.tb01816.x

Miyamoto, D., 2023. Neural circuit plasticity for complex non-declarative sensorimotor memory consolidation during sleep. Neurosci. Res. 189, 37–43. https://doi.org/10.1016/j.neures.2022.12.020

Mohns, E.J., Blumberg, M.S., 2008. Synchronous bursts of neuronal activity in the developing hippocampus: modulation by active sleep and association with emerging gamma and theta rhythms. J. Neurosci. Off. J. Soc. Neurosci. 28, 10134–10144. https://doi.org/10.1523/JNEUROSCI.1967-08.2008

Molholm, S., Murphy, J.W., Bates, J., Ridgway, E.M., Foxe, J.J., 2020. Multisensory Audiovisual Processing in Children With a Sensory Processing Disorder (I): Behavioral and Electrophysiological Indices Under Speeded Response Conditions. Front. Integr. Neurosci. 14, 1–15. https://doi.org/10.3389/fnint.2020.00004

Molholm, S., Ritter, W., Javitt, D.C., Foxe, J.J., 2004. Multisensory visual-auditory object recognition in humans: a high-density electrical mapping study. Cereb. Cortex 14, 452–465. https://doi.org/10.1093/cercor/bhh007

Molholm, S., Ritter, W., Murray, M.M., Javitt, D.C., Schroeder, C.E., Foxe, J.J., 2002. Multisensory auditory-visual interactions during early sensory processing in humans: a high-density electrical mapping study. Brain Res. Cogn. Brain Res. 14, 115–128.

https://doi.org/10.1016/s0926-6410(02)00066-6

Molholm, S., Sehatpour, P., Mehta, A.D., Shpaner, M., Gomez-Ramirez, M., Ortigue, S., Dyke, J.P., Schwartz, T.H., Foxe, J.J., 2006. Audio-visual multisensory integration in superior parietal lobule revealed by human intracranial recordings. J. Neurophysiol. 96, 721–729. https://doi.org/10.1152/jn.00285.2006

Moll, H., Meltzoff, A.N., Merzsch, K., Tomasello, M., 2013. Taking versus confronting visual perspectives in preschool children. Dev. Psychol. 49, 646–654. https://doi.org/10.1037/a0028633

Morelli, F., Schiatti, L., Cappagli, G., Martolini, C., Gori, M., Signorini, S., 2023. Clinical assessment of the TechArm system on visually impaired and blind children during uni- and multi-sensory perception tasks. Front. Neurosci. 17, 1158438. https://doi.org/10.3389/fnins.2023.1158438

Morison, R.S., Bassett, D.L., 1945. ELECTRICAL ACTIVITY OF THE THALAMUS AND BASAL GANGLIA IN DECORTICATE CATS. J. Neurophysiol. 8, 309–314. https://doi.org/10.1152/jn.1945.8.5.309

Mullen, T., Kothe, C., Chi, Y.M., Ojeda, A., Kerth, T., Makeig, S., Cauwenberghs, G., Jung, T.P., 2013. Real-time modeling and 3D visualization of source dynamics and connectivity using wearable EEG, in: Proceedings of the Annual International Conference of the IEEE Engineering in Medicine and Biology Society, EMBS. https://doi.org/10.1109/EMBC.2013.6609968

Mullen, T.R., Kothe, C.A.E., Chi, Y.M., Ojeda, A., Kerth, T., Makeig, S., Jung, T.-P., Cauwenberghs, G., 2015. Real-Time Neuroimaging and Cognitive Monitoring Using Wearable Dry EEG. IEEE Trans. Biomed. Eng. 62, 2553–2567. https://doi.org/10.1109/TBME.2015.2481482

Murata, Y., Colonnese, M.T., 2019. Thalamic inhibitory circuits and network activity development. Brain Res. 1706, 13–23. https://doi.org/https://doi.org/10.1016/j.brainres.2018.10.024

Murray, M.M., Michel, C.M., Grave de Peralta, R., Ortigue, S., Brunet, D., Gonzalez Andino, S., Schnider, A., 2004. Rapid discrimination of visual and multisensory memories revealed by electrical neuroimaging. Neuroimage 21, 125–135. https://doi.org/10.1016/j.neuroimage.2003.09.035

Murray, M.M., Molholm, S., Michel, C.M., Heslenfeld, D.J., Ritter, W., Javitt, D.C., Schroeder, C.E., Foxe, J.J., 2005. Grabbing your ear: Rapid auditory-somatosensory multisensory interactions in low-level sensory cortices are not constrained by stimulus alignment. Cereb. Cortex 15, 963–974. https://doi.org/10.1093/cercor/bhh197

Murray, M.M., Thelen, A., Thut, G., Romei, V., Martuzzi, R., Matusz, P.J., 2016. The multisensory function of the human primary visual cortex. Neuropsychologia 83, 161–169. https://doi.org/10.1016/j.neuropsychologia.2015.08.011

Musacchia, G., Schroeder, C.E., 2009. Neuronal mechanisms , response dynamics and perceptual functions of multisensory interactions in auditory cortex. Hear. Res. 258, 72–79. https://doi.org/10.1016/j.heares.2009.06.018

Nardini, M., Bedford, R., Mareschal, D., 2010. Fusion of visual cues is not mandatory in children. Proc. Natl. Acad. Sci. U. S. A. 107, 17041–17046. https://doi.org/10.1073/pnas.1001699107

Nardini, M., Begus, K., Mareschal, D., 2013. Multisensory uncertainty reduction for hand localization in children and adults. J. Exp. Psychol. Hum. Percept. Perform. 39, 773–787. https://doi.org/10.1037/a0030719

Nardini, M., Jones, P., Bedford, R., Braddick, O., 2008. Development of Cue Integration in Human Navigation. Curr. Biol. 18, 689–693. https://doi.org/10.1016/j.cub.2008.04.021

Neil, P.A., Chee-Ruiter, C., Scheier, C., Lewkowicz, D.J., Shimojo, S., 2006. Development of multisensory spatial integration and perception in humans. Dev. Sci. 9, 454–464. https://doi.org/10.1111/j.1467-7687.2006.00512.x

Niedermeyer, E., 1997. Alpha rhythms as physiological and abnormal phenomena. Int. J. Psychophysiol. 26, 31–49. https://doi.org/10.1016/S0167-8760(97)00754-X

Noebels, J.L., Roth, W.T., Kopell, B.S., 1978. Cortical slow potentials and the occipital EEG in congenital blindness. J Neurol Sci 37, 51–58.

Novikova, L.A., 1974. Blindness and the electrical activity of the brain: electroencephalographic studies of the effects of sensory impairment. American Foundation for the Blind.

Olsho, L.W., 1984. Infant frequency discrimination. Infant Behav. Dev. 7, 27–35. https://doi.org/10.1016/S0163-6383(84)80020-X

Olsho, L.W., Koch, E.G., Carter, E.A., Halpin, C.F., Spetner, N.B., 1986. Pure-tone sensitivity of human infants. J. Acoust. Soc. Am. 80, S123–S123. https://doi.org/10.1121/1.2023630

Oostenveld, R., Fries, P., Maris, E., Schoffelen, J.-M., Oostenveld, R., Fries, P., Maris, E., Schoffelen, J.-M., 2011. FieldTrip: Open Source Software for Advanced Analysis of MEG, EEG, and Invasive Electrophysiological Data, FieldTrip: Open Source Software for Advanced Analysis of MEG, EEG, and Invasive Electrophysiological Data. Comput. Intell. Neurosci. https://doi.org/10.1155/2011/156869, 10.1155/2011/156869

Ortiz-terán, L., Diez, I., Ortiz, T., Perez, D.L., Ignacio, J., Costumero, V., 2017. Brain circuit – gene expression relationships and neuroplasticity of multisensory cortices in blind children 2–7. https://doi.org/10.1073/pnas.1619121114

Ossandón, J.P., König, P., Heed, T., 2020. No Evidence for a Role of Spatially Modulated a -Band Activity in Tactile Remapping and Short-Latency , Overt Orienting Behavior 40, 9088–9102.

Ossandón, J.P., Stange, L., Gudi-Mindermann, H., Rimmele, J.M., Sourav, S., Bottari, D., Kekunnaya, R., Röder, B., 2023. The development of oscillatory and aperiodic resting state activity is linked to a sensitive period in humans. Neuroimage 275, 120171. https://doi.org/10.1016/j.neuroimage.2023.120171

Page, J., Lustenberger, C., Fröhlich, F., 2018. Social, motor, and cognitive development through the lens of sleep network dynamics in infants and toddlers between 12 and 30 months of age. Sleep 41. https://doi.org/10.1093/sleep/zsy024

Pagel, B., Heed, T., Ro, B., 2009. Change of reference frame for tactile localization during child development 6, 929–937. https://doi.org/10.1111/j.1467-7687.2009.00845.x

Palmiero, M., 2014. La cognizione spaziale : uno sguardo alla rappresentazione dello spazio e alle modalità di navigazione.

Park, H.-J., Lee, J.D., Kim, E.Y., Park, B., Oh, M.-K., Lee, S., Kim, J.-J., 2009. Morphological alterations in the congenital blind based on the analysis of cortical thickness and surface area. Neuroimage 47, 98–106. https://doi.org/10.1016/j.neuroimage.2009.03.076

Pasqualotto, A., Proulx, M.J., 2012. The role of visual experience for the neural basis of spatial cognition. Neurosci. Biobehav. Rev. 36, 1179–1187. https://doi.org/10.1016/j.neubiorev.2012.01.008

Paus, T., 2005. Mapping brain development and aggression. Can. child Adolesc. psychiatry Rev. = La Rev. Can. Psychiatr. l'enfant l'adolescent 14, 10–15.

Peirano, P.D., Algarín, C.R., 2007. Sleep in brain development. Biol. Res. 40, 471–478. https://doi.org/10.4067/S0716-97602007000500008

Pernet, C.R., Latinus, M., Nichols, T.E., Rousselet, G.A., 2015. Cluster-based computational methods for mass univariate analyses of event-related brain potentials/fields: A simulation study. J. Neurosci. Methods 250, 85–93. https://doi.org/10.1016/j.jneumeth.2014.08.003

Petersén, I., Eeg-Olofsson, O., 1971. The development of the electroencephalogram in normal children from the age of 1 through 15 years. Non-paroxysmal activity. Neuropadiatrie 2, 247–304. https://doi.org/10.1055/s-0028-1091786

Petrini, K., Remark, A., Smith, L., Nardini, M., 2014. When vision is not an option: Children's integration of auditory and haptic information is suboptimal. Dev. Sci. 17, 376–387. https://doi.org/10.1111/desc.12127

Petsche, H., Kaplan, S., Von Stein, A., Filz, O., 1997. The possible meaning of the upper and lower alpha frequency ranges for cognitive and creative tasks. Int. J. Psychophysiol. 26, 77–97.

Pfurtscheller, G., Lopes da Silva, F.H., 1999. Event-related EEG/MEG synchronization and desynchronization: basic principles. Clin. Neurophysiol. Off. J. Int. Fed. Clin. Neurophysiol. 110, 1842–1857. https://doi.org/10.1016/s1388-2457(99)00141-8

Pion-Tonachini, L., Kreutz-Delgado, K., Makeig, S., 2019. ICLabel: An automated electroencephalographic independent component classifier, dataset, and website. Neuroimage 198, 181–197. https://doi.org/10.1016/j.neuroimage.2019.05.026

Poirier, C., Collignon, O., DeVolder, A.G., Renier, L., Vanlierde, A., Tranduy, D., Scheiber, C., 2005. Specific activation of the V5 brain area by auditory motion processing: An fMRI study. Cogn. Brain Res. 25, 650–658.

https://doi.org/10.1016/j.cogbrainres.2005.08.015

Poulsen, A.T., Pedroni, A., Langer, N., Hansen, L.K., 2018. Microstate EEGlab toolbox: An introductory guide. bioRxiv 1–30. https://doi.org/10.1101/289850

Puentes-Mestril, C., Roach, J., Niethard, N., Zochowski, M., Aton, S.J., 2019. How rhythms of the sleeping brain tune memory and synaptic plasticity. Sleep 42. https://doi.org/10.1093/sleep/zsz095

R Core Team, 2021. R: A Language and Environment for Statistical Computing.

Radziun, D., Korczyk, M., Szwed, M., Ehrsson, H.H., 2024. Are blind individuals immune to bodily illusions? Somatic rubber hand illusion in the blind revisited. Behav. Brain Res. 460, 114818. https://doi.org/10.1016/j.bbr.2023.114818

Rakic, P., Suñer, I., Williams, R.W., 1991. A novel cytoarchitectonic area induced experimentally within the primate visual cortex. Proc. Natl. Acad. Sci. U. S. A. https://doi.org/10.1073/pnas.88.6.2083

Rasch, B., Born, J., 2013. About Sleep's Role in Memory. Physiol. Rev. 93, 681–766. https://doi.org/10.1152/physrev.00032.2012

Raven, J.C., Court, J.H., Raven, J., 1996. Raven Manual: Section 3 Standard ProgressiveMatrices With Adult US Norms by JC Raven, JH Court AndJ. Raven. Oxford Psychologist Press.

Ray, L.B., Sockeel, S., Soon, M., Bore, A., Myhr, A., Stojanoski, B., Cusack, R., Owen, A.M., Doyon, J., Fogel, S.M., 2015. Expert and crowd-sourced validation of an individualized sleep spindle detection method employing complex demodulation and individualized normalization. Front. Hum. Neurosci. 9, 507. https://doi.org/10.3389/fnhum.2015.00507

Recanzone, G.H., 1998. Rapidly induced auditory plasticity: The ventriloquism aftereffect. Proc. Natl. Acad. Sci. 95, 869–875. https://doi.org/10.1073/pnas.95.3.869

Red'ka, I. V, Mayorov, O.Y., 2014. Spectral characteristics of the ongoing electroencephalogram in children suffering from visual dysfunctions. Neurophysiology 46, 149–159.

Renier, L., De Volder, A.G., 2005. Cognitive and brain mechanisms in sensory substitution of vision: a contribution to the study of human perception. J. Integr. Neurosci. 4, 489–503. https://doi.org/10.1142/s0219635205000999

Renier, L., De Volder, A.G., Rauschecker, J.P., 2014. Cortical plasticity and preserved function in early blindness. Neurosci. Biobehav. Rev. 41, 53–63. https://doi.org/10.1016/j.neubiorev.2013.01.025

Revelle, W., 2009. An introduction to psychometric theory with applications in R.

Reynell, J., 1978. Developmental patterns of visually handicapped children. Child. Care. Health Dev. 4, 291–303.

Ricci, A., He, F., Calhoun, S.L., Fang, J., Vgontzas, A.N., Liao, D., Bixler, E.O., Younes, M., Fernandez-Mendoza, J., 2021. Sex and Pubertal Differences in the Maturational Trajectories of Sleep Spindles in the Transition from Childhood to Adolescence: A

Population-Based Study. eNeuro 8. https://doi.org/10.1523/ENEURO.0257-21.2021

Ricciardi, E., Bonino, D., Pellegrini, S., Pietrini, P., 2014. Mind the blind brain to understand the sighted one! Is there a supramodal cortical functional architecture? Neurosci. Biobehav. Rev. 41, 64–77. https://doi.org/10.1016/j.neubiorev.2013.10.006

Richardson, H., Saxe, R., Bedny, M., 2023. Developmental Cognitive Neuroscience Neural correlates of theory of mind reasoning in congenitally blind children. Dev. Cogn. Neurosci. 63, 101285. https://doi.org/10.1016/j.dcn.2023.101285

Rigato, S., Begum Ali, J., Van Velzen, J., Bremner, A.J., 2014. The neural basis of somatosensory remapping develops in human infancy. Curr. Biol. 24, 1222–1226. https://doi.org/10.1016/j.cub.2014.04.004

Rigato, S., Bremner, A.J., Mason, L., Pickering, A., Davis, R., van Velzen, J., 2013. The electrophysiological time course of somatosensory spatial remapping: Vision of the hands modulates effects of posture on somatosensory evoked potentials. Eur. J. Neurosci. 38, 2884–2892. https://doi.org/10.1111/ejn.12292

Ringland, K.E., Zalapa, R., Neal, M., Escobedo, L., Tentori, M., Hayes, G.R., 2014. SensoryPaint : A Multimodal Sensory Intervention for Children with SensoryPaint : A Multimodal Sensory Intervention for C hildren with N eurodevelopmental D isorders. https://doi.org/10.1145/2632048.2632065

Rockland, K.S., Ojima, H., 2003. Multisensory convergence in calcarine visual areas in macaque monkey. Int. J. Psychophysiol. Off. J. Int. Organ. Psychophysiol. 50, 19–26. https://doi.org/10.1016/s0167-8760(03)00121-1

Röder, B., 2012. Sensory deprivation and the development of multisensory integration. Multisensory Dev. https://doi.org/10.1093/acprof:oso/9780199586059.003.0013

Röder, B., Heed, T., Badde, S., 2014. Development of the spatial coding of touch: ability vs. automaticity. Dev. Sci. 17, 944–945. https://doi.org/https://doi.org/10.1111/desc.12186

Röder, B., Pagel, B., Heed, T., 2013. The implicit use of spatial information develops later for crossmodal than for intramodal temporal processing. Cognition 126, 301–306. https://doi.org/https://doi.org/10.1016/j.cognition.2012.09.009

Röder, B., Rösler, F., Neville, H.J., 2000. Event-related potentials during auditory language processing in congenitally blind and sighted people. Neuropsychologia 38, 1482–1502. https://doi.org/10.1016/s0028-3932(00)00057-9

Röder, B., Rösler, F., Spence, C., 2004. Early Vision Impairs Tactile Perception in the Blind. Curr. Biol. 14, 121–124. https://doi.org/10.1016/j.cub.2003.12.054

Röder, B., Teder-Sälejärvi, W., Sterr, A., Rösler, F., Hillyard, S.A., Neville, H.J., 1999. Improved auditory spatial tuning in blind humans. Nature 400, 162–166. https://doi.org/10.1038/22106

Roffwarg, H.P., Muzio, J.N., Dement, W.C., 1966. Ontogenetic development of the human sleep-dream cycle. Science (80-.). https://doi.org/10.1126/science.152.3722.604

Ronga, I., Galigani, M., Bruno, V., Noel, J.P., Gazzin, A., Perathoner, C., Serino, A.,

Garbarini, F., 2021. Spatial tuning of electrophysiological responses to multisensory stimuli reveals a primitive coding of the body boundaries in newborns. Proc. Natl. Acad. Sci. U. S. A. 118, 1–3. https://doi.org/10.1073/pnas.2024548118

Rossetti, Y., Gaunet, F., Thinus-Blanc, C., 1996. Early visual experience affects memorization and spatial representation of proprioceptive targets. Neuroreport 7, 1219–1223. https://doi.org/10.1097/00001756-199604260-00025

Rothschild, G., 2019. The transformation of multi-sensory experiences into memories during sleep. Neurobiol. Learn. Mem. 160, 58–66. https://doi.org/10.1016/j.nlm.2018.03.019

Ruggiero, G., D'Errico, O., Iachini, T., 2016. Development of egocentric and allocentric spatial representations from childhood to elderly age. Psychol. Res. 80, 259–272. https://doi.org/10.1007/s00426-015-0658-9

Russo, N., Foxe, J.J., Brandwein, A.B., Altschuler, T., Gomes, H., Molholm, S., 2010. Multisensory processing in children with autism: High-density electrical mapping of auditory-somatosensory integration. Autism Res. 3, 253–267. https://doi.org/10.1002/aur.152

Sabbagh, M.A., Bowman, L.C., Evraire, L.E., Ito, J.M.B., 2009. Neurodevelopmental correlates of theory of mind in preschool children. Child Dev. 80, 1147–1162. https://doi.org/10.1111/j.1467-8624.2009.01322.x

Saby, J.N., Meltzoff, A.N., Marshall, P.J., 2015. Neural body maps in human infants: Somatotopic responses to tactile stimulation in 7-month-olds. Neuroimage 118, 74–78. https://doi.org/10.1016/j.neuroimage.2015.05.097

Sadato, N., Pascual-Leone, A., Grafman, J., Ibañez, V., Deiber, M.P., Dold, G., Hallett, M., 1996. Activation of the primary visual cortex by Braille reading in blind subjects. Nature 380, 526–528. https://doi.org/10.1038/380526a0

Salvador, R., Molaee-ardekani, B., Mekonnen, A., Merlet, I., Soria-frish, A., Ruffini, G., Miranda, P.C., Wendling, F., 2013. From Oscillatory Transcranial Current Stimulation to Scalp EEG Changes : A Biophysical and Physiological Modeling Study 8, 1–12. https://doi.org/10.1371/journal.pone.0057330

Sankupellay, M., Wilson, S., Heussler, H.S., Parsley, C., Yuill, M., Dakin, C., 2011. Characteristics of sleep EEG power spectra in healthy infants in the first two years of life. Clin. Neurophysiol. Off. J. Int. Fed. Clin. Neurophysiol. 122, 236–243. https://doi.org/10.1016/j.clinph.2010.06.030

Sann, C., Streri, A., 2007. Perception of object shape and texture in human newborns : evidence from cross-modal transfer tasks 3, 399–410. https://doi.org/10.1111/j.1467-7687.2007.00593.x

Schabus, M., Dang-Vu, T.T., Albouy, G., Balteau, E., Boly, M., Carrier, J., Darsaud, A., Degueldre, C., Desseilles, M., Gais, S., Phillips, C., Rauchs, G., Schnakers, C., Sterpenich, V., Vandewalle, G., Luxen, A., Maquet, P., 2007. Hemodynamic cerebral correlates of sleep spindles during human non-rapid eye movement sleep. Proc. Natl. Acad. Sci. U. S. A. 104, 13164–13169. https://doi.org/10.1073/pnas.0703084104

Scheier, C., Lewkowicz, D.J., Shimojo, S., 2003. Sound induces perceptual reorganization of an ambiguous motion display in human infants. Dev. Sci. 6, 233–241. https://doi.org/https://doi.org/10.1111/1467-7687.00276

Schiatti, L., Cappagli, G., Martolini, C., Maviglia, A., Signorini, S., Gori, M., Crepaldi, M., 2020. A Novel Wearable and Wireless Device to Investigate Perception in Interactive Scenarios. Proc. Annu. Int. Conf. IEEE Eng. Med. Biol. Soc. EMBS 2020-July, 3252–3255. https://doi.org/10.1109/EMBC44109.2020.9176167

Schipke, C.S., Knoll, L.J., Friederici, A.D., Oberecker, R., 2012. Preschool children's interpretation of object-initial sentences: Neural correlates of their behavioral performance. Dev. Sci. https://doi.org/10.1111/j.1467-7687.2012.01167.x

Schoch, S.F., Kurth, S., Werner, H., 2021. Actigraphy in sleep research with infants and young children: Current practices and future benefits of standardized reporting. J. Sleep Res. 30. https://doi.org/10.1111/jsr.13134

Scholle, S., Beyer, U., Bernhard, M., Eichholz, S., Erler, T., Graness, P., Goldmann-Schnalke, B., Heisch, K., Kirchhoff, F., Klementz, K., Koch, G., Kramer, A., Schmidtlein, C., Schneider, B., Walther, B., Wiater, A., Scholle, H.C., 2011. Normative values of polysomnographic parameters in childhood and adolescence: quantitative sleep parameters. Sleep Med. 12, 542–549. https://doi.org/10.1016/j.sleep.2010.11.011

Schubert, J.T.W., Buchholz, V.N., Föcker, J., Engel, A.K., Röder, B., Heed, T., 2019. Alpha-band oscillations reflect external spatial coding for tactile stimuli in sighted , but not in congenitally blind humans 1–14. https://doi.org/10.1038/s41598-019-45634-w

Schubert, J.T.W., Buchholz, V.N., Föcker, J., Engel, A.K., Röder, B., Heed, T., 2015. Oscillatory activity reflects differential use of spatial reference frames by sighted and blind individuals in tactile attention. Neuroimage 117, 417–428. https://doi.org/10.1016/j.neuroimage.2015.05.068

Schubert, R., Ritter, P., Wu, T., Franklin, B., 2008. Spatial Attention Related SEP Amplitude Modulations Covary with BOLD Signal in S1 — A Simultaneous EEG — fMRI Study. https://doi.org/10.1093/cercor/bhn029

Sciutti, A., Burr, D., Saracco, A., Sandini, G., Gori, M., 2014. Development of context dependency in human space perception. Exp. brain Res. 232, 3965–3976. https://doi.org/10.1007/s00221-014-4021-y

Scurry, A.N., Chifamba, K., Jiang, F., 2020. Electrophysiological Dynamics of Visual-Tactile Temporal Order Perception in Early Deaf Adults. Front. Neurosci. 14. https://doi.org/10.3389/fnins.2020.544472

Senkowski, D., Gomez-Ramirez, M., Lakatos, P., Wylie, G.R., Molholm, S., Schroeder, C.E., Foxe, J.J., 2007. Multisensory processing and oscillatory activity: Analyzing non-linear electrophysiological measures in humans and simians. Exp. Brain Res. 177, 184–195. https://doi.org/10.1007/s00221-006-0664-7

Serino, A., 2019. Peripersonal space (PPS) as a multisensory interface between the

individual and the environment, defining the space of the self. Neurosci. Biobehav. Rev. 99, 138–159. https://doi.org/https://doi.org/10.1016/j.neubiorev.2019.01.016

Setti, W., Engel, I.A.M., Cuturi, L.F., Gori, M., Picinali, L., 2022. The Audio-Corsi: an acoustic virtual reality-based technological solution for evaluating audio-spatial memory abilities. J. Multimodal User Interfaces 16, 207–218. https://doi.org/10.1007/s12193-021-00383-x

Shaw, P., Kabani, N.J., Lerch, J.P., Eckstrand, K., Lenroot, R., Gogtay, N., Greenstein, D., Clasen, L., Evans, A., Rapoport, J.L., Giedd, J.N., Wise, S.P., 2008. Neurodevelopmental trajectories of the human cerebral cortex. J. Neurosci. Off. J. Soc. Neurosci. 28, 3586–3594. https://doi.org/10.1523/JNEUROSCI.5309-07.2008

Shen, G., Allison, O.N., Weiss, S.M., Meltzoff, A.N., Marshall, P.J., 2021. Exploring developmental changes in infant anticipation and perceptual processing : EEG responses to tactile stimulation 97–114. https://doi.org/10.1111/infa.12438

Shen, G., Meltzoff, A.N., Weiss, S.M., Marshall, P.J., 2020. Body representation in infants: Categorical boundaries of body parts as assessed by somatosensory mismatch negativity. Dev. Cogn. Neurosci. 44, 100795. https://doi.org/10.1016/j.dcn.2020.100795

Sherman, S.M., Spear, P.D., 1982. Organization of visual pathways in normal and visually deprived cats. Physiol. Rev. https://doi.org/10.1152/physrev.1982.62.2.738

Sherrington, C.S., 1956. Man on his Nature. British Journal for the Philosophy of Science, Cambridge. https://doi.org/DOI: 10.1017/CBO9780511694196

Shinomiya, S., Nagata, K., Takahashi, K., Masumura, T., 1999. Development of sleep spindles in young children and adolescents. Clin. Electroencephalogr. 30, 39–43. https://doi.org/10.1177/155005949903000203

Shonkoff, J.P., Phillips, D.A. (Eds.), 2000. From Neurons to Neighborhoods: The Science of Early Childhood Development. Washington (DC). https://doi.org/10.17226/9824

Siclari, F., Bernardi, G., Riedner, B.A., LaRocque, J.J., Benca, R.M., Tononi, G., 2014. Two Distinct Synchronization Processes in the Transition to Sleep: A High-Density Electroencephalographic Study. Sleep 37, 1621–1637. https://doi.org/10.5665/sleep.4070

Silva, L.R., Amitai, Y., Connors, B.W., 1991. Intrinsic oscillations of neocortex generated by layer 5 pyramidal neurons. Science 251, 432–435. https://doi.org/10.1126/science.1824881

Smith, G.B., Hein, B., Whitney, D.E., Fitzpatrick, D., Kaschube, M., 2018. Distributed network interactions and their emergence in developing neocortex. Nat. Neurosci. 21, 1600–1608. https://doi.org/10.1038/s41593-018-0247-5

Sokoloff, G., Dooley, J.C., Glanz, R.M., Wen, R.Y., Hickerson, M.M., Evans, L.G., Laughlin, H.M., Apfelbaum, K.S., Blumberg, M.S., 2021. Twitches emerge postnatally during quiet sleep in human infants and are synchronized with sleep spindles. Curr. Biol. 31, 3426-3432.e4. https://doi.org/https://doi.org/10.1016/j.cub.2021.05.038

Somogyi, E., Jacquey, L., Heed, T., Hoffmann, M., Lockman, J.J., Granjon, L., Fagard, J., O'Regan, J.K., 2018. Which limb is it? Responses to vibrotactile stimulation in early infancy. Br. J. Dev. Psychol. 36, 384–401. https://doi.org/10.1111/bjdp.12224

Soto-Faraco, S., Azañón, E., 2013. Electrophysiological correlates of tactile remapping. Neuropsychologia 51, 1584–1594. https://doi.org/10.1016/j.neuropsychologia.2013.04.012

Spiess, M., Bernardi, G., Kurth, S., Ringli, M., Wehrle, F.M., Jenni, O.G., Huber, R., Siclari, F., 2018. How do children fall asleep ? A high-density EEG study of slow waves in the transition from wake to sleep 178, 23–35. https://doi.org/10.1016/j.neuroimage.2018.05.024

Stefanou, M.E., Dundon, N.M., Bestelmeyer, P.E.G., Ioannou, C., Bender, S., Biscaldi, M., Smyrnis, N., Klein, C., 2020. Late attentional processes potentially compensate for early perceptual multisensory integration deficits in children with autism: evidence from evoked potentials. Sci. Rep. 10, 1–13. https://doi.org/10.1038/s41598-020-73022-2

Stein, B.E., 1998. Neural mechanisms for synthesizing sensory information and producing adaptive behaviors, in: Experimental Brain Research. Springer-Verlag, pp. 124–135. https://doi.org/10.1007/s002210050553

Stein, B.E., Meredith, M.A., 1993. The merging of the senses., The merging of the senses., Cognitive neuroscience. The MIT Press, Cambridge, MA, US.

Stein, B.E., Stanford, T.R., Rowland, B.A., 2009. The Neural Basis of Multisensory Integration in the Midbrain: Its Organization and Maturation. Attention, Perception, Psychophys. 82, 1–7. https://doi.org/10.1038/jid.2014.371

Steriade, M., 1999. Brainstem activation of thalamocortical systems. Brain Res. Bull. 50, 391–392. https://doi.org/10.1016/s0361-9230(99)00119-7

Steriade, M., Deschênes, M., Domich, L., Mulle, C., 1985. Abolition of spindle oscillations in thalamic neurons disconnected from nucleus reticularis thalami. J. Neurophysiol. 54, 1473–1497. https://doi.org/10.1152/jn.1985.54.6.1473

Steriade, M., Jones, E.G., Llinás, R.R., 1990. Thalamic oscillations and signaling. John Wiley & Sons.

Streri, A., 2003. Cross-modal recognition of shape from hand to eyes in human newborns. Somatosens. Mot. Res. 20, 13–18. https://doi.org/10.1080/0899022031000083799

Streri, A., Gentaz, E., 2004. Cross-modal recognition of shape from hand to eyes and handedness in human newborns. Neuropsychologia 42, 1365–1369. https://doi.org/https://doi.org/10.1016/j.neuropsychologia.2004.02.012

Striem-Amit, E., Amedi, A., 2014. Visual cortex extrastriate body-selective area activation in congenitally blind people "Seeing" by using sounds. Curr. Biol. 24, 687–692. https://doi.org/10.1016/j.cub.2014.02.010

Striem-Amit, E., Cohen, L., Dehaene, S., Amedi, A., 2012. Reading with sounds: sensory substitution selectively activates the visual word form area in the blind. Neuron 76,

640–652. https://doi.org/10.1016/j.neuron.2012.08.026

Stroganova, T.A., Orekhova, E. V, Posikera, I.N., 1999. EEG alpha rhythm in infants. Clin. Neurophysiol. Off. J. Int. Fed. Clin. Neurophysiol. 110, 997–1012. https://doi.org/10.1016/s1388-2457(98)00009-1

Sur, S., Sinha, V.K., 2009. Event-related potential: An overview. Ind. Psychiatry J. 18, 70–73. https://doi.org/10.4103/0972-6748.57865

Tahara, Y., Aoyama, S., Shibata, S., 2017. The mammalian circadian clock and its entrainment by stress and exercise. J. Physiol. Sci. https://doi.org/10.1007/s12576-016-0450-7

Tamaki, M., Matsuoka, T., Nittono, H., Hori, T., 2008. Fast sleep spindle (13-15 hz) activity correlates with sleep-dependent improvement in visuomotor performance. Sleep 31, 204–211. https://doi.org/10.1093/sleep/31.2.204

Tanaka, Y., Kanakogi, Y., Kawasaki, M., Myowa, M., 2018. The integration of audio−tactile information is modulated by multimodal social interaction with physical contact in infancy. Dev. Cogn. Neurosci. 30, 31–40. https://doi.org/10.1016/j.dcn.2017.12.001

Tarokh, L., Carskadon, M.A., Achermann, P., 2014. Early Adolescent Cognitive Gains Are Marked by Increased Sleep EEG Coherence. PLoS One 9, 1–5. https://doi.org/10.1371/journal.pone.0106847

Taylor-Clarke, M., Kennett, S., Haggard, P., 2002. Vision Modulates Somatosensory Cortical Processing. Curr. Biol. 12, 233–236. https://doi.org/https://doi.org/10.1016/S0960-9822(01)00681-9

Teller, D.Y., McDonald, M.A., Preston, K., Sebris, S.L., Dobson, V., 1986. Assessment of Visual Acuity in Infants and Children; the Acuity Card Procedure. Dev. Med. Child Neurol. 28, 779–789. https://doi.org/10.1111/j.1469-8749.1986.tb03932.x

Thorpe, S.G., Cannon, E.N., Fox, N.A., 2016. Spectral and source structural development of mu and alpha rhythms from infancy through adulthood. Clin. Neurophysiol. 127, 254–269. https://doi.org/10.1016/j.clinph.2015.03.004

Tiihonen, J., Hari, R., Kajola, M., Karhu, J., Ahlfors, S., Tissari, S., 1991. Magnetoencephalographic 10-Hz rhythm from the human auditory cortex. Neurosci. Lett. 129, 303–305. https://doi.org/10.1016/0304-3940(91)90486-d

Timofeev, I., Chauvette, S., 2013. The Spindles: Are They Still Thalamic? Sleep.

Timofeev, I., Steriade, M., 1996. Low-frequency rhythms in the thalamus of intact-cortex and decorticated cats. J. Neurophysiol. 76, 4152–4168. https://doi.org/10.1152/jn.1996.76.6.4152

Tinti, C., Adenzato, M., Tamietto, M., Cornoldi, C., 2006. Visual experience is not necessary for efficient survey spatial cognition: evidence from blindness. Q. J. Exp. Psychol. (Hove). 59, 1306–1328. https://doi.org/10.1080/17470210500214275

Tiriac, A., Bistrong, K., Pitcher, M.N., Tworig, J.M., Feller, M.B., 2022. The influence of spontaneous and visual activity on the development of direction selectivity maps in

mouse retina. Cell Rep. 38, 110225. https://doi.org/10.1016/j.celrep.2021.110225

Tomé, D., Barbosa, F., Nowak, K., Marques-Teixeira, J., 2015. The development of the N1 and N2 components in auditory oddball paradigms: a systematic review with narrative analysis and suggested normative values. J. Neural Transm. https://doi.org/10.1007/s00702-014-1258-3

Tomé, D.F., Sadeh, S., Clopath, C., 2022. Coordinated hippocampal-thalamic-cortical communication crucial for engram dynamics underneath systems consolidation. Nat. Commun. 13, 1–18. https://doi.org/10.1038/s41467-022-28339-z

Tononi, G., Cirelli, C., 2014. Sleep and the Price of Plasticity: From Synaptic and Cellular Homeostasis to Memory Consolidation and Integration. Neuron 81, 12–34. https://doi.org/https://doi.org/10.1016/j.neuron.2013.12.025

Trommershäuser, J., Kording, K., Landy, M.S. (Eds.), 2011. Sensory Cue Integration. https://doi.org/10.1093/acprof:oso/9780195387247.001.0001

Tröndle, M., Popov, T., Dziemian, S., Langer, N., 2022. Decomposing the role of alpha oscillations during brain maturation 1–34.

Turrigiano, G.G., Nelson, S.B., 2004. Homeostatic plasticity in the developing nervous system. Nat. Rev. Neurosci. 5, 97–107. https://doi.org/10.1038/nrn1327

Uhl, F., Franzen, P., Lindinger, G., Lang, W., Deecke, L., 1991. On the functionality of the visually deprived occipital cortex in early blind persons. Neurosci. Lett. 124, 256–259. https://doi.org/10.1016/0304-3940(91)90107-5

Uppal, N., Foxe, J.J., Butler, J.S., Acluche, F., Molholm, S., 2023. The neural dynamics of somatosensory processing and adaptation across childhood : a high-density electrical mapping study 1605–1619. https://doi.org/10.1152/jn.01059.2015

Van Boven, R.W., Hamilton, R.H., Kauffman, T., Keenan, J.P., Pascual-Leone, A., 2000. Tactile spatial resolution in blind braille readers. Neurology 54, 2230–2236. https://doi.org/10.1212/wnl.54.12.2230

Van De Ville, D., Britz, J., Michel, C.M., 2010. EEG microstate sequences in healthy humans at rest reveal scale-free dynamics. Proc. Natl. Acad. Sci. U. S. A. 107, 18179–18184. https://doi.org/10.1073/pnas.1007841107

Vidyasagar, T.R., 1978. Possible plasticity in the rat superior colliculus. Nature 275, 140–141.

Vitali, H., Campus, C., De Giorgis, V., Signorini, S., Gori, M., 2022. The vision of dreams: from ontogeny to dream engineering in blindness. J. Clin. sleep Med. JCSM Off. Publ. Am. Acad. Sleep Med. 18, 2051–2062. https://doi.org/10.5664/jcsm.10026

Vollebregt, M.A., Zumer, J.M., Castricum, J., Buitelaar, J.K., Jensen, O., 2015. NeuroImage Lateralized modulation of posterior alpha oscillations in children. Neuroimage 123, 245–252. https://doi.org/10.1016/j.neuroimage.2015.06.054

Voss, P., Gougoux, F., Zatorre, R.J., Lassonde, M., Lepore, F., 2008. Differential occipital responses in early- and late-blind individuals during a sound-source discrimination task. Neuroimage 40, 746–758. https://doi.org/10.1016/j.neuroimage.2007.12.020

Voss, P., Lassonde, M., Gougoux, F., Fortin, M., Guillemot, J.-P., Lepore, F., 2004. Early- and Late-Onset Blind Individuals Show Supra-Normal Auditory Abilities in Far-Space Patrice. Curr. Biol. 14, 1734–1738. https://doi.org/10.1016/j

Voss, P., Zatorre, R.J., 2012. Organization and reorganization of sensory-deprived cortex. Curr. Biol. 22, R168–R173. https://doi.org/10.1016/j.cub.2012.01.030

Wakai, R.T., Lutter, W.J., 2016. Slow rhythms and sleep spindles in early infancy. Neurosci. Lett. 630, 164–168. https://doi.org/10.1016/j.neulet.2016.07.051

Wallace, M.T., Jr, T.J.P., Hairston, W.D., Stein, B.E., 2004. Visual Experience Is Necessary for the Development of Multisensory Integration 24, 9580–9584. https://doi.org/10.1523/JNEUROSCI.2535-04.2004

Wallace, M.T., Stein, B.E., Carolina, N., 2001. Sensory and Multisensory Responses in the Newborn Monkey Superior Colliculus 21, 8886–8894.

Wechsler, D., 2003. Wechsler Intelligence Scale for Children-Fourth Edition (WISCIV). San Antonio, Tx.

Weeks, R., Horwitz, B., Aziz-Sultan, A., Tian, B., Wessinger, C.M., Cohen, L.G., Hallett, M., Rauschecker, J.P., 2000. A positron emission tomographic study of auditory localization in the congenitally blind. J. Neurosci. 20, 2664–2672. https://doi.org/10.1523/JNEUROSCI.20-07-02664.2000

Welch, R.B., Warren, D.H., 1980. Immediate perceptual response to intersensory discrepancy. Psychol. Bull. 88, 638–667.

Weliky, M., Katz, L.C., 1999. Correlational structure of spontaneous neuronal activity in the developing lateral geniculate nucleus in vivo. Science 285, 599–604. https://doi.org/10.1126/science.285.5427.599

Wenzhi, S., Yang, D., 2009. Layer-specific network oscillation and spatiotemporal receptive field in t he visual cortex. Proc. Natl. Acad. Sci. U. S. A. https://doi.org/10.1073/pnas.0903962106

Whitehead, K., Meek, J., Fabrizi, L., 2018. Developmental trajectory of movement-related cortical oscillations during active sleep in a cross-sectional cohort of pre-term and full-term human infants. Sci. Rep. 8, 1–8. https://doi.org/10.1038/s41598-018-35850-1

Whitford, T.J., Rennie, C.J., Grieve, S.M., Clark, C.R., Gordon, E., Williams, L.M., 2007. Brain maturation in adolescence: concurrent changes in neuroanatomy and neurophysiology. Hum. Brain Mapp. 28, 228–237. https://doi.org/10.1002/hbm.20273

Wilkinson, G.N., Rogers, C.E., 1973. Symbolic Description of Factorial Models for Analysis of Variance. J. R. Stat. Soc. Ser. C (Applied Stat. 22, 392–399.

Wong, M., Gnanakumaran, V., Goldreich, D., 2011. Tactile spatial acuity enhancement in blindness: Evidence for experience-dependent mechanisms. J. Neurosci. 31, 7028–7037. https://doi.org/10.1523/JNEUROSCI.6461-10.2011

Yordanova, J., Kolev, V., 1997. Alpha response system in children: Changes with age. Int. J. Psychophysiol. 26, 411–430. https://doi.org/10.1016/S0167-8760(97)00779-4

Yordanova, J.Y., Kolev, V.N., 1996. Developmental changes in the alpha response system. Electroencephalogr. Clin. Neurophysiol. 99, 527–538. https://doi.org/10.1016/S0013-4694(96)95562-5

Yoshida, M., Shinohara, H., Kodama, H., 2015. Assessment of nocturnal sleep architecture by actigraphy and one-channel electroencephalography in early infancy. Early Hum. Dev. 91, 519–526. https://doi.org/10.1016/j.earlhumdev.2015.06.005

Zwiers, M.P., Van Opstal, A.J., Cruysberg, J.R., 2001. A spatial hearing deficit in early-blind humans. J. Neurosci. 21, RC142: 1-5. https://doi.org/10.1523/JNEUROSCI.21-09-j0002.2001

Zwiers, M.P., Van Opstal, A.J., Paige, G.D., 2003. Plasticity in human sound localization induced by compressed spatial vision. Nat. Neurosci. 6, 175–181. https://doi.org/10.1038/nn999